# Investigating the Biological Mechanisms underlying the Initiation of Autoimmunity against Beta Cell Antigens in Type 1 Diabetes

PAR

## Chiara CIANCIARUSO

ÉCOLE POLYTECHNIQUE
FÉDÉRALE DE LAUSANNE

Suisse
2017

# Acknowledgements

I would like to thank the following people who helped me towards the completion of my PhD:

My thesis advisor and co-director, Prof. Steinunn Baekkeskov, for her supervision, for giving me the opportunity of doing my PhD in a stimulating research environment and for letting me develop my own ideas.

My thesis director, Prof. Jeffrey Alan Hubbell, for his advice and availability.

The members of my thesis committee, Prof. Gisou van der Goot, Prof. Johan Auwerx, Prof. Decio Laks Eizirik and Prof. Pierre Maechler for reviewing my thesis.

Prof. Nicola Harris for her mentorship.

Prof. Michele De Palma for his help and scientific support.

Prof. Edward Allen Phelps and Miriella Pasquier, for being the best colleagues I could have wished for and for their being such genuine and supportive friends.

Sonja Bodmer and Ingrid Margot for administrative assistance during my thesis.

Gabriele Galliverti, for always being there for me throughout all of this, for his extraordinary patience and for sharing good (and bad) times with me.

My four parents, with a special thanks to my mother, and my sister Alice for their understanding and unconditional support.

# Abstract

Type 1 diabetes (T1D) is an autoimmune disease characterized by circulating autoantibodies, lymphocytic infiltration of pancreatic islets of Langerhans, and cell-specific destruction of beta cells, leading to insulin deficiency and symptomatic hyperglycemia. Some of the major target autoantigens in T1D are intracellular proteins, such as GAD65, IA-2 and proinsulin, whose initial encounter with the immune system is poorly understood.

Here we describe a method for culturing monolayers of primary pancreatic islet cells *in vitro*, which enables detailed observation of proteins and sub-cellular processes in primary human and rat beta cells by super-resolution and live-cell light microscopy. This technical advance is broadly applicable to obtaining novel biological insights as demonstrated by our identification of a mechanism to control proliferation in primary beta cells through growth and disassembly of primary cilia.

This protocol also allowed us to identify two novel interrelated mechanisms for how beta cell proteins, such as the antigen GAD65, can become target of autoimmunity and initiate T1D. A triggering factor that these two pathways have in common is represented by endoplasmic reticulum (ER) stress, to which pancreatic islet beta cells are particularly susceptible, and can be induced by inflammatory factors such as Th1 cytokines.

In the first mechanism, we show that ER stress in beta cells perturbs the palmitoylation cycle controlling GAD65 endomembrane distribution, resulting in aberrant accumulation of the palmitoylated form in Golgi membranes. The palmitoylated form has heightened immunogenicity, exhibiting increased uptake by antigen presenting cells (APCs) and T cell stimulation compared to the non-palmitoylated form. Similar accumulation of GAD65 in Golgi membranes is observed in human beta cells in pancreatic sections from GAD65 autoantibody positive individuals, who have not yet progressed to clinical onset of T1D, and T1D patients

with residual beta cell mass and ongoing T cell infiltration of islets. Thus, aberrant accumulation of immunogenic GAD65 in Golgi membranes facilitates inappropriate presentation to the immune system following release from stressed and/or damaged beta cells, triggering autoimmunity.

In the second mechanism, we present that, following a pathway originating from the Golgi, both rat and human pancreatic islets release the intracellular beta cell autoantigens GAD65, IA-2 and proinsulin in a subtype of extracellular vesicles called exosomes. Islet-exosomes are then taken up by and can activate APCs including dendritic cells. Accordingly, anchoring of GAD65 to exosome-mimetic liposomes strongly boosts antigen presentation and T cell activation in the context of the human T1D susceptibility haplotype HLA-DR4. Furthermore, cytokine-induced ER stress enhances exosome secretion by beta cells, induces exosomal release of the immunostimulatory chaperones calreticulin, Gp96 and ORP150 and increases exosomal stimulation of APCs. Therefore, stress-induced exosomal release of intracellular autoantigens and immunostimulatory chaperones may play a role in initiation of autoimmune responses in T1D.

# Riassunto

Il diabete di tipo 1 è una malattia autoimmune caratterizzata dalla presenza di anticorpi circolanti, infiltrazione linfocitaria nelle isole di Langerhans e distruzione delle cellule beta pancreatiche, con conseguente insulino-deficienza e iperglicemia sintomatica. Alcuni dei più importanti autoantigeni nel diabete di tipo I sono proteine intracellulari come GAD65, IA-2 e la proinsulina. Le modalità tramite cui avviene l'incontro iniziale di questi antigeni con il sistema immunitario sono ancora poco conosciute.

Nella presente tesi di dottorato viene descritto un metodo che permette la coltivazione *in vitro* di monostrati di cellule pancreatiche primarie. Con l'aiuto di tecniche di microscopia a super-risoluzione ed in tempo reale, tale metodo consente di effettuare osservazioni dettagliate su proteine e processi sub-cellulari in cellule beta pancreatiche di uomo o ratto. Questa tecnica può essere utilizzata per ottenere nuove conoscenze a livello biologico. Ad esempio, grazie a questo sistema, siamo riusciti a individuare un meccanismo di controllo della proliferazione mediato dalla crescita e successivo disassemblaggio delle ciglia primarie nelle cellule beta pancreatiche.

Questo protocollo ci ha inoltre permesso di identificare due nuovi meccanismi interconnessi che spiegano come le proteine delle cellule beta pancreatiche, tra cui GAD65, possono diventare bersaglio dell'autoimmunità e portare all'insorgenza del diabete di tipo I. Un fattore scatenante, che questi due meccanismi hanno in comune, è rappresentato dallo stress del Reticolo Endoplasmatico (RE), al quale le cellule beta pancreatiche sono particolarmente suscettibili e che può essere indotto da fattori infiammatori come le citochine di tipo Th1.

Riguardo al primo meccanismo, mostriamo che lo stress del RE nelle cellule beta pancreatiche perturba il ciclo di palmitoilazione che controlla la distribuzione di

GAD65 tra le membrane, causando un accumulo anormale della forma palmitoilata di questo antigene nel Golgi. Rispetto alla forma non palmitoilata, la proteina GAD65 palmitoilata presenta una maggiore immunogenicità, viene più facilmente catturata dalle cellule presentanti l'antigene (cellule APC) ed è in grado di indurre una più forte stimolazione dei linfociti T. Un simile accumulo di GAD65 nelle membrane del Golgi è inoltre osservabile all'interno di cellule beta umane presenti in sezioni istologiche di pancreas derivate sia da individui pre-diabetici positivi per autoanticorpi contro GAD65 che da pazienti diabetici con massa beta cellulare residua ed infiltrazione linfocitaria nelle isole pancreatiche. Pertanto, l'accumulo anomalo di GAD65 nel Golgi, insieme al suo rilascio da parte di cellule in condizioni di stress e/o danneggiate, potrebbe facilitare la sua anormale presentazione al sistema immunitario, scatenando così il processo di autoimmunità.

Il secondo meccanismo qui presentato mostra che, seguendo un percorso intracellulare che vede la sua origine nel Golgi, le isole pancreatiche umane e di ratto rilasciano gli autoantigeni intracellulari GAD65, IA-2 e la proinsulina in un sottotipo di vescicole extracellulari chiamate esosomi. Questi esosomi sono poi catturati da cellule APC, in particolare cellule dendritiche, inducendo la loro attivazione. Analogamente, la coniugazione di GAD65 a liposomi simil-esosomi (ovvero generati in maniera tale da mimare gli esosomi) porta alla presentazione di questo antigene e ad una forte attivazione delle cellule T in presenza dell'aplotipo HLA-DR4 correlato a suscettibilità al diabete. Inoltre, lo stress del RE indotto da citochine aumenta la secrezione di esosomi da parte delle cellule beta e delle proteine chaperone con proprietà immunostimolatorie (tra cui calreticulina, Gp96 e ORP150) ad essi associate e, di conseguenza, aumenta la stimolazione delle cellule APC. Pertanto il rilascio, indotto da stress e mediato da esosomi, di autoantigeni intracellulari e proteine chaperone immunostimolatorie potrebbe avere un ruolo importante nella generazione della risposta autoimmune.

# Table of contents

## CHAPTER 3
**Aberrant accumulation of the diabetes autoantigen GAD65 in Golgi membranes in conditions of ER stress and autoimmunity**          83

## CHAPTER 4
**Primary human and rat beta cells release the intracellular autoantigens GAD65, IA-2 and proinsulin in exosomes together with cytokine-induced enhancers of immunity**  **119**

## CHAPTER 5
**Conclusion**  **161**

# CHAPTER 1

# Introduction

## 1.1 BACKGROUND

### 1.1.1  T1D and target islet autoantigens

Type 1 Diabetes (T1D) results from the immune-mediated destruction of insulin-producing beta cells in the islets of Langerhans in the pancreas. Loss of pancreatic beta cells leads to a decrease in insulin production, elevated blood sugar levels (hyperglycemia) and the onset of T1D (1). The prevalence of T1D in humans between the ages of 0 and 19 years was reported to be 1.7 per 1000 and has been rising globally and by as much as 5.3% annually in the United States (2).

Although the etiology of T1D is not fully understood, a well-accepted view is that T1D is an autoimmune disease caused by genetic and environmental factors (1). There are several lines of evidence showing the autoimmune nature of T1D. First, certain haplotypes of the human leukocyte antigen (HLA) have strong linkage with disease, especially HLA-DR3, DQ2 and HLA-DR4, DQ8 (2). These HLA genes are also associated with other autoimmune diseases, such as coeliac disease and rheumatoid arthritis (3,4). Second, the presence of circulating antibodies to islet autoantigens occurs many years before clinical onset of T1D (5), and these autoantibodies are predictive and diagnostic markers for the development of the disease (**Figure 1**). Third, lymphocytic infiltrates (insulitis) appear in the islets during the beta cell destruction and development of T1D. Finally, autoreactive CD4 and CD8 T cells recognizing islet antigens are often present in recently diagnosed diabetic patients and in high-risk subjects (5-7).

The presence of autoantibodies and autoreactive T cells indicates that certain islet antigens are erroneously recognized as foreign resulting in induction of

autoimmunity against beta cells. The major antigens implicated in human T1D include (pro)insulin (8), GAD65 (9), ZnT8 (10) and IA-2 (11).

In the next paragraphs, I will give a brief introduction to the major target antigens in human T1D.

### 1.1.1.1  GAD65 and IA-2

Early identification of the smaller isoform of the enzyme L-glutamic acid decarboxylase, GAD65, and a tyrosine phosphatase like protein, IA-2 as T1D autoantigens came from immunoprecipitation studies involving incubation of non-ionic detergent solubilized human islets of Langerhans with sera from newly diagnosed T1D patients or controls, showing that the diabetic sera specifically recognize and precipitate conformational but not linear epitopes in a 64 kDa islet cell protein (12). Immunoreactivity to the 64-kDa antigen was observed in about 80% of new-onset T1D patients (12) and in pre-T1D subjects, and was found to be present several years before the clinical onset (13). Thereafter, an amphiphilic component of the 64-kDa autoantigen in T1D was identified as GAD65 (9) while a second component of the 64-kDa autoantigen was identified as IA-2alpha (14). Subsequent research on humoral autoimmunity in diabetes led to the development of new assays to detect autoantibodies against conformational and not linear epitopes of GAD65 and IA-2. These assays are now widely used (15).

### 1.1.1.2  GAD65

GAD65 and a highly homologous second isoform of glutamic acid decarboxylase, GAD67, are the major synthesizing enzymes for production of the neurotransmitter gamma-amino butyric acid (GABA). GAD67 is not an independent autoantigen in T1D but is recognized by cross-reactive conformational GAD65 antibodies in a fraction of patients (16). The GAD enzymes require a cofactor,

pyridoxal 5'-phosphate (PLP, activated vitamin B6) for activity and are principally found in GABAergic neurons. However, they are also expressed in other tissues such as ovary and testis, and especially in pancreatic islet beta cells (17).

GAD67 is a constitutively active holoenzyme, stably bound to PLP, and produces the majority of brain GABA, while GAD65 fluctuates between a PLP-bound active holoenzyme and PLP-free inactive apoenzyme and is critical for fine tuning of GABAergic neurotransmission in response to changes in GABA demand (18).

GAD65 and GAD67 have some differences in their structure, with GAD65 having more flexibility in the carboxy-terminal region, a feature that has been suggested to play a role in its antigenicity (19). Early humoral autoimmune response to GAD65 in T1D has been detected against epitopes primarily in the middle and carboxyl terminal regions of GAD65 (20). While autoantibodies in T1D are an important marker for prediction and as a diagnostic tool, they are not believed to play a role in beta cells destruction, which is mediated by Th1 T-helper cells and cytotoxic T-cells (21). However, autoantigen-specific B lymphocytes seem to play an important role in uptake of autoantigen through their membrane bound immunoglobulin receptor and presentation to T cells (22). Interestingly, the epitope specificity of the B cell can enhance or suppress T cell epitopes (23). Additionally, structural crystallography studies aided by monoclonal antibody testing of antigenic determinants have indicated that the more flexible carboxy-terminal region of GAD65 shows a close grouping of autoantibody and T cell antigenic determinants, raising the possibility that antigen–antibody complexes could contribute to GAD65-induced T cell reactivity (24). Although the importance of the middle region and the carboxyl terminus bearing major immunoreactive epitopes is recognized, epitope spreading to the amino-terminal region of GAD65 as well as to GAD67 can occur later (15).

GAD65 is localized differently from the other autoantigens in beta cells (25), which are associated with dense-core insulin secretory granules. Analogous to neuronal cells, both GAD65 and GAD67 are initially synthesized as cytosolic proteins

in beta cells rather than the ER, and are subject to different translational regulation than proinsulin or other autoantigens contained in secretory granules (26). GAD65 undergoes a two-step post-translational modification by hydrophobic residues. The first step results in a form that is weakly membrane associated and cycles on and off the cytosolic face of ER and *cis*-Golgi membranes. The second step involves palmitoylation of two cysteine residues in the amino-terminal region (27) and is required for trafficking of GAD65 through the *trans*-Golgi network (TGN) and targeting to synaptic vesicles in neurons (28) or small peripheral vesicles in beta cells (29). The hydrophobic modifications and consequent membrane anchoring of GAD65 to GABA-secreting vesicles may be significant for its role as an islet autoantigen (15).

In the last years, the Diamyd vaccine, based on the whole recombinant human GAD65 molecule suspended in alum, has provided an interesting development in the area of tolerance induction in T1D. Phase I clinical trials in late onset autoimmune diabetes in adults and adolescents with newly diagnosed type 1 diabetes have suggested benefit. Treatment with this vaccine seemed to induce a deviation of the GAD65–specific T cell response toward a protective immune profile and reduce C-peptide decline in recently diagnosed patients (30). However, these observations were not confirmed in subsequent phase II and III clinical trials leading to the conclusion that, at for such a late intervention, induction of immune deviation of the GAD65 response to a more tolerogenic phenotype was not sufficient to block beta cell decline (30).


*1.1.1.3  IA-2*

IA-2 (also known as ICA512) is a transmembrane proteins located to the insulin secretory granule membrane in beta cells (15). Autoantibodies against this protein can be detected decades before diabetes onset in first-degree relatives of T1D probands (31). Due to epitope spreading, IA-2β (also known as phogrin) can become

target antigen in small groups of T1D patients who develop autoantibodies to cross-reactive epitopes in IA-2 and phogrin.

IA-2 and IA-2 β have domains with close homology (88%) to protein phosphotyrosine phosphatases (PTPs), although they do not seem to possess such enzyme activity. IA-2 and IA-2 β are both initially synthesized as proprotein precursors that are proteolytically processed in coordination with proinsulin (see below). The mature IA-2 and IA-2 β proteins are type 1 integral membrane proteins, with the PTP domain oriented on the cytosolic side of the granule membrane and a short amino-terminal domain located on the inside of the granule (15).

The actual function of IA-2 and IA-2β remains unknown, although in beta cells it has been postulated that they may play a role in regulating insulin secretory granule content and possibly beta cell growth (15). Indeed, the IA-2 and IA-2β knockout mice are glucose intolerant and exhibit reduced insulin secretion (32). Deletion of IA-2 and/or IA-2β results in a marked decrease in the number of dense-core vesicles (DCVs) in beta cells and a decrease in beta cell intracellular calcium handling (33).

Naturally processed HLA class II allele-specific epitopes recognized by CD4 T cells were found to correspond to the intracellular domain of IA-2. These epitopes were identified after delivering the native IA-2 antigen to Epstein-Barr virus (EBV)-transformed B cells followed by mass spectrometry analyses of eluted peptides (34). Dendritic cell subsets can facilitate the processing and presentation of IA-2 antigen to CD4 T cells. Specifically, at times near the onset of T1D, the plasmacytoid subset of dendritic cells is overrepresented in the blood compared to the myeloid cell type. Both dendritic cell subsets process and present soluble IA-2 to CD4 T cells, but only plasmacytoid dendritic cells show a distinctive ability to capture islet autoantigenic immune complexes and enhance autoantigen presentation in the presence of serum from IA-2 autoantibody-positive patient. This may suggest a synergistic

proinflammatory role for plasmacytoid dendritic cells and IA-2 autoantibodies in T1D (35).

### 1.1.1.4 Insulin and proinsulin

Functional variation of the INS gene promoter conferred by the variable number of tandem repeats (VNTR) polymorphism, or mutations at other genetic loci, can lead to reduced insulin expression in the thymus and lymphoid organs resulting in a loss of tolerance to insulin (36). In susceptible mice, both CD4 and CD8 T cell clones that recognize insulin can transfer the disease (37).

Insulin represents up to 50% of the total production of beta cell protein under stimulated conditions (38). In beta cells, delivery of newly synthesized preproinsulin into the lumen of the ER is initiated by signal peptide binding to the signal recognition particle, followed by docking and translocation at the ER membrane, and cleavage of the signal peptide associated with completion of proinsulin biosynthesis (15). The preproinsulin signal peptide is one of the sites containing epitopes to which cytotoxic T lymphocytes and insulin autoantibodies can be directed (39,40). Subsequently, in the secretory pathway, coordinated proteolytic cleavages excise the C peptide of proinsulin to produce the mature two-chain hormone linked by two interchain disulfide bonds. The enzymatic reactions converting proinsulin to insulin occur primarily within immature secretory granules beginning at the time of their emergence from the *trans*-Golgi network (15).

Pathogenic T lymphocytes in NOD mice developing autoimmune diabetes recognize an immunodominant epitope contained within residues S(B9)–G(B23) of proinsulin, and this is also true in patients with recent-onset T1D (41). In T1D patients with the HLA-DRB1*0401 (DR4) DQ8 haplotype, another immunodominant epitope has been reported within proinsulin, which includes the carboxy-terminal

portion of the C-peptide running through the endoproteolytic cleavage site contiguous with the A chain (42).

Insulin-related peptides continue to attract great interest in tolerogenic vaccine development. An altered peptide ligand of the immunodominant insulin peptide S(B9)–G(B23) (NBI-6024; Neurocrine Biosciences) completed phase I trials with a suggestion of immunologic efficacy (43) but was not effective in phase II trials (44). Phase I studies based on intradermal administration of the proinsulin peptide 19-A3 have been completed, reporting that the treatment was safe and well tolerated but not particularly effective (45).

The human clinical trials conducted to date using insulin as a therapeutic or prophylactic immunotherapy have shown disappointing results. Indeed, although clinical trials based on oral and intranasal administrations of insulin in recent-onset diabetic individuals showed reduced insulin-specific T cell responses, none of them was able to induce significant differences in C-peptide level between the treated and control groups (46).


*1.1.1.5  ZnT8*

Beta cells maintain an unusually high level of cellular zinc, and the most consistently expressed beta cell zinc transporter is ZnT8 (encoded by SLC30A8), a 369 amino acid poly-topic, dimeric membrane protein whose pancreatic expression is concentrated in the islets (47). In beta cells, ZnT8 resides primarily in the membrane of insulin secretory granules where it serves to take up zinc that forms a complex with insulin molecules. ZnT8 has been shown to be a target of humoral autoimmunity in a large fraction of newly-onset T1D patients (48). SLC30A8 polymorphisms have been found associated with both type 2 (49) and type 1 diabetes (50). Autoantibodies against ZnT8 as well as T cell responses against ZnT8 are produced in patients who develop autoimmune diabetes (15).

In turn, ZnT8 expression in beta cells is down-regulated by cytokines, and this down-regulation has been proposed to play a role in beta cell dysfunction and apoptosis (15). Beta cells express several different zinc transporters. While the specific role of ZnT8 in beta cell physiology remains poorly understood, it appears to play a role in optimum secretion and storage of insulin. Thus, ZnT8-deficient mice display a decrease in glucose-stimulated insulin secretion (51) and develop glucose intolerance when fed a diabetogenic diet (52). Furthermore, knock-down of ZnT8 in beta cell lines results in a decrease in glucose stimulated insulin secretion (53), and double knockdown of ZnT8 and ZnT3 (another zinc transporter abundant in insulin secretory granules (54)) reportedly triggers cell death in pancreatic beta cell lines (55), perhaps owing to cytosolic or nuclear zinc intoxication. Altogether, these studies indicate that downregulation of ZnT8 expression can contribute to beta cell dysfunction and diminished survival, whereas its exposure as an autoantigen can trigger immune responses (15).
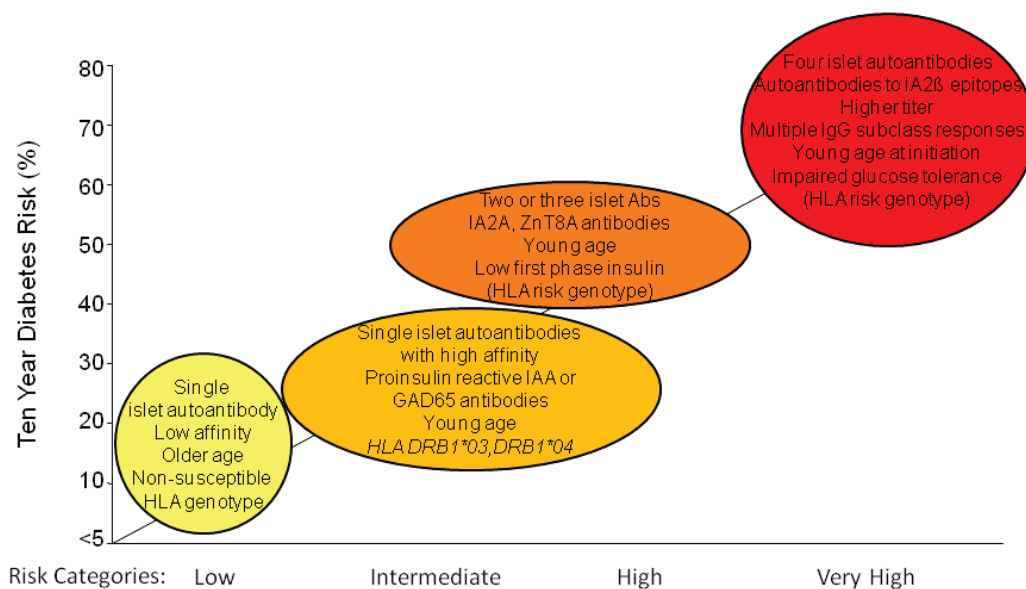


**Figure 1. Type 1 diabetes risk stratification by islet autoantibody properties.**
Increase in T1D risk is associated with progression of islet autoantibodies from single to multiple autoantibodies. Characteristics of the initial antibody response can help predict disease progression. (IAA, insulin autoantibodies; GAD65, glutamic acid decarboxylase 65; IA-2, islet-associated autoantibody 2; ZnT8, zinc transporter 8) (from 56).

22

### 1.1.2  Animal models in T1D

Multiple animal models are available to study immune-mediated diabetes. The spontaneous models, the Biobreeding (BB) rat and the non-obese diabetic (NOD) mouse have been instructive for elucidating basic molecular mechanisms involved in autoimmune destruction of pancreatic beta cells. However, these models do not carry human MHC-class II molecules and the nature of the primary target antigens differ from the human disease, except that insulin seems to have a major role in T1D in the NOD mouse (57).

In NOD mice, diabetes development starts at 5 weeks of age with an initial insulitis that manifests by means of leukocytic aggregates at the perimeter of the islets and a lymphocytic infiltration into the pancreatic islets. The dominant initial insulitis population consists of CD4 T cells and is followed by infiltration of CD8 T cells, macrophages and B cells in smaller numbers. The majority of female NOD mice develop diabetes by 12-40 weeks, but incidence in males is lower (57). The NOD mouse has several features, which distinguish it from the human disease. First, many islet autoantigens in NOD mice are different from those targeted in the human T1D (58). For example, distinct from humans and rats beta cells, mouse pancreatic beta cells do not express detectable levels of one of the major autoantigen in the human disease, GAD65, but they express the 67kDa isoform of GAD (59). In addition, the induction of organ-specific autoimmunity in humans may be caused by human pathogens and/or toxins, while autoimmunity seems to be the default mechanism in the NOD mouse (57) and infections block the development of autoimmunity and disease.

In the case of the BB rat, spontaneous T cell mediated diabetes is significantly distinct from the human disease in that it is accompanied by autoantibodies to lymphocytes and a severe lymphocytopenia, which is essential for development of beta cell autoimmunity and diabetes in this model (57).

In an attempt to develop better models of diabetes, 'humanized' transgenic mice that express diabetes-susceptibility human MHC-class II molecules were developed. Since these animals did not develop spontaneous diabetes, many were backcrossed into the NOD background. However, such backcrossing failed to induce diabetes in most cases (57,60).

Other animal models of T1D, some of them carrying human MHC-class II diabetes-susceptibility genes, were developed by inducing expression of ectopic antigens in pancreatic islets using the rat insulin promoter (RIP). While diabetes did not develop spontaneously in those models, autoimmunity and beta cell destruction was induced following immunization with the ectopic antigen or infection with a virus expressing the antigen (57).

Pharmacological models are also available. These diabetes-inducible models take advantage of alloxan and streptozotocin (STZ), which are toxic glucose analogues that preferentially accumulate in pancreatic beta cells via the GLUT2 glucose transporter. Alloxan and high doses of STZ selectively kill the insulin-producing beta cells, whereas multiple low doses of STZ generate $H_2O_2$ and induce expression of GAD65 and GAD67 autoantigens, triggering beta cell-specific autoimmunity (57).

### 1.1.3  ER stress in T1D

There is a growing experimental evidence suggesting that dysregulation of the endoplasmic reticulum (ER) homeostasis contributes to T1D pathogenesis through multiple potential mechanisms that eventually lead to beta cell death (38,61-63). For example, acute and chronic stimulation of beta cells by nutrients such as glucose, arginine, or lipids, induces the production of large amounts of insulin, which places a continuous demand on the ER for increasing protein synthesis, folding, trafficking and secretion. When the folding capacity of the ER is exceeded, misfolded or

unfolded proteins accumulate in the ER lumen, triggering the unfolded protein response (UPR) (64). The UPR is an integrated response program that reduces translation, increases chaperone availability, and enhances the degradation of misfolded proteins in an attempt to restore ER homeostasis (64). Although physiological stimulation of the UPR may be beneficial for beta cell function and acute adaptation to stress, severe or prolonged ER stress response that fails to reestablish homeostasis results in induction of apoptosis (65,66). In experimental animal models and in humans, mutations in genes critical for ER function result in beta cell failure and severe early-onset diabetes (67,68). In fact, misfolded insulin alone can cause diabetes in both mice and humans (69,70). Pro-inflammatory cytokines produced by islet-infiltrating immune cells also lead to beta cell destruction by direct cytotoxicity and enhancement of immune recognition (38). Putative inflammatory mediators of beta cell loss in T1D, such as interleukin-1beta (IL1β), tumor necrosis factor-alpha (TNFα) and interferon-gamma (IFNγ), were all shown to induce ER stress through several intracellular pathways (71,72), leading to the depletion of ER calcium, dysfunction of ER chaperones, and a severe disruption in ER homeostasis (73). Thus, cytokine-induced alterations in ER function can affect cell adaptation and amplify pro-apoptotic pathways. Reciprocally, chronic ER stress can engage stress and inflammatory pathways through activation of c-Jun N-terminal kinase (JNK), inhibitor of nuclear factor kB kinase (IKK), and protein kinase R (PKR), and this low-grade chronic inflammation may also contribute to eventual islet destruction (62).

Indicators of ER stress are present in inflamed islets of both diabetes-prone NOD mice (74) and patients with T1D (75). Viral infection, environmental toxins, chronic inflammation, abnormal protein folding, and a surplus of nutrients all can cause ER stress and trigger the UPR (76). In addition, when stress is prolonged and unresolved, the UPR can engage apoptotic pathways. The canonical UPR operates through inositol-requiring protein 1 (IRE1), protein kinase RNA-like ER kinase

(PERK), and activating transcription factor 6 (ATF6), all of which are localized in the ER membrane and respond to stress by relaying signals from the ER to the cytoplasm and nucleus.

A recent study showed the importance of ER stress and the beneficial effects of restoring organelle function through using a UPR-modulating chemical chaperone in the context of T1D in the NOD mouse (64).


### 1.1.4  Posttranslational modifications in T1D

A total of 20 amino acids constitute the building blocks of human proteins, but this number increases to more than 140 building blocks after accounting for posttranslational modifications (PTM) through enzymatic modifications (e.g. deamidation, citrullination, glycosylation) and nonenzymatic (spontaneous) modifications (e.g. methylation, carbamylation, oxidation, nitration). Data on PTM of islet autoantigens is emerging. In T1D, both citrullinated and deamidated autoantigens have been identified, indicating a role for peptidylarginine deiminases (PADs) and tissue transglutaminase (tTG) respectively, in the generation of islet neo-autoantigens (77).

In human islets, tTG is active during insulin secretion, acting on cytosolic, mitochondrial and nuclear substrates (78). Therefore, islets have the potential to generate neo-autoantigens through tTG-mediated deamidation. Inflammatory stimuli can result in deamidation of the proinsulin C-peptide (79). T cells reactive to this deamidated C-peptide were found in patients with T1D (80), linking neo-antigen generation in human islets with the induction of autoreactive T cells. tTG is also present in cells of the myeloid lineage and direct vesicular transfer of islet material to resident antigen presenting cells (APCs) has been demonstrated in both mice and humans, suggesting that islet proteins can be deamidated by tTG during antigen processing within the APC (81). PAD expression and activity have not been

26

investigated in human islets, but APCs, such as human monocytes and macrophages, contain both PAD2 and PAD4 transcripts and active PAD2 and PAD4, indicating that cells of the monocytic lineage have the potential to citrullinate self-proteins (82).

HLA binding is a key factor in the selection of processed (neo)epitopes presented by APC and beta cells. The genetic association of T1D with HLA-DQ can potentially be explained by the deamidating function of tTG, which creates more negatively charged peptides that can be exceptionally potent HLA-DQ binders. Indeed, deamidation of a naturally processed and presented peptide of preproinsulin (PPI) enhanced binding to HLA-DQ2/8 molecules and specifically to DQ8trans, a heterodimeric HLA molecule composed of the DQ2 alpha and DQ8 beta chains, and patient T cell responses (IFNγ) were increased after stimulation with the deamidated PPI peptide (80). Citrullinated GAD65 peptides displayed enhanced binding to HLA-DR4 and were recognized by autoreactive CD4 T cells isolated from patients with T1D (83). Citrullinated glucose-regulated protein 78 was identified as a modified autoantigen in murine beta cells and was a target for autoreactive T cells in mice (84). Citrullination could increase the binding affinity to predisposing HLA molecules by making the peptide more acidic, resulting in enhanced immunogenicity. The common factor linking these modifications is the increase in HLA binding affinity that results from PTM. As such, stringent selection of a high-affinity TCR repertoire against modified islet proteins is likely to play a role in T1D pathogenesis (77).

## 1.1.5 Extracellular vesicles and exosomes in T1D

Exosomes (EXOs) are small (diameter 30-100nm) biologically active vesicles that are secreted in the extracellular space by many different cell types (85). Thanks to their biological composition, these vesicles, particularly enriched in lipid raft containing cholesterol and sphingomyelin, are highly stable in body fluids, including

blood, saliva and urine (86). Many studies of EXO proteomics have been performed and the possible application of these extracellular vesicles as novel disease biomarkers is drawing considerable interest in numerous fields of research (87). The molecular mechanism of EXO biogenesis is not fully understood, but is believed to share a common pathway involving formation of multivesicular bodies (MVBs). Indeed, in addition to the conventional pathway based on the fusion of MVBs with lysosomes for degradation, MVBs can fuse with the plasma membrane releasing EXOs in the extracellular space (85).

EXOs can display immunostimulatory or immunoregulatory functions (85,88). For example, vaccination with tumor antigen-loaded EXOs resulted in tumor rejection in an antigen-specific manner (89). In the context of T1D, EXOs released by the mouse insulinoma cell line MIN6 were able to stimulate autoreactive T cells in NOD mice (90). These EXOs contain insulin and possibly GAD65, although we have been unable to detect any GAD65 in MIN6 cells (Chapter 4). Moreover, EXOs from MIN6 cells were found to stimulate autoreactive marginal zone-like B cells accumulating in prediabetic NOD mice (91). The same group also showed that islet mesenchymal stem cell-like cells produce immunostimulatory EXOs that can activate autoreactive T and B cells in NOD mice (92).

In addition to exosomes, other types of extracellular vesicles (EVs) have been described. Among these, the best known are microparticles (MPs), also called shed vesicles or microvesicles (MVs), and apoptotic bodies. MPs present irregular shape and have a size between 100 and 1000 nm (93). They are released by budding of the plasma membrane upon activation of cell surface receptors or apoptosis and subsequent increase of intracellular calcium (94). MPs are mainly produced by platelets, red blood cells and endothelial cells, and they have been shown to have a pro-coagulant activity (95), a role in IL1β secretion (96) and in promoting tumor invasiveness (97). Compared to other extracellular vesicles, apoptotic bodies are the least characterized. They are 1-5 μm in diameter and are released as blebs of cells

undergoing apoptosis (93). They are generally characterized by phosphatidylserine externalization (due to its exposure in the outer leaflet of the plasma membrane during apoptosis) and may contain fragmented DNA (98). Examples of key functions of apoptotic bodies are horizontal transfer of oncogenes (99) and DNA (100). In vitro experiments have shown that apoptotic bodies can also deliver T cell epitopes that are presented on MHC I molecules upon uptake by phagocytic cells (101). Furthermore, apoptotic bodies seem to be involved in the presentation of autoantigens to B cells (102). Uptake of apoptotic bodies has been shown to lead to immunosuppression (93). Protocols capable of isolating the different types of EVs, especially exosomes, are available, although potential contaminations among different extracellular vesicles need to be carefully addressed (93).

In the study by Palmisano et al. (103), EXOs and MPs were shown to be released by a rat insulinoma cell line, especially during cytokine-induced apoptosis. A quantitative study of proteins from cell-derived EVs, using stable isotope labeled amino acids (SILAC) in cell culture combined with mass spectrometry, mapped the most distinctive changes in protein content between EVs generated with and without cytokine stimulation to several cell death and cell signaling molecules. These included TNF receptor superfamily member 1A, TNF, alpha-induced protein 3, TNF-interacting kinase receptor-interacting serine-threonine kinase 1 and intercellular adhesion molecule (103). Despite this increasing interest in studying EXOs and MPs in the context of T1D, no studies aimed at extensively characterizing the proteomics of EVs released by primary pancreatic islets have been reported thus far.

### 1.1.6 Bioengineering approach to designing synthetic exosome mimetics

Purification of EVs, especially exosomes, from cell culture supernatants is hampered by several disadvantages, such as very low yield and limited reproducibility among different preparations. The realization that synthetic exosome

mimetics may overcome these issues opens potential applications in numerous fields of research, such as drug delivery, gene therapy, vaccine design and treatment of autoimmune and inflammatory diseases.

It is possible that not every component in natural exosomes is required for specific and efficient delivery of cargo to the target cell. By extensive characterization of the lipid, protein, and nucleic acid content of exosomes, functional components could be used for selective conjugation or incorporation in synthetic exosome mimetics. Given that natural exosomes exist as spherical lipid bilayer structures, liposomes would provide a logical basis for the generation of exosome mimetics (104).

Similar to exosomes, liposomes are bilayered phospholipid structures with adjustable diameters around 100 nm (from 25 nm to 2.5 µm), which can be loaded with a variety of proteins, nucleic acids or drug molecules. The liposome bilayer can be composed of either synthetic or natural phospholipids. The predominant physical and chemical properties of a liposome are based on the net properties of the constituent phospholipids, including permeability, charge density and steric hindrance. The lipid bilayer closes in on itself due to interactions between water molecules and the hydrophobic phosphate groups of the phospholipids. This process of liposome formation is spontaneous because the amphiphilic phospholipids self-associate into bilayers. Loading of proteins into liposomes can be achieved through (i) liposome formation in an aqueous solution saturated with a soluble drug; (ii) the use of organic solvents and solvent exchange mechanisms; (iii) the use of lipophilic drugs; and (iv) pH gradient methods. In addition, liposomes can easily be manipulated by adding additional molecules to the outer surface of the lipid bilayer (105).

Liposomes have been shown to be valuable tools in drug delivery; several liposome-based drug delivery systems are currently in preclinical development and clinical trials, while others have been approved for clinical development. Production

30

of exosome mimetics is more easily scalable for use in preclinical or clinical settings. In addition, the assembly process of exosome mimetics is controllable and results in the formation of "clean", well characterized drug delivery systems with high pharmaceutical acceptability. Moreover, the use of exosome mimetics allows us to study the effect of each component separately. However, the components which are likely to be required for proper functioning of exosome mimetics as drug delivery systems are not yet well defined in the literature (104). Thus, elucidating the mechanisms by which exosomes mediate intracellular delivery of biomolecules may also identify design strategies to guide the development of synthetic exosomes (106).

Exosomes are enriched in sphingomyelins, cholesterol, glycolipid GM3, and glycerophospholipids with long and saturated fatty acyl chains. Rigid lipid compositions such as those of exosomes may increase circulation stability of lipid particles, which may be beneficial for increasing liposome half-life in the blood. Some exosomal components, including phosphatidylserine, integrins and tetraspanins, increase uptake by recipient cells. Exosomes also display complement inhibitors CD55 and CD59, which minimize exosome lysis upon incubation with serum. Since liposome-mediated activation of complement can induce lethal immune stimulation, incorporation of complement inhibitors found in exosomes may increase the safety of liposomes (106).

In conclusion, in the effort to elucidate physiological roles and biophysical properties of exosomal components, liposomes could be valuable tools for displaying defined exosomal components, either individually or in combination. This would allow for a better understanding of the isolated effects of each component of exosomes, as well as providing a method for discovering potential synergistic effects between combinations of components (106).

## 1.2 OVERVIEW OF THE THESIS

The reasons for the loss of tolerance to beta cell antigens and the activation of autoreactive T cells in T1D are not fully understood. Before lymphocytic infiltration (insulitis), physiological islet abnormalities have been described in both humans and in animal models, such as upregulation of inflammatory cytokines (107) and increased endoplasmic reticulum (ER) stress in beta cells (74). It is well known that cytokines and other cytolytic components can induce beta cell stress and death (108). In addition, these factors may also lead to alterations in the normal trafficking pathways of the islet antigens resulting in their release in the extracellular space. The main target autoantigens in the human disease, insulin, proinsulin, GAD65, ZnT8 and IA-2, are proteins expressed in pancreatic beta cells. Except for insulin that is released by exocytosis of secretory granules, the other target autoantigens are intracellular membrane proteins, thus potentially not visible by the immune system (15). The mechanisms underlying how these antigens can be recognized by the immune system, taken up by APCs and presented to self-reactive T cells are not clarified yet.

The present PhD thesis results from the combination of three scientific manuscripts, whose overall purpose is the identification of the possible mechanisms underlying the development of autoimmunity in T1D.

The first manuscript presented here is the description of a novel methodology for culturing monolayers of pancreatic endocrine cells dissociated from human and rat islets of Langerhans. Inspired by culture techniques normally applied to neurons (with which endocrine islet cells share many similarities), we were able to overcome the difficulties in obtaining high-quality monolayers of dissociated islet cells, thus allowing the application of high resolution imaging techniques and the visualization of intracellular biological phenomena with un unprecedented level of clarity and resolution. This procedure made possible most of the observations reported in the subsequent two manuscripts reported here.

In the second publication, we show that ER stress induced by pro-inflammatory factors or saturated fatty acids leads to a block in the palmitoylation cycle of the antigen GAD65 and a consequent accumulation of the palmitoylated form of this protein in Golgi membranes. The palmitoylated form of GAD65 is highly immunogenic and can stimulate a stronger activation of GAD65-specific T cells compared to the form not carrying this post-translation modification. In addition, accumulation of GAD65 in Golgi membranes seems to occur in humans during T1D, as demonstrated by direct observation on human beta cells in pancreatic sections from both GAD65-autoantibody positive individuals right before the onset of the disease and in T1D patients with ongoing T cell infiltration in the islets.

The third manuscript, which constitutes the core of my thesis project, illustrates a possible mechanism by which intracellular beta cells antigens, such as GAD65, IA-2 and proinsulin, might be released in extracellular vesicles, especially exosomes, and consequently become potential target of the immune system. The route of antigen release seems to involve an exosomal pathway originating from the *trans*-Golgi network (TGN). Once released, such exosomes can be taken up by APCs resulting in their activation. In addition, cell stress induced by pro-inflammatory cytokines increases the release of islet-exosomes and fosters the association of pro-inflammatory ER proteins with the autoantigens, conditions that overall could potentially contribute to the initiation of autoimmunity.

We also adopted bioengineering approaches to design exosome-mimetic liposomes carrying relevant features of pancreatic islet-derived exosomes. Using this platform, we were able to show that the activation of autoantigen-specific T cells is about 50 times stronger when antigens, such as GAD65, are associated to exosome-like structures compared to when they are present in the extracellular space in the form of free proteins.

## 1.3 REFERENCES

1. Lehuen A, Diana J, Zaccone P, Cooke A. Immune cell crosstalk in type 1 diabetes. Nat Rev Immunol 2010;10(7):501–13
2. van Belle TL, Coppieters KT, von Herrath MG. Type 1 diabetes: etiology, immunology, and therapeutic strategies. Physiol Rev 2011;91(1):79–118
3. Moustakas AK, van de Wal Y, Routsias J, Kooy YM, van Veelen P, Drijfhout JW, et al. Structure of celiac disease-associated HLA-DQ8 and non-associated HLA-DQ9 alleles in complex with two disease-specific epitopes. Int Immunol 2000;12(8):1157–66
4. Singal DP, Green D, Reid B, Gladman DD, Buchanan WW. HLA-D region genes and rheumatoid arthritis (RA): importance of DR and DQ genes in conferring susceptibility to RA. Ann Rheum Dis 1992;51(1):23–8
5. Zhang L, Eisenbarth GS. Prediction and prevention of Type 1 diabetes mellitus. J Diabetes 2011;3(1):48–57
6. Reijonen H, Novak EJ, Kochik S, Heninger A, Liu AW, Kwok WW, et al. Detection of GAD65-specific T-cells by major histocompatibility complex class II tetramers in type 1 diabetic patients and at-risk subjects. Diabetes 2002;51(5):1375–82
7. Coppieters KT, Dotta F, Amirian N, Campbell PD, Kay TWH, Atkinson MA, et al. Demonstration of islet-autoreactive CD8 T cells in insulitic lesions from recent onset and long-term type 1 diabetes patients. J Exp Med 2012;209(1):51–60
8. Palmer JP, Asplin CM, Clemons P, Lyen K, Tatpati O, Raghu PK, et al. Insulin antibodies in insulin-dependent diabetics before insulin treatment. Science 1983;222(4630):1337–9
9. Baekkeskov S, Aanstoot HJ, Christgau S, Reetz A, Solimena M, Cascalho M, et al. Identification of the 64K autoantigen in insulin-dependent diabetes as the GABA-synthesizing enzyme glutamic acid decarboxylase. Nature 1990;347(6289):151–6
10. Wenzlau JM, Juhl K, Yu L, Moua O, Sarkar SA, Gottlieb P, et al. The cation efflux transporter ZnT8 (Slc30A8) is a major autoantigen in human type 1 diabetes. Proc Natl Acad Sci U S A 2007;104(43):17040–5
11. Bonifacio E, Lampasona V, Bingley PJ. IA-2 (islet cell antigen 512) is the primary target of humoral autoimmunity against type 1 diabetes-associated tyrosine phosphatase autoantigens. J Immunol 1998;161(5):2648–54
12. Baekkeskov S, Nielsen JH, Marner B, Bilde T, Ludvigsson J, Lernmark A. Autoantibodies in newly diagnosed diabetic children immunoprecipitate human pancreatic islet cell proteins. Nature 1982;298(5870):167–9
13. Baekkeskov S, Landin M, Kristensen JK, Srikanta S, Bruining GJ, Mandrup-Poulsen T, et al. Antibodies to a 64,000 Mr human islet cell antigen precede the clinical onset of insulin-dependent diabetes. J Clin Invest 1987;79(3):926–34
14. Payton MA, Hawkes CJ, Christie MR. Relationship of the 37,000- and 40,000-M(r) tryptic fragments of islet antigens in insulin-dependent diabetes to the protein tyrosine phosphatase-like molecule IA-2 (ICA512). J Clin Invest 1995;96(3):1506–11
15. Arvan P, Pietropaolo M, Ostrov D, Rhodes CJ. Islet autoantigens: structure, function, localization, and regulation. Cold Spring Harb Perspect Med 2012;2(8):a007658
16. Velloso LA, Kämpe O, Hallberg A, Christmanson L, Betsholtz C, Karlsson FA. Demonstration of GAD-65 as the main immunogenic isoform of glutamate decarboxylase in type 1 diabetes and determination of autoantibodies using a radioligand produced by eukaryotic expression. J Clin Invest 1993;91(5):2084–90
17. Wang C, Mao R, Van de Casteele M, Pipeleers D, Ling Z. Glucagon-like peptide-1 stimulates GABA formation by pancreatic beta-cells at the level of glutamate decarboxylase. Am J Physiol Endocrinol Metab 2007;292(4):E1201-6

18. Battaglioli G, Liu H, Martin DL. Kinetic differences between the isoforms of glutamate decarboxylase: implications for the regulation of GABA synthesis. J Neurochem 2003;86(4):879–87

19. Fenalti G, Buckle AM. Structural biology of the GAD autoantigen. Autoimmun Rev 2010;9(3):148–52

20. Ronkainen MS, Hoppu S, Korhonen S, Simell S, Veijola R, Ilonen J, et al. Early epitope- and isotype-specific humoral immune responses to GAD65 in young children with genetic susceptibility to type 1 diabetes. Eur J Endocrinol 2006;155(4):633–42

21. Atkinson MA. The pathogenesis and natural history of type 1 diabetes. Cold Spring Harb Perspect Med 2012;2(11)

22. Serreze D V, Silveira PA. The role of B lymphocytes as key antigen-presenting cells in the development of T cell-mediated autoimmune type 1 diabetes. Curr Dir Autoimmun 2003;6:212–27

23. Jaume JC, Parry SL, Madec A-M, Sønderstrup G, Baekkeskov S. Suppressive effect of glutamic acid decarboxylase 65-specific autoimmune B lymphocytes on processing of T cell determinants located within the antibody epitope. J Immunol 2002;169(2):665–72

24. Fenalti G, Hampe CS, Arafat Y, Law RHP, Banga JP, Mackay IR, et al. COOH-terminal clustering of autoantibody and T-cell determinants on the structure of GAD65 provide insights into the molecular basis of autoreactivity. Diabetes 2008;57(5):1293–301

25. Sorenson RL, Garry DG, Brelje TC. Structural and functional considerations of GABA in islets of Langerhans. Beta-cells and nerves. Diabetes 1991;40(11):1365–74

26. Uchizono Y, Alarcón C, Wicksteed BL, Marsh BJ, Rhodes CJ. The balance between proinsulin biosynthesis and insulin secretion: where can imbalance lead? Diabetes Obes Metab 2007;9 Suppl 2:56–66

27. Christgau S, Aanstoot HJ, Schierbeck H, Begley K, Tullin S, Hejnaes K, et al. Membrane anchoring of the autoantigen GAD65 to microvesicles in pancreatic beta-cells by palmitoylation in the NH2-terminal domain. J Cell Biol 1992;118(2):309–20

28. Kanaani J, Patterson G, Schaufele F, Lippincott-Schwartz J, Baekkeskov S. A palmitoylation cycle dynamically regulates partitioning of the GABA-synthesizing enzyme GAD65 between ER-Golgi and post-Golgi membranes. J Cell Sci 2008;121(Pt 4):437–49

29. Kanaani J, Cianciaruso C, Phelps E a., Pasquier M, Brioudes E, Billestrup N, et al. Compartmentalization of GABA synthesis by GAD67 differs between pancreatic beta cells and neurons. PLoS One 2015;10(2):e0117130

30. Rewers M, Gottlieb P. Immunotherapy for the prevention and treatment of type 1 diabetes: human trials and a look into the future. Diabetes Care 2009;32(10):1769–82

31. Morran MP, Casu A, Arena VC, Pietropaolo S, Zhang Y-J, Satin LS, et al. Humoral autoimmunity against the extracellular domain of the neuroendocrine autoantigen IA-2 heightens the risk of type 1 diabetes. Endocrinology 2010;151(6):2528–37

32. Kubosaki A, Gross S, Miura J, Saeki K, Zhu M, Nakamura S, et al. Targeted disruption of the IA-2beta gene causes glucose intolerance and impairs insulin secretion but does not prevent the development of diabetes in NOD mice. Diabetes 2004;53(7):1684–91

33. Cai T, Hirai H, Zhang G, Zhang M, Takahashi N, Kasai H, et al. Deletion of Ia-2 and/or Ia-2β in mice decreases insulin secretion by reducing the number of dense core vesicles. Diabetologia 2011;54(9):2347–57

34. Peakman M, Stevens EJ, Lohmann T, Narendran P, Dromey J, Alexander A, et al. Naturally processed and presented epitopes of the islet cell autoantigen IA-2 eluted from HLA-DR4. J Clin Invest 1999;104(10):1449–57

35. Allen JS, Pang K, Skowera A, Ellis R, Rackham C, Lozanoska-Ochser B, et al. Plasmacytoid dendritic cells are proportionally expanded at diagnosis of type 1 diabetes and enhance islet autoantigen presentation to T-cells through immune complex capture. Diabetes 2009;58(1):138–45

36. Vafiadis P, Ounissi-Benkalha H, Palumbo M, Grabs R, Rousseau M, Goodyer CG, et al. Class III alleles of the variable number of tandem repeat insulin polymorphism associated with silencing of thymic insulin predispose to type 1 diabetes. J Clin Endocrinol Metab 2001;86(8):3705–10

37. Wong FS, Siew LK, Scott G, Thomas IJ, Chapman S, Viret C, et al. Activation of insulin-reactive CD8 T-cells for development of autoimmune diabetes. Diabetes 2009;58(5):1156–64

38. Eizirik DL, Colli ML, Ortis F. The role of inflammation in insulitis and beta-cell loss in type 1 diabetes. Nat Rev Endocrinol 2009;5(4):219–26

39. Toma A, Laïka T, Haddouk S, Luce S, Briand J-P, Camoin L, et al. Recognition of human proinsulin leader sequence by class I-restricted T-cells in HLA-A*0201 transgenic mice and in human type 1 diabetes. Diabetes 2009;58(2):394–402

40. Berg H, Walter M, Mauch L, Seissler J, Northemann W. Recombinant human preproinsulin. Expression, purification and reaction with insulin autoantibodies in sera from patients with insulin-dependent diabetes mellitus. J Immunol Methods 1993;164(2):221–31

41. Alleva DG, Crowe PD, Jin L, Kwok WW, Ling N, Gottschalk M, et al. A disease-associated cellular immune response in type 1 diabetics to an immunodominant epitope of insulin. J Clin Invest 2001;107(2):173–80

42. Congia M, Patel S, Cope AP, De Virgiliis S, Sønderstrup G. T cell epitopes of insulin defined in HLA-DR4 transgenic mice are derived from preproinsulin and proinsulin. Proc Natl Acad Sci U S A 1998;95(7):3833–8

43. Alleva DG, Maki RA, Putnam AL, Robinson JM, Kipnes MS, Dandona P, et al. Immunomodulation in Type 1 Diabetes by NBI-6024, an Altered Peptide Ligand of the Insulin B(9-23) Epitope. Scand J Immunol 2006;63(1):59–69

44. Walter M, Philotheou A, Bonnici F, Ziegler A-G, Jimenez R, NBI-6024 Study Group. No effect of the altered peptide ligand NBI-6024 on beta-cell residual function and insulin needs in new-onset type 1 diabetes. Diabetes Care 2009;32(11):2036–40

45. Thrower SL, James L, Hall W, Green KM, Arif S, Allen JS, et al. Proinsulin peptide immunotherapy in type 1 diabetes: report of a first-in-man Phase I safety study. Clin Exp Immunol 2009;155(2):156–65

46. Clemente-Casares X, Tsai S, Huang C, Santamaria P. Antigen-specific therapeutic approaches in Type 1 diabetes. Cold Spring Harb Perspect Med 2012;2(2):a007773

47. Chimienti F, Devergnas S, Pattou F, Schuit F, Garcia-Cuenca R, Vandewalle B, et al. In vivo expression and functional characterization of the zinc transporter ZnT8 in glucose-induced insulin secretion. J Cell Sci 2006;119(Pt 20):4199–206

48. Wenzlau JM, Juhl K, Yu L, Moua O, Sarkar SA, Gottlieb P, et al. The cation efflux transporter ZnT8 (Slc30A8) is a major autoantigen in human type 1 diabetes. Proc Natl Acad Sci U S A 2007;104(43):17040–5

49. Cauchi S, Del Guerra S, Choquet H, D'Aleo V, Groves CJ, Lupi R, et al. Meta-analysis and functional effects of the SLC30A8 rs13266634 polymorphism on isolated human pancreatic islets. Mol Genet Metab 2010;100(1):77–82

50. Wenzlau JM, Liu Y, Yu L, Moua O, Fowler KT, Rangasamy S, et al. A common nonsynonymous single nucleotide polymorphism in the SLC30A8 gene determines ZnT8 autoantibody specificity in type 1 diabetes. Diabetes 2008;57(10):2693–7

51. Pound LD, Sarkar SA, Benninger RKP, Wang Y, Suwanichkul A, Shadoan MK, et al. Deletion of the mouse Slc30a8 gene encoding zinc transporter-8 results in impaired insulin secretion. Biochem J 2009;421(3):371–6

52. Lemaire K, Ravier MA, Schraenen A, Creemers JWM, Van de Plas R, Granvik M, et al. Insulin crystallization depends on zinc transporter ZnT8 expression, but is not required for normal glucose homeostasis in mice. Proc Natl Acad Sci U S A 2009;106(35):14872–7

53. Fu Y, Tian W, Pratt EB, Dirling LB, Shyng S-L, Meshul CK, et al. Down-regulation of ZnT8 expression in INS-1 rat pancreatic beta cells reduces insulin content and glucose-inducible insulin secretion. PLoS One 2009;4(5):e5679

54. Smidt K, Larsen A, Brønden A, Sørensen KS, Nielsen J V, Praetorius J, et al. The zinc transporter ZNT3 co-localizes with insulin in INS-1E pancreatic beta cells and influences cell survival, insulin secretion capacity, and ZNT8 expression. Biometals 2016;29(2):287–98

55. Petersen AB, Smidt K, Magnusson NE, Moore F, Egefjord L, Rungby J. siRNA-mediated knock-down of ZnT3 and ZnT8 affects production and secretion of insulin and apoptosis in INS-1E cells. APMIS 2011;119(2):93–102

56. Ziegler A-G, Nepom GT. Prediction and pathogenesis in type 1 diabetes. Immunity 2010;32(4):468–78

57. Van Belle TL, Taylor P, von Herrath MG. Mouse Models for Type 1 Diabetes. Drug Discov Today Dis Models 2009;6(2):41–5

58. Stadinski BD, Delong T, Reisdorph N, Reisdorph R, Powell RL, Armstrong M, et al. Chromogranin A is an autoantigen in type 1 diabetes. Nat Immunol 2010;11(3):225–31

59. Kim J, Richter W, Aanstoot HJ, Shi Y, Fu Q, Rajotte R, et al. Differential expression of GAD65 and GAD67 in human, rat, and mouse pancreatic islets. Diabetes 1993;42(12):1799–808

60. Fugger L, Michie SA, Rulifson I, Lock CB, McDevitt GS. Expression of HLA-DR4 and human CD4 transgenes in mice determines the variable region beta-chain T-cell repertoire and mediates an HLA-DR-restricted immune response. Proc Natl Acad Sci U S A 1994;91(13):6151–5

61. Mathis D, Vence L, Benoist C. beta-Cell death during progression to diabetes. Nature 2001;414(6865):792–8

62. Eizirik DL, Miani M, Cardozo AK. Signalling danger: endoplasmic reticulum stress and the unfolded protein response in pancreatic islet inflammation. Diabetologia 2013;56(2):234–41

63. Todd DJ, Lee A-H, Glimcher LH. The endoplasmic reticulum stress response in immunity and autoimmunity. Nat Rev Immunol 2008;8(9):663–74

64. Engin F, Yermalovich A, Nguyen T, Ngyuen T, Hummasti S, Fu W, et al. Restoration of the unfolded protein response in pancreatic β cells protects mice against type 1 diabetes. Sci Transl Med 2013;5(211):211ra156

65. Fonseca SG, Burcin M, Gromada J, Urano F. Endoplasmic reticulum stress in beta-cells and development of diabetes. Curr Opin Pharmacol 2009;9(6):763–70

66. Scheuner D, Kaufman RJ. The unfolded protein response: a pathway that links insulin demand with beta-cell failure and diabetes. Endocr Rev 2008;29(3):317–33

67. Ladiges WC, Knoblaugh SE, Morton JF, Korth MJ, Sopher BL, Baskin CR, et al. Pancreatic beta-cell failure and diabetes in mice with a deletion mutation of the endoplasmic reticulum molecular chaperone gene P58IPK. Diabetes 2005;54(4):1074–81

68. Song B, Scheuner D, Ron D, Pennathur S, Kaufman RJ. Chop deletion reduces oxidative stress, improves beta cell function, and promotes cell survival in multiple mouse models of diabetes. J Clin Invest 2008;118(10):3378–89

69. Støy J, Edghill EL, Flanagan SE, Ye H, Paz VP, Pluzhnikov A, et al. Insulin gene mutations as a cause of permanent neonatal diabetes. Proc Natl Acad Sci U S A 2007;104(38):15040–4

70. Wang J, Takeuchi T, Tanaka S, Kubo SK, Kayo T, Lu D, et al. A mutation in the insulin 2 gene induces diabetes with severe pancreatic beta-cell dysfunction in the Mody mouse. J Clin Invest 1999;103(1):27–37

71. Størling J, Binzer J, Andersson AK, Züllig RA, Tonnesen M, Lehmann R, et al. Nitric oxide contributes to cytokine-induced apoptosis in pancreatic beta cells via potentiation of JNK activity and inhibition of Akt. Diabetologia 2005;48(10):2039–50

72. Cardozo AK, Ortis F, Storling J, Feng Y-M, Rasschaert J, Tonnesen M, et al. Cytokines downregulate the sarcoendoplasmic reticulum pump Ca2+ ATPase 2b and deplete endoplasmic reticulum Ca2+, leading to induction of endoplasmic reticulum stress in pancreatic beta-cells. Diabetes 2005;54(2):452–61

73. Chambers KT, Unverferth JA, Weber SM, Wek RC, Urano F, Corbett JA. The role of nitric oxide and the unfolded protein response in cytokine-induced beta-cell death. Diabetes 2008;57(1):124–32

74. Tersey SA, Nishiki Y, Templin AT, Cabrera SM, Stull ND, Colvin SC, et al. Islet β-cell endoplasmic reticulum stress precedes the onset of type 1 diabetes in the nonobese diabetic mouse model. Diabetes 2012;61(4):818–27

75. Marhfour I, Lopez XM, Lefkaditis D, Salmon I, Allagnat F, Richardson SJ, et al. Expression of endoplasmic reticulum stress markers in the islets of patients with type 1 diabetes. Diabetologia 2012;55(9):2417–20

76. Bernales S, Papa FR, Walter P. Intracellular signaling by the unfolded protein response. Annu Rev Cell Dev Biol 2006;22:487–508

77. McLaughlin RJ, Spindler MP, van Lummel M, Roep BO. Where, How, and When: Positioning Posttranslational Modification Within Type 1 Diabetes Pathogenesis. Curr Diab Rep 2016;16(7):63

78. Sileno S, D'Oria V, Stucchi R, Alessio M, Petrini S, Bonetto V, et al. A possible role of transglutaminase 2 in the nucleus of INS-1E and of cells of human pancreatic islets. J Proteomics 2014;96:314–27

79. McLaughlin RJ, de Haan A, Zaldumbide A, de Koning EJ, de Ru AH, van Veelen PA, et al. Human islets and dendritic cells generate post-translationally modified islet autoantigens. Clin Exp Immunol 2016;185(2):133–40

80. van Lummel M, Duinkerken G, van Veelen PA, de Ru A, Cordfunke R, Zaldumbide A, et al. Posttranslational modification of HLA-DQ binding islet autoantigens in type 1 diabetes. Diabetes 2014;63(1):237–47

81. Vomund AN, Zinselmeyer BH, Hughes J, Calderon B, Valderrama C, Ferris ST, et al. Beta cells transfer vesicles containing insulin to phagocytes for presentation to T cells. Proc Natl Acad Sci U S A 2015;112(40):E5496-502

82. Foulquier C, Sebbag M, Clavel C, Chapuy-Regaud S, Al Badine R, Méchin M-C, et al. Peptidyl arginine deiminase type 2 (PAD-2) and PAD-4 but not PAD-1, PAD-3, and PAD-6 are expressed in rheumatoid arthritis synovium in close association with tissue inflammation. Arthritis Rheum 2007;56(11):3541–53

83. McGinty JW, Chow I-T, Greenbaum C, Odegard J, Kwok WW, James EA. Recognition of posttranslationally modified GAD65 epitopes in subjects with type 1 diabetes. Diabetes 2014;63(9):3033–40

84. Rondas D, Crèvecoeur I, D'Hertog W, Ferreira GB, Staes A, Garg AD, et al. Citrullinated glucose-regulated protein 78 is an autoantigen in type 1 diabetes. Diabetes 2015;64(2):573–86

85. Théry C, Ostrowski M, Segura E. Membrane vesicles as conveyors of immune responses. Nat Rev Immunol 2009;9(8):581–93

86. Rahman MJ, Regn D, Bashratyan R, Dai YD. Exosomes released by islet-derived mesenchymal stem cells trigger autoimmune responses in NOD mice. Diabetes 2014;63(3):1008–20

87. Choi D-S, Kim D-K, Kim Y-K, Gho YS. Proteomics, transcriptomics and lipidomics of exosomes and ectosomes. Proteomics 2013;13(10–11):1554–71

88. Robbins PD, Morelli AE. Regulation of immune responses by extracellular vesicles. Nat Rev Immunol 2014;14(3):195–208

89. Zitvogel L, Regnault A, Lozier A, Wolfers J, Flament C, Tenza D, et al. Eradication of established murine tumors using a novel cell-free vaccine: dendritic cell derived exosomes. Nat Med 1998;4(5):594–600

90. Sheng H, Hassanali S, Nugent C, Wen L, Hamilton-Williams E, Dias P, et al. Insulinoma-released exosomes or microparticles are immunostimulatory and can activate autoreactive T cells spontaneously developed in nonobese diabetic mice. J Immunol. 2011;187(4):1591–600.

91. Bashratyan R, Sheng H, Regn D, Rahman MJ, Dai YD. Insulinoma-released exosomes activate autoreactive marginal zone-like B cells that expand endogenously in prediabetic NOD mice. Eur J Immunol 2013;43(10):2588–97

92. Rahman MJ, Regn D, Bashratyan R, Dai YD. Exosomes released by islet-derived mesenchymal stem cells trigger autoimmune responses in NOD mice. Diabetes 2014;63(3):1008–20

93. György B, Szabó TG, Pásztói M, Pál Z, Misják P, Aradi B, et al. Membrane vesicles, current state-of-the-art: emerging role of extracellular vesicles. Cell Mol Life Sci 2011;68(16):2667–88

94. Baroni M, Pizzirani C, Pinotti M, Ferrari D, Adinolfi E, Calzavarini S, et al. Stimulation of P2 (P2X7) receptors in human dendritic cells induces the release of tissue factor-bearing microparticles. FASEB J 2007;21(8):1926–33

95. Leroyer AS, Tedgui A, Boulanger CM. Role of microparticles in atherothrombosis. J Intern Med 2008;263(5):528–37

96. MacKenzie A, Wilson HL, Kiss-Toth E, Dower SK, North RA, Surprenant A. Rapid secretion of interleukin-1beta by microvesicle shedding. Immunity 2001;15(5):825–35

97. Giusti I, D'Ascenzo S, Millimaggi D, Taraboletti G, Carta G, Franceschini N, et al. Cathepsin B mediates the pH-dependent proinvasive activity of tumor-shed microvesicles. Neoplasia 2008;10(5):481–8

98. Beyer C, Pisetsky DS. The role of microparticles in the pathogenesis of rheumatic diseases. Nat Rev Rheumatol 2010;6(1):21–9

99. Bergsmedh A, Szeles A, Henriksson M, Bratt A, Folkman MJ, Spetz AL, et al. Horizontal transfer of oncogenes by uptake of apoptotic bodies. Proc Natl Acad Sci U S A 2001;98(11):6407–11

100. Holmgren L, Szeles A, Rajnavölgyi E, Folkman J, Klein G, Ernberg I, et al. Horizontal transfer of DNA by the uptake of apoptotic bodies. Blood 1999;93(11):3956–63

101. Bellone M, Iezzi G, Rovere P, Galati G, Ronchetti A, Protti MP, et al. Processing of engulfed apoptotic bodies yields T cell epitopes. J Immunol 1997;159(11):5391–9

102. Cocca BA, Cline AM, Radic MZ. Blebs and apoptotic bodies are B cell autoantigens. J Immunol 2002;169(1):159–66

103. Palmisano G, Jensen SS, Le Bihan M-C, Lainé J, McGuire JN, Pociot F, et al. Characterization of membrane-shed microvesicles from cytokine-stimulated β-cells using proteomics strategies. Mol Cell Proteomics 2012;11(8):230–43

104. Kooijmans SAA, Vader P, van Dommelen SM, van Solinge WW, Schiffelers RM. Exosome mimetics: a novel class of drug delivery systems. Int J Nanomedicine 2012;7:1525–41

105. Malam Y, Loizidou M, Seifalian AM. Liposomes and nanoparticles: nanosized vehicles for drug delivery in cancer. Trends Pharmacol Sci 2009;30(11):592–9

106. Marcus ME, Leonard JN. FedExosomes: Engineering Therapeutic Biological Nanoparticles that Truly Deliver. Pharmaceuticals (Basel) 2013;6(5):659–80

107.   Toyoda H, Formby B, Magalong D, Redford A, Chan E, Takei S, et al. In situ islet cytokine gene expression during development of type I diabetes in the non-obese diabetic mouse. Immunol Lett 1994;39(3):283–8

108.   Turley S, Poirot L, Hattori M, Benoist C, Mathis D. Physiological beta cell death triggers priming of self-reactive T cells by dendritic cells in a type-1 diabetes model. J Exp Med 2003;198(10):1527–37

# CHAPTER 2

# Advances in pancreatic islet monolayer culture permit super-resolution microscopy and reveal a cilia-centric mechanism of beta cell proliferation

Adapted from the original manuscript

Edward A. Phelps*, Chiara Cianciaruso*, Jaime Santo-Domingo, Miriella Pasquier, Gabriele Galliverti, Lorenzo Piemonti, Ekaterine Berishvili, Andreas Wiederkehr, Jeffrey A. Hubbell, Steinunn Baekkeskov

* These authors contributed equally to this work

## 2.1  ABSTRACT

The field of islet cell biology has been hampered by insufficient techniques to culture monolayers of primary islet cells on glass coverslips for study by light microscopy. Guided by an observation that dispersed islet cells spread and adhere well on surfaces in neuronal co-culture, we demonstrate that in the absence of neurons, well-defined surface coatings combined with components of neuronal culture media collectively support robust monolayers of primary human or rat islet cells on glass surfaces. The resultant islet cell monolayers stably maintain endocrine cell phenotype and exhibit glucose-sensitive calcium signaling similar to whole islets. This technical advance enabled detailed observation of sub-cellular processes in primary human and rat islet cells by super-resolution and live-cell light microscopy. The protocol is broadly applicable to obtaining novel biological insights as demonstrated by our identification of a mechanism to control proliferation in primary beta cells through growth and disassembly of primary cilia.

## 2.2  INTRODUCTION

Light microscopy is a cornerstone of cell biology facilitating the understanding of how cells function. Powerful staining methods permit the labeling of specific molecules within live and fixed cells and the emergence of super-resolution techniques continue to push the boundaries of scientific discovery through light microscopy. Yet, applications of the latest advanced imaging techniques in the field of pancreatic islet biology have been hampered by the limitations of resolving sub-organelle level structures in intact islets and an inability to culture dissociated primary islet cells on the surface of glass coverslips (1-3). Imaging targets in close proximity to the surface of glass coverslips are a general requirement for visualization with high power objectives. Super-resolution microscopy techniques (4) such as stimulated emission depletion (STED) microscopy, which permit the sub-diffraction limit discernment of biological structures, require cells to be grown on 0.17 mm glass coverslips for optimal performance and are incompatible with plastic substrates. While cell lines derived from pancreatic endocrine tumors such as INS-1 (5) and MIN6 (6) are amenable for culturing on glass, they have lost many of the characteristics of primary beta cells. A robust method enabling generation of primary islet cell monolayers on glass, particularly from human islets, would represent a major advancement for high-resolution light microscopy studies of islet cells and allow detailed imaging of subcellular activities such as insulin granule secretion, calcium signaling, mitochondrial function or cytoskeletal dynamics.

Previous efforts to generate two-dimensional cultures of dispersed primary islet cells include surface coatings of extracellular matrix (ECM) secreted from 804G rat bladder carcinoma cells (2,3,7), HTB-9 human bladder carcinoma cells (3,8,9), A-431 human epidermoid carcinoma cells (10), and bovine corneal epithelial cell matrix (BCEM) (3,10,11). While somewhat effective for promoting primary islet cell adhesion on tissue-culture treated plastic surfaces, these cell-line ECMs do not permit sufficient islet cell adhesion on glass surfaces, particularly when islet cells are

cultured in traditional islet media. In addition, cell-line derived ECMs have a high batch to batch variability and are sub-optimal for sensitive biological studies of single islet cells as they are poorly characterized and have been shown to promote de-differentiation of beta cells (9,12).

Pancreatic islet endocrine cells display a protruding primary cilium proposed to play a role in glucose homeostasis, insulin signaling and risk of developing type 2 diabetes (13). Primary cilia act as major hubs for cell signaling, cell differentiation, and cell polarity. Disassembly of primary cilia precedes entry into the cell cycle for many cell types (14,15). Islet beta cells are mainly quiescent and identification of a protocol to promote proliferation and expand beta cell mass in vitro for treatment of diabetes is a major goal (16). Intriguingly, factors reported to induce proliferation of insulin-producing beta cells such as increased Wnt/beta-catenin signaling (17,18), Rho Kinase (ROCK) inhibition (18) and overexpression of Aurora Kinase A (19) are also implicated in pathways controlling primary cilia function, formation and/or disassembly. In mouse embryonic fibroblasts ciliary disassembly leads to nuclear translocation of beta-catenin and activation of transcription factors responsible for cell cycle progression, while the presence of primary cilia restrains Wnt/beta-catenin signaling (20). ROCK inhibition leads to cilia resorption through promoting cytoskeletal rearrangements, basal body repositioning and centrosome splitting (21,22). Furthermore, the beta cell mitogenic protein Aurora Kinase A stimulates cell cycle progression by specifically mediating cilia disassembly in multiple cell types (14,23).

In this study, we show that defined surface coatings of collagen IV or laminin combined with a cell culture medium with features formulated for primary neurons promotes superior adhesion, spreading and viability of human and rat islet cell monolayers respectively while retaining key features of differentiated islet endocrine cells. Analyses of such monolayer cultures of primary islet cells on glass by high resolution microscopy enabled visibility of cilia expression and length on primary beta

cells and the identification of a mechanistic correlation between disassembly of primary cilia and stimulation of beta cell proliferation.

## 2.3 METHODS

### 2.3.1 Islet isolation and culture

Rat islets were isolated from pancreases of P5 Sprague Dawley rats (Charles River) as previously described (11) except using Liberase TL (Roche) for pancreas digestion. Hand-picked islets were cultured at 37°C in 10 cm non-adherent cell culture dishes (500 islets/dish) in islet basal medium: RPMI 1640 medium with GlutaMAX (Gibco), 11 mM glucose, 10% fetal bovine serum (FBS). One-percent Penicillin/Streptomycin was added to the islet basal medium for whole islet culture but not for islet cell monolayer culture.

Human pancreatic islets were obtained through the European Consortium on Islet Transplantation, (ECIT), Islets for Basic Research Program. Human islets were cultured at 24°C in 10 cm non-adherent cell culture dishes (500 islets/dish) in CMRL medium with 2% glutamine, 10% FBS, 10 mM HEPES and 1% Penicillin/Streptomycin. Human islets used in this study were obtained from three normal non-diabetic donors, two male and one female, ranging in age 18-59 years with a body mass index of 20-29 kg/m$^2$.

### 2.3.2 Co-culture of islet cells and neurons

Primary rat hippocampal neurons were prepared from P2-P3 Sprague Dawley rats, as described by Codazzi et al. (24). Neurons were seeded on round poly-L-ornithine-coated glass or Thermanox coverslips (Nunc), at 100,000 cells per coverslip in a 24-well plate and in 1 ml of neuronal medium: Minimum essential medium (MEM) with GlutaMAX (Gibco), 11 mM glucose, 5% FBS, 1 mM sodium

pyruvate, 10 mM HEPES and 1X B-27 Supplement (25) (Gibco). One day after isolation, 3 µM of the chemotherapeutic agent ARA-C (Sigma-Aldrich) was added to the culture medium to eliminate astrocytes and obtain a neuronal culture of high purity (> 90% neurons). Three-four days after preparation of a neuronal culture, without changing the medium, a suspension of either human or rat islet cells was prepared as described below, and 50,000 islet cells in 50 µL of neuronal medium were added per well to the established neurons.

### 2.3.3  Preparation of matrix-coated coverslips

Lab-Tek 4-well Chambered Coverglass (Nunc, Thermo Fisher Scientific) were used for live/dead cell staining. Round 12 mm diameter and 0.17 mm thickness borosilicate glass coverslips (Electron Microscopy Sciences) were used for immunofluorescence staining. Coverglass-bottom Fluorodishes (World Precision Instruments) and MatTek dishes (MatTek Corporation) were used for live cell imaging experiments. Glass surfaces were coated with purified laminin (Gibco) or purified collagen IV (Sigma Aldrich) at 50 µg/ml in HBSS with $Ca^{2+}/Mg^{2+}$ for 1 hour at 37°C, then washed 3x in HBSS with $Ca^{2+}/Mg^{2+}$. HTB-9 matrix was generated from HTB-9 human bladder carcinoma cells (ATCC) grown to 95% confluence, lysed with 20 mM $NH_4OH$ + 0.5% Triton X-100 in pyrogen-free water, followed by three washes in pyrogen-free water. Coverslips were also prepared with Poly-L-ornithine coating (400 µg/ml).

### 2.3.4  Preparation of human and rat islet cell monolayer cultures

Within one week of isolation, rat or human islets were hand-picked from suspension cultures, collected in a 15 ml tube and washed twice in PBS without $Ca^{2+}$ and $Mg^{2+}$ (Gibco). Islets were dissociated into a suspension of single islet cells by continuous gentle pipetting in 0.3 ml 0.05% trypsin-EDTA (Gibco) per 500 islets for 3

minutes at 37°C. Trypsin digestion was halted by adding neuronal or islet basal medium to a total volume of 15 ml, followed by pelleting of islet cells by centrifugation for 5 min at 800 rpm (47 x g) and resuspension in neuronal or islet basal medium. Islet cells were seeded on matrix-coated surfaces at approximately 35,000 cells/cm$^2$ in neuronal medium for all experiments except for groups indicated as seeded in islet basal medium. Islet cells required 3-4 days of culture to adhere and spread on surfaces before further experimentation. While typically not necessary, elimination of fibroblast like cells in human islet cell monolayer cultures maintained for 7 days or longer, could be achieved by adding 3 µM of ARA-C to the culture medium one day after islet cell seeding. ARA-C was used for establishing the neuronal cultures seeded with islet cells in Figure 1 and for islet cell monolayer cultures shown in Supplementary Figure 1.

### 2.3.5 Live / dead cell staining

Calcein AM (2 µM), ethidium homodimer-1 (4 µM) and Hoechst 33342 (8 µM) (Molecular Probes) were added directly to cell monolayers without removing culture media to avoid removal of non-adherent cells. Cells were incubated for 30 minutes at room temperature and imaged live with a Zeiss LSM700 confocal microscope with 20x/0.8 NA Plan-Apochromat air objective. Analyses of cell adhesion, spreading and viability were performed in ImageJ (26).

### 2.3.6 Immunofluorescence staining

Human pancreas sections obtained from the Network for Pancreatic Organ Donors with Diabetes (nPOD case ID #6174 and 6230) were deparaffinized followed by acidic-pH heat-mediated antigen retrieval according to the nPOD standard operating procedure for immunopathology (27). Whole islets, monolayers of pancreatic islet cells and co-cultures of islet cells and neurons were fixed with 4%

EM-grade PFA (Electron Microscopy Sciences) at room temperature for 20 minutes or 1 hour, respectively. Samples were blocked and permeabilized in PBS + 0.3% Triton X-100 with 10% goat or donkey serum. Primary antibodies were incubated overnight at 4°C. Alexa Fluor 405, 488, 568, and 647 conjugated secondary antibodies (Molecular Probes) were incubated at 1:200 dilution in 0.3% Triton X-100 in PBS for 30 minutes at room temperature. Coverslips were mounted with ProLong Gold Antifade Reagent (Molecular Probes). Immunostained whole islets were handled in 1.5 ml Eppendorf tubes by centrifugation between immunostaining steps and mounted beneath glass coverslips.

For alpha-tubulin staining, cells were washed in 37°C PHEM buffer (60 mM PIPES, 25 mM HEPES, 10 mM EGTA, 4 mM $MgSO_4$), fixed for 10 min at 37°C in 3.2% EM-grade PFA (Electron Microscopy Sciences) with 0.05% EM-grade glutaraldehyde (Electron Microscopy Sciences), washed three times with PBS and permeabilized for 15 min with 0.3% TX-100 in PBS. Unreacted aldehydes were quenched by 3 x 10 min washes with 1 mg/mL sodium borohydride in PBS. Immunostaining was performed as above.


### 2.3.7  Microscopy

Standard confocal microscopy was performed on multi-color immunostained samples on a Zeiss LSM700 confocal microscope with 20x/0.8 NA Plan-Apochromat air, 40x/1.30 and 63x/1.40 NA Plan-Apochromat oil-immersion objectives.

Super-resolution microscopy was performed on rat and human islet cell monolayers cultured on laminin (for rat) or collagen IV (for human) coated 0.17 mm thickness glass coverslips. Cells were immunostained for insulin detected with Alexa Fluor 488 secondary antibody and alpha tubulin detected with Alexa Fluor 532 secondary antibody; or stained for actin with Alexa Fluor 488 phalloidin (Molecular Probes). STED super-resolution microscopy was performed on Leica TCS SP5

STED CW white light laser (WLL) and Leica SP8 STED 3X microscopes with HC PL APO 100x/1.40 NA oil immersion objectives, 488 nm WLL excitation line with 592 nm depletion laser or 532 nm WLL excitation line with 660 nm depletion laser, Hybrid detector (HyD) with timing gate 1.0-6.5 ns, and with 21 nm/pixel xy resolution. Images were processed and measured in ImageJ (26).

3D-SIM microscopy was performed on a Nikon N-SIM configured Nikon Eclipse Ti inverted microscope with Apochromat total internal reflection fluorescence (TIRF) 100x/1.49 NA objective and electron-multiplying charge-coupled device camera (EMCCD, IXON3; Andor Technology) at 512 x 512 pixels with 63 nm/pixel resolution in the x,y coordinates and 60 nm/voxel resolution in the z coordinate. Super-resolution images were reconstructed using built-in algorithms of NIS-Elements software (28). Reconstruction parameters were: contrast 0.70; apodization 1.00; and Widh3DFilter 0.20.

Live-cell imaging of insulin granule motility was measured in rat islet cell monolayers transfected with pVenus-N1-NPY plasmid (NPY-Venus) (29,30) plasmid using Lipofectamine 2000 (Invitrogen). Twenty-four hours after transfection, 1-5 minute time-lapse videos with 730 ms temporal resolution were captured during static incubation in KREBS buffer with 2 mM or 11 mM glucose, on a Leica TCS SP5 WLL microscope with HCX PL APO CS 100x/1.46 NA oil immersion objective. Automated particle-tracking analysis and diffusivity constant calculations were performed on 60 s clips from each time-lapse video using the Mosaic Particle Tracker 2D plugin (31) for ImageJ.

Cytosolic $Ca^{2+}$ was measured in monolayer cultures of rat islet cells transduced with adenovirus encoding the Cameleon ratiometric $Ca^{2+}$ sensor $YC3.6_{cyto}$ (32) under the control of the rat insulin promoter ($Ad\text{-}RIP\text{-}YC3.6_{cyto}$) (33). Rat islet cells, cultured for four days in neuronal medium on laminin-coated MatTek dishes, were infected with $3\times10^6$ infectious units (IFU) $Ad\text{-}RIP\text{-}YC3.6_{cyto}$ adenovirus for 24h at 37°C. Two days after infection, rat islet cell monolayers were washed 4 times in Krebs-Ringer

bicarbonate HEPES buffer (KRBH): 140 mM NaCl, 3.6 mM KCl, 0.5 mM $NaH_2PO_4$,

0.5 mM $MgSO_4$, 1.5 mM $CaCl_2$, 10 mM HEPES, 5 mM $NaHCO_3$, 2.5 mM glucose, pH

7.4. Calcium imaging was performed in a thermostatic chamber at 37°C on a

DMI6000 B inverted fluorescence microscope with HCX PL APO 40x/1.30 NA oil

immersion objective (Leica), Evolve 512 EMCCD (Photometrics), BP436/20 nm

excitation filter, and BP480/40 nm and BP535/30 nm emission filters. Small volumes

of concentrated solutions were added by hand to cells in KRBH at the given time

points to produce a final concentration of 16.7 mM glucose, 100 μM diazoxide, or 35

mM KCl. Fluorescence ratios were calculated in MetaFluor 7.0 (Meta Imaging

Series).

Counting of primary cilia in beta cells and analyses of cilia length were

performed on images acquired with a Leica DM5500B fluorescence microscope with

a 40x air objective. Analyses of beta cell density were performed on images captured

with Olympus Slide Scanner VS120-L100 with a 10x/0.40 UPLSAPO air objective.

For transmission electron microscopy (TEM), Co-cultures of islet cells with

neurons or whole rat islets were fixed in 2.5% glutaraldehyde / 2.0%

paraformaldehyde in 0.1 M phosphate buffer, pH 7.4 for 2 hours, washed with

cacodylate (0.1 M, pH 7.4), post-fixed for 40 min in 1.0 % osmium tetroxide, followed

by 40 min wash in 1% uranyl acetate in water, dehydrated through increasing

concentrations of alcohol and embedded in Durcupan ACM (Sigma Aldrich). Sections

(50 nm thickness) contrasted with lead citrate and uranyl acetate were imaged on a

Tecnai Spirit microscope with Eagle CCD camera (FEI Company).

### 2.3.8  Antibodies

The following unconjugated primary antibodies were used for

immunofluorescence staining: guinea pig anti-insulin (Linco 4011-01) 1:10,000 (for

STED and SIM microscopy); chicken anti-insulin (Abcam ab14042) 1:2000 (for multi-

color confocal microscopy); GAD6, a mouse monoclonal antibody specific for GAD65 (34) 1:1000; chicken anti-MAP2 (Abcam ab5392) 1:10,000; sheep anti-somatostatin (Abcam ab35425) 1:200; rabbit anti-pancreatic polypeptide (Abcam ab113694) 1:1000; rabbit anti-Ki67 (Abcam ab16667) 1:100; mouse anti-beta actin (Sigma A1978) 1:500; rabbit anti-calnexin (Abcam ab22595) 1:200; rabbit anti-alpha-tubulin (Abcam ab18251) 1:200; guinea-pig anti-PDX1 (Abcam ab47308) 1:2000; mouse anti-NKX6-1 (Developmental Studies Hybridoma Bank F55A12s) 1:6; mouse anti-acetylated alpha tubulin (Sigma T7451.) 1:1000; rabbit anti-pericentrin (Abcam ab4448) 1:5000.

### 2.3.9  Cilia-disassembly and beta cell proliferation

Neonatal rat islet monolayers were established during an initial 3-day culture period in complete neuronal medium with 11 mM glucose. To encourage cilia formation and growth, culture medium was replaced with serum and B-27-free neuronal medium containing 5.5 mM or 11 mM glucose for 36 hours. To induce cilia reabsorption and cell cycle progression following serum starvation, medium was replaced with complete neuronal medium containing 11 mM or 17 mM glucose and/or 15 µm ROCK inhibitor Y-27632 for 36 hours followed by fixation of cells in 4% EM-grade paraformaldehyde (PFA) for analysis.

### 2.3.10  Statistical analyses

Means among three or more groups were compared by analysis of variance (ANOVA) in GraphPad Prism 6 software. If deemed significant, Tukey's post-hoc pairwise comparisons were performed. Means between two groups were compared by Student $t$ test. A confidence level of 95% was considered significant. Statistical significance of the data is indicated as follows: * $P < 0.05$, ** $P < 0.01$, *** $P < 0.001$, ns no significant difference.

### 2.3.11 Ethical approval

Animals were used under EPFL animal regulation guidelines and an IACUC approved protocol. Human islets were received from the University Hospital of Geneva and San Raffaele Scientific Institute, Milan through the ECIT islets for basic research program and were approved by the Institutional Review Board of the University Hospital of Geneva (CER Nr. 05–028) and by the Ethics Committee of the San Raffaele Scientific Institute of Milan (IPF002-2014). Human pancreatic sections obtained via the nPOD tissue bank, University of Florida, Gainesville, FL, USA were harvested from cadaveric organ donors by certified organ procurement organizations partnering with nPOD in accordance with organ donation laws and regulations and classified as "Non-Human Subjects" by the University of Florida Institutional Review Board (35,36). EPFL grants permit for the use of human material as long as the provider can certify that the samples were obtained according to local laws and regulations, as well as good practices in the country were they were collected.

## 2.4 RESULTS

### 2.4.1 Co-culture of primary islet cells with primary hippocampal neurons

Pancreatic islets are innervated by the autonomic nervous system posing intriguing questions about the role of neuronal signaling in islet function and the possibility of sensory feedback of islet activities (37). We questioned whether co-culture with primary neurons would support the growth of monolayers of primary pancreatic islet cells. When islet cells derived from dispersed human or rat islets were seeded in minimum essential medium (MEM) containing 5% FBS and 2% B-27 medium supplement onto established cultures of rat neurons on glass coverslips, the seeded islet cells exhibited excellent cell adhesion and spreading **(Figure 1A)**, far surpassing the quality of islet cell monolayer cultures we had previously produced on HTB-9 or bovine corneal epithelial cell ECM (11). Islet cells seeded in neuronal culture medium on poly-ornithine coated glass but without neurons failed to adhere (**Figure 1B**). The islet cells cultured with neurons formed an interconnected network with readily apparent neuronal-islet cell contacts observed by immunostaining for insulin, the beta cell and GABA-ergic neuronal cell marker GAD65, and the neuronal cell marker MAP2 (**Figure 1C, D**). By transmission electron microscopy (TEM), we identified neuronal axons forming synapse-like structural interactions with islet endocrine cells, including insulin producing beta cells (**Figure 1E**). The islet-neuronal experiment, while raising intriguing questions for future studies of this system,

52

importantly established that conditions in the co-culture provided primary islet cells with adhesion and survival factors enabling high quality islet cell monolayers on glass substrates.
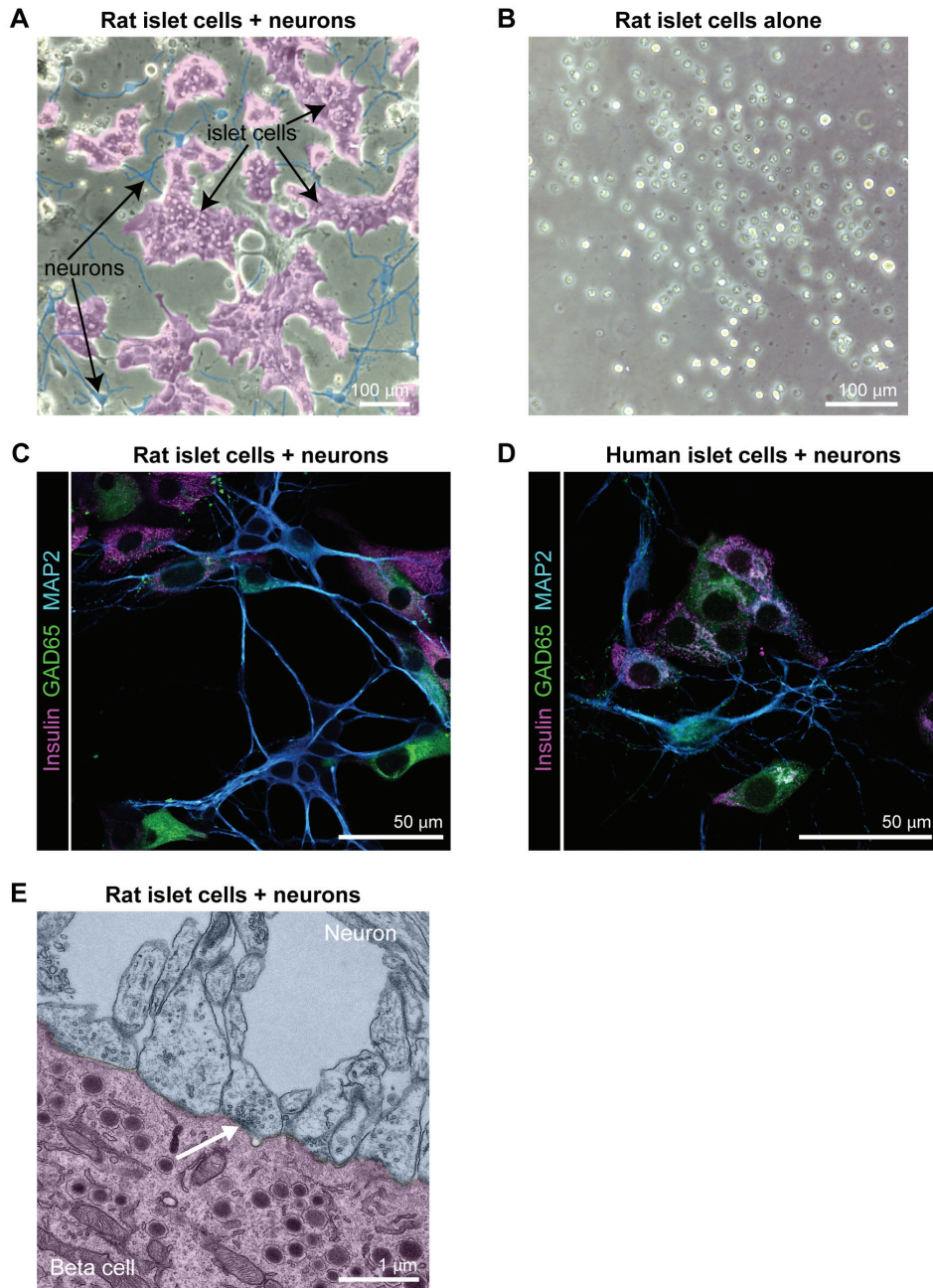


**Figure 1. Neuron and rat islet cell co-culture.**
(**A**) A representative transmitted light image of rat islet cells (magenta) co-cultured with rat neurons (blue) on polyornithine-coated coverslips in neuronal medium, pseudocoloring added to highlight cell types identified by morphology. (**B**) A Representative transmitted light image of rat islet cells seeded alone on polyornithine-coated coverslips in neuronal medium. (**C**) Co-culture of neurons and rat islet cells immunostained for insulin expressed in beta cells, GAD65 expressed in both beta cells and in the

soma and axons of GABA-ergic neurons, and MAP2 expressed in dendrites of all neurons. (**D**) Co-culture of neurons and human islet cells immunostained for insulin, expressed in beta cells, GAD65 expressed in beta cells and in the soma and axons of GABA-ergic neurons and MAP2 expressed in dendrites of all neuronal cells. (**E**) TEM image of rat islet cells co-cultured with rat neurons showing synapse-like cell junctions (arrow) between neuron (blue) containing synaptic vesicles and a beta cell (magenta) containing insulin granules, pseudo-coloring added to highlight cell types.

## 2.4.2  Monolayer primary islet cell culture in neuronal medium with defined surface-coating

We hypothesized that ECM deposited by the neuronal cultures could be a key factor enabling the impressive primary islet cell adhesion. Integrin subunit β1 is highly expressed in islet cells (1,10,38-41) and mediates islet cell-adhesion to laminin (42) and collagen IV (39) which are abundant in the ECM of native islets (43). We investigated the potential of purified laminin or collagen IV as a surface coating to replace neurons and the importance of culturing islet cells in medium formulated for primary neurons.

Glass coverslips were coated with laminin or collagen IV, followed by seeding single neonatal rat or adult human islet cells in either neuronal medium or islet basal medium. We also prepared uncoated coverslips and coverslips coated with polyornithine or HTB-9 matrix. Both human and rat islet cells required culture in neuronal medium for strong attachment and spreading, and failed to adhere to any glass surface coating when cultured in islet basal medium (**Figure 2**). When grown in neuronal medium, rat islet cells attached and spread well on both laminin and HTB-9 matrix but not on other surface coatings (**Figure 2A-D**). Rat islet cell density was 40% higher on laminin than on HTB-9 matrix. Laminin and HTB-9 matrix supported comparable levels of rat islet cell spreading. Viability of rat islet cells was high across all conditions. In contrast to rat islet cells, human islet cells grown in neuronal medium attached and spread best on collagen IV and did not adhere well to laminin (**Figure 2E-H**). Human islet cell spreading on HTB-9 matrix was higher than for the other conditions except for collagen IV, however human islet cell density on HTB-9

matrix was low. Neuronal medium promoted increased viability of human islet cells compared to islet basal medium on all surface coatings. The HTB-9 matrix promoted the attachment and proliferation of fibroblast-like cells, particularly from human islets. These fibroblast-like cells were also observed in low numbers in human islet cells cultured on collagen IV, but did not appear to interfere with endocrine cell attachment or survival. For long-term culture of human islet cell monolayers, it was possible to largely eliminate the fibroblast-like cells by adding the chemotherapeutic drug ARA-C to the culture medium (**Supplementary Figure 1**).
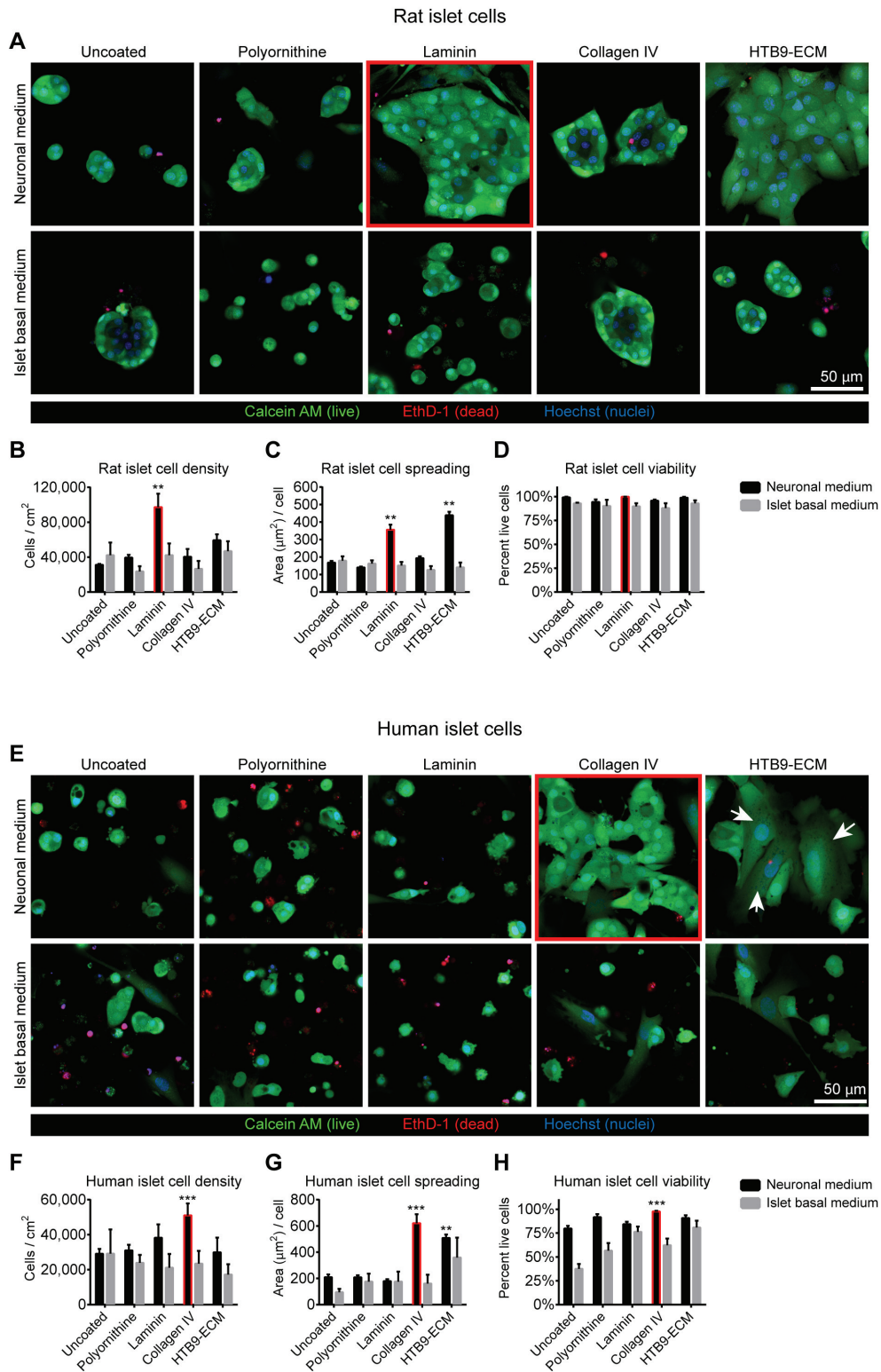
**Figure 2. Optimization of primary islet monolayer conditions.**

Monolayer cultures of rat (**A-D**) and human (**E-H**) islet cells 4 days after seeding onto glass coverslips with different coatings. (**A, E**) Representative confocal images of rat (**A**) and human (**E**) islet cells grown in neuronal media stained with calcein AM (live cells), ethidium homodimer 1 (dead cell nuclei) and counterstained by Hoechst 33342 (total nuclei). White arrows indicate fibroblast-like non endocrine cells.

(**B-D, F-H**) Quantification of islet cell density (**B, F**), islet cell spreading (**C, G**) and islet cell viability (**D, H**) for rat (**B-D**) and human (**F-H**) islet cells cultured in neuronal or islet basal media. Mean ± SEM ($n$ = 6 image random fields per condition). Statistical analysis by one-way ANOVA (** $p < 0.01$, *** $p < 0.001$, Tukey's post-hoc pairwise comparisons of coated versus uncoated cover slips in the same medium condition).

### 2.4.3 Monolayer primary islet cell cultures retain key characteristics of differentiated endocrine cells

Human and rat islet cell monolayers organized into clusters of differentiated endocrine cells expressing endocrine hormones glucagon, insulin, somatostatin and pancreatic polypeptide in alpha, beta, delta, and PP cells, respectively, which occurred in similar proportions as in native islets (**Figure 3A-D**). Insulin-positive beta cells in human and rat islet cell monolayers maintained high nuclear expression of the beta cell markers PDX1 and NKX6.1 after 2 weeks of monolayer culture (**Figure 3E-H**). No bihormonal expressing cells were observed. After a week of culture, considerable proliferation of neonatal rat islet beta cells grown on laminin was observed in neuronal but not islet basal medium by Ki67 staining (**Supplementary Figure 2A, B**). Proliferation in adult human islet beta cells grown on collagen IV in neuronal medium was extremely rare (**Supplementary Figure 2C**). Standard confocal microscopy on islet cell monolayers stained for insulin, the neuroendocrine GABA-synthesizing enzyme GAD65, and the endoplasmic reticulum marker calnexin enabled detailed imaging of subcellular structures unresolvable on whole islets (**Supplementary Figure 2D)** and revealed islet monolayer cells adopting typical polarized polyhedron morphology (44) and rosette-like micro-societies (44) (**Supplementary Figure 2E**).
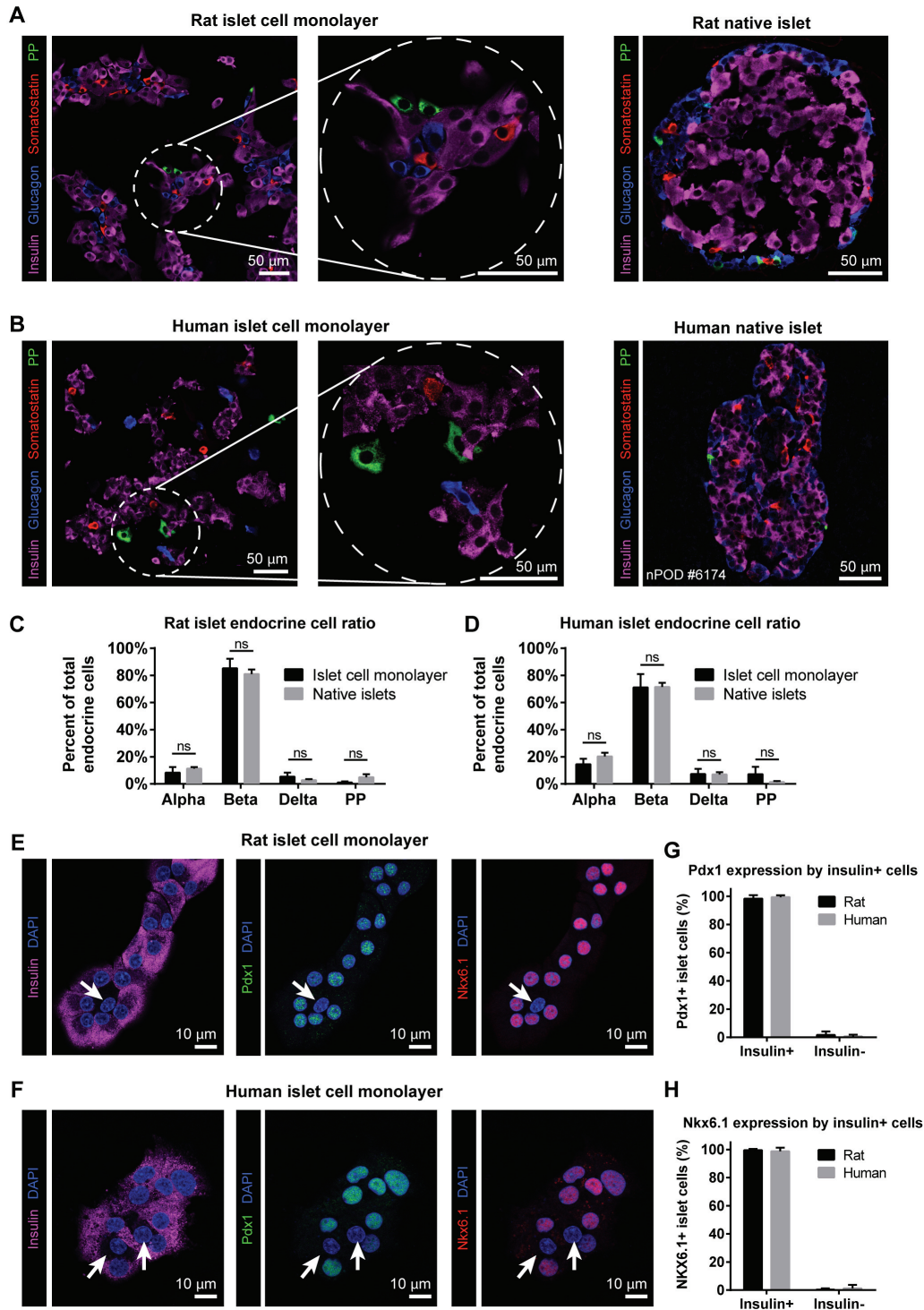
**Figure 3. Maintenance of endocrine cell phenotype in primary islet monolayer cultures.**

(**A**) Rat islet cells cultured for four days on laminin-coated coverslips in neuronal medium and (**B**) human islet cells cultured for four days on collagen IV-coated coverslips in neuronal medium and immunostained for glucagon, insulin, somatostatin and pancreatic polypeptide (PP) to identify islet alpha, beta, delta and PP cells, respectively. Left image panels show monolayer islet cell cultures.

Middle panels show increased magnification of the encircled regions in the left panel. Right panels show native islets from sections of rat and human pancreas. (**C, D**) Quantification of cell type distribution in rat (**C**) and human (**D**) islet cell monolayers and pancreatic tissue sections. Mean ± SEM (*n* = 6 random image fields from each of 2 different donors). Statistical analysis by Student's *t*-test (ns, no significant difference). (**E, F**) Expression of beta cell markers PDX1 and NKX6-1 persist 2 weeks after seeding in monolayers in rat (**E**) and human (**F**) cultures. Arrows indicate lack of PDX1 and NKX6.1 expression in insulin-negative cells. Mean ± SEM (*n* = 6 random image fields). Images are representative of 3 independent experiments. (**G**) Quantification of PDX1 and (**H**) NKX6.1 expression in insulin-positive and insulin-negative islet cells in rat and human islet cell monolayer cultures.

To test the functionality of primary islet cell monolayers, we acquired time-lapse videos of cytosolic calcium signaling in primary rat beta cells expressing the cytosolic Cameleon $Ca^{2+}$ sensor YC3.6cyto (32) under the control of the rat insulin promoter (Ad-RIP-YC3.6cyto) (**Figure 4A-C**). The beta cells in the islet cell monolayers displayed characteristic islet-like calcium signaling behavior. Calcium transients were absent under resting glucose (2.5 mM) conditions whereas rhythmic coordinated calcium spikes were observed in response to glucose stimulation (16.7 mM) and depolarization with KCl caused a large calcium rise. High-glucose stimulated calcium signaling was abolished by maintaining the ATP-dependent K+ channels in its open state using diazoxide. Together, these data indicate that differentiated primary endocrine cell phenotypes are maintained in our monolayer culture system.
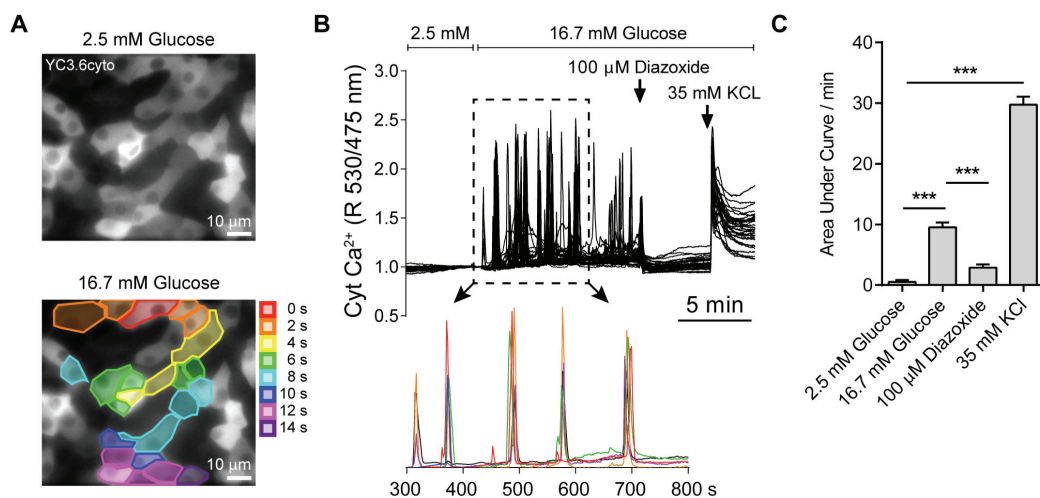
**Figure 4. Functional calcium-responsive glucose sensing in islet cell monolayer cultures.**
(**A**) Rat islet cell monolayers transduced with adenovirus to express Cameleon cytosolic $Ca^{2+}$ sensor YC3.6$_{cyto}$ under the control of the rat insulin promoter. Top panel shows localization of YC3.6$_{cyto}$ in the cytosol. Bottom panel shows wavelike propagation of $Ca^{2+}$ signaling between adjacent beta cells during high glucose stimulation. (**B**) A representative $Ca^{2+}$ imaging experiment in primary rat beta cells showing simultaneously-recorded $Ca^{2+}$ traces from 41 beta cells in a single field-of-view. Lower panel shows strongly coordinated $Ca^{2+}$ activity in subsets of beta cells during 16.7 mM glucose stimulation. Each color represents an individual cell recording (6 cell traces shown). Colors do not correspond to those in (**A**). (**C**) Quantification of the number of beta cells transiting $Ca^{2+}$ per min during recording experiments shown in (**B**). Mean ± SD ($n$ = 3 independent experiments). Statistical analysis by one-way ANOVA (*** $p < 0.001$, Tukey's post-hoc pairwise comparisons).

## 2.4.4 Live-cell microscopy of plasmid-transfected primary islet cell cultures

We acquired time-lapse videos of insulin vesicular trafficking dynamics in primary rat beta cells transfected with the insulin-granule targeting neuronal peptide NPY-Venus (30), (**Figure 5A-D**). We observed characteristic glucose concentration-dependent behavior of insulin granule motility. In low glucose (2 mM), insulin granules appeared to be completely static within the beta cell**.** Under high glucose stimulation (11 mM), insulin granules exhibited high intracellular motility. Glucose-dependent motility of insulin granules was previously reported with lower image resolution in insulinoma cells (45) and whole islets (46) and attributed to interactions between insulin granules and microtubule and actin cytoskeleton networks (47) that reorganize in response to glucose stimulation. We measured microtubule network spacing in rat islet monolayers by confocal microscopy and confirmed the previous reports that inter-microtubule spacing and insulin granule motility are both inversely correlated with glucose concentration (**Figure 5E-G**).
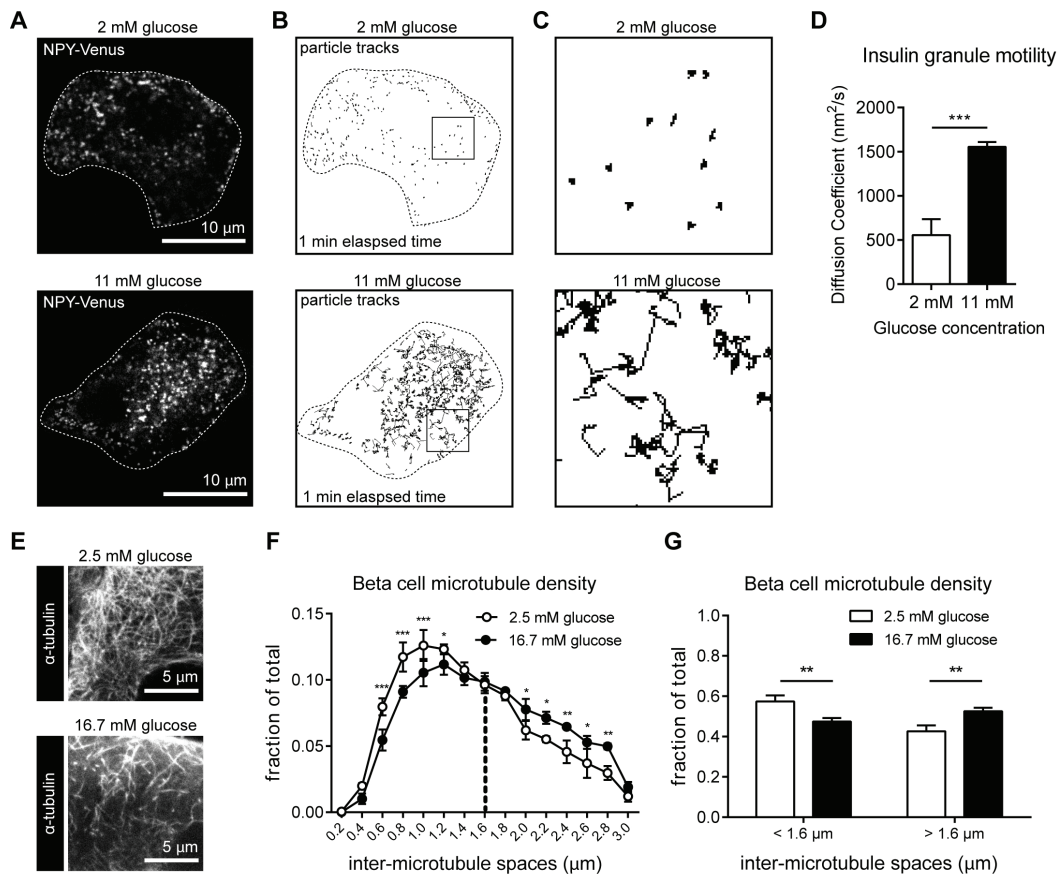
**Figure 5. Live-cell imaging of insulin granule dynamics in rat islet cells monolayers.**

(**A**) Representative still frames from time-lapse live-cell confocal microscopy videos of NPY-Venus labeled insulin granules during exposure to KREBS buffer containing 2 mM or 11 mM glucose. Dashed line indicates cell outline. (**B**) Particle tracking analysis of 1-min clips of time-lapse of NPY-Venus labeled insulin granule movement showing particle tracks. Dashed line indicates cell outline. (**C**) Increased magnification of NPY-Venus particle tracks of bounded region shown in (**B**). (**D**) Diffusion coefficients of insulin granules calculated from particle tacking analysis of NPY-Venus. Mean ± SD (*n* = 3 independent experiments) Statistical analysis by Student's *t*-test (*** p < 0.001). (**E**) Representative confocal images of primary rat beta cells fixed after exposure to 2.5 mM or 16.7 mM glucose for 1 h and immunostained for α-tubulin. (**F**) Quantification of microtubule density in confocal images of rat beta cells following exposure to 2.5 mM or 16.7 mM glucose for 1 h displayed as a 15-bin histogram. Statistical analysis by one-way ANOVA (* p < 0.05, ** p < 0.01, *** p < 0.001, Tukey's post-hoc pairwise comparisons respective to 2.5 mM glucose condition of same bin-width). (**G**) Same data as in F, but displayed as a 2-bin histogram. Statistical analysis by Student's *t*-test (** p < 0.01).

### 2.4.5  Super-resolution microscopy of primary islet cell cultures

We performed STED super-resolution imaging of insulin granules, microtubules, and actin filaments in primary rat and human islet cells (**Figure 6 and Supplementary Figure 3**). The size of insulin granules and cytoskeletal features imaged by STED demonstrate successful sub-diffraction limit imaging of cellular structures on length-scales below the resolving power of traditional light microscopy, in agreement with measurements made by transmission electron microscopy (TEM) (**Supplementary Figure 4**). STED imaging of insulin on human beta cells fixed following a brief incubation in high glucose revealed individual insulin granules docked at the plasma membrane (**Figure 6E**). We observed that the cell-cell interface between adjacent beta cells is characterized by a dense cortical actin network (**Figure 6F**) which is implicated in the recruitment and docking of secretory granules (44). We also captured three-dimensional (3D) super-resolution images of human islet beta cells immunostained for insulin by the alternative super-resolution method of structured illumination microscopy (SIM) (48) (**Figure 6G**). To our knowledge, this is the first example of high-quality super-resolution microscopy of primary human beta cell monolayers.
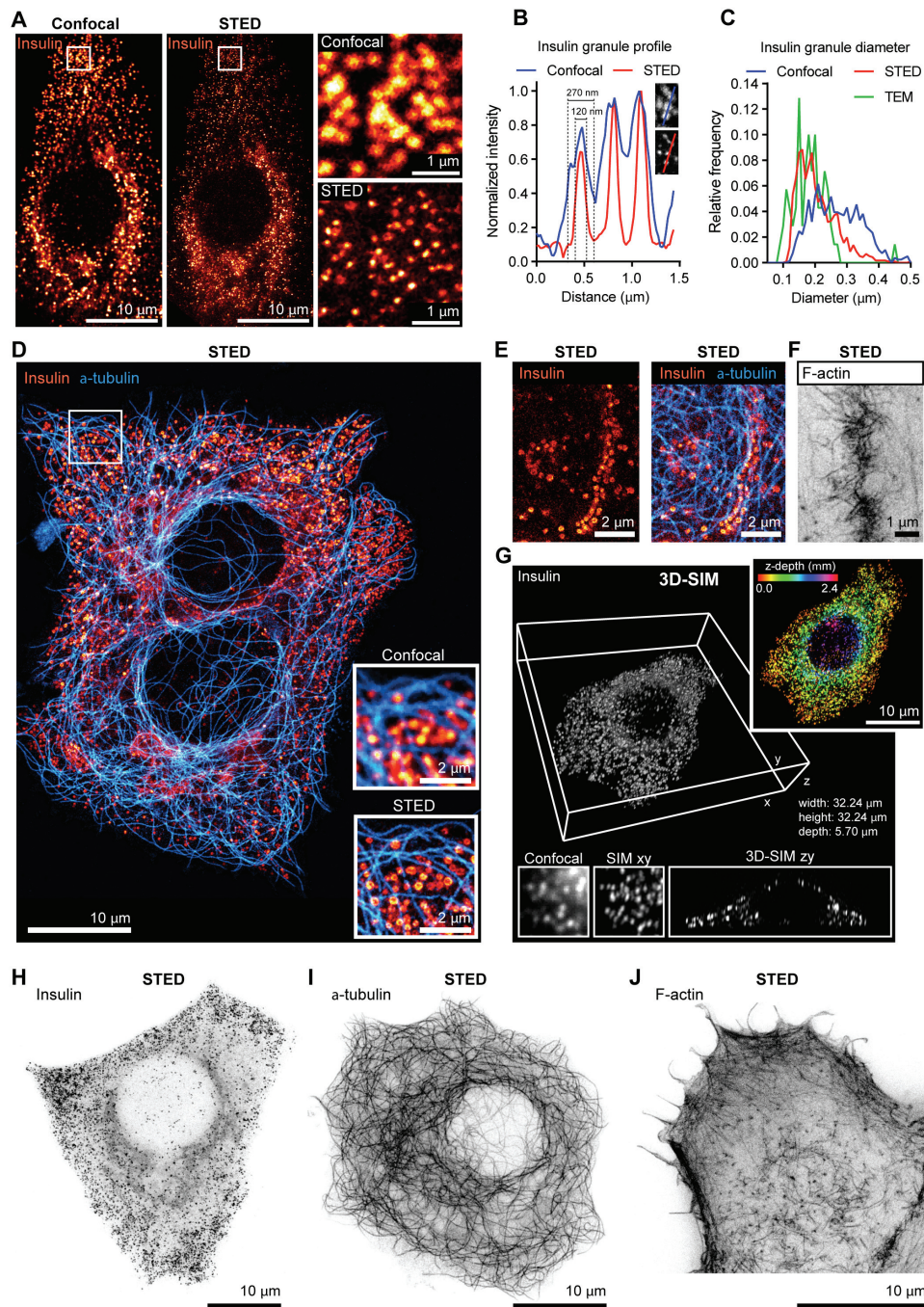
**Figure 6. Super-resolution microscopy techniques applied to islet cell monolayers on glass.**
(**A**) Representative confocal and STED super-resolution microscopy images of rat islet cell monolayers immunostained for insulin. Right panels show increased magnification of the boxed regions in the left panels. (**B**) Representative intensity profile measurement across a group of three insulin granules according to confocal or STED microscopy. Feature sizes measured as full width at half maximum. (**C**) Size distribution of insulin granules as measured by confocal, STED or TEM microscopy. (**D**) Comparison of confocal and STED super-resolution microscopy portrait of a human islet beta cell monolayers immunostained for insulin and α-tubulin. Inset frames show higher magnification of boxed

63

region. (**E**) STED image of insulin granule recruitment and docking to plasma membranes at a cell-cell interface in rat islet cell monolayers following a brief exposure to high glucose. (**F**) STED image of the cortical F-actin network at a cell-cell interface in human islet cell monolayers. (**G**) 3D-SIM super resolution microscopy of a human islet beta cell, immunostained for insulin. (**H**) Representative STED image of insulin granules in a human beta cell. (**I**) Representative STED image of α-tubulin in a human beta cell. (**J**) Representative STED image of F-actin in a rat beta cell.

### 2.4.6   Induction of beta cell proliferation by repression of primary cilia formation

To take advantage of the technical development described above, islet cell monolayer cultures on glass were used to observe primary cilia by immunostaining for the cilia marker acetylated alpha tubulin and the centrosomal protein pericentrin (**Supplementary Figure 5 and Figure 7**). The new method enabled identification of individual cilia-expressing beta cells, the length of their cilium and the subcellular localization of ciliary proteins.

We noted that the percentage of ciliated beta cells was 3 fold higher in human islet cell monolayers compared to neonatal rat islet cell monolayers (48% vs 16% of insulin-positive cells) (**Figure 7A, B**). Because analyses of expression of the proliferative marker Ki67 indicated a lower rate of proliferation of adult human beta cells than neonatal rat beta cells (**Supplementary Figure 2**), we speculated that the lower incidence of primary cilia in rat islet cells might reflect differences in cell cycle status between the two cultures. In support of this hypothesis, we observed that primary cilia were uniformly absent from proliferating Ki67-positive rat islet beta cells (**Figure 7C, D**), indicating an inverse correlation between presence of cilia and beta cell proliferation state. Furthermore, images of primary beta cells undergoing cell division showed acetylated alpha tubulin localized to the mitotic spindle during mitosis rather than in ciliary structures (**Figure 7E**). Together these observations implicate an inverse correlation between the presence of primary cilia and cell cycle progression in primary beta cells.
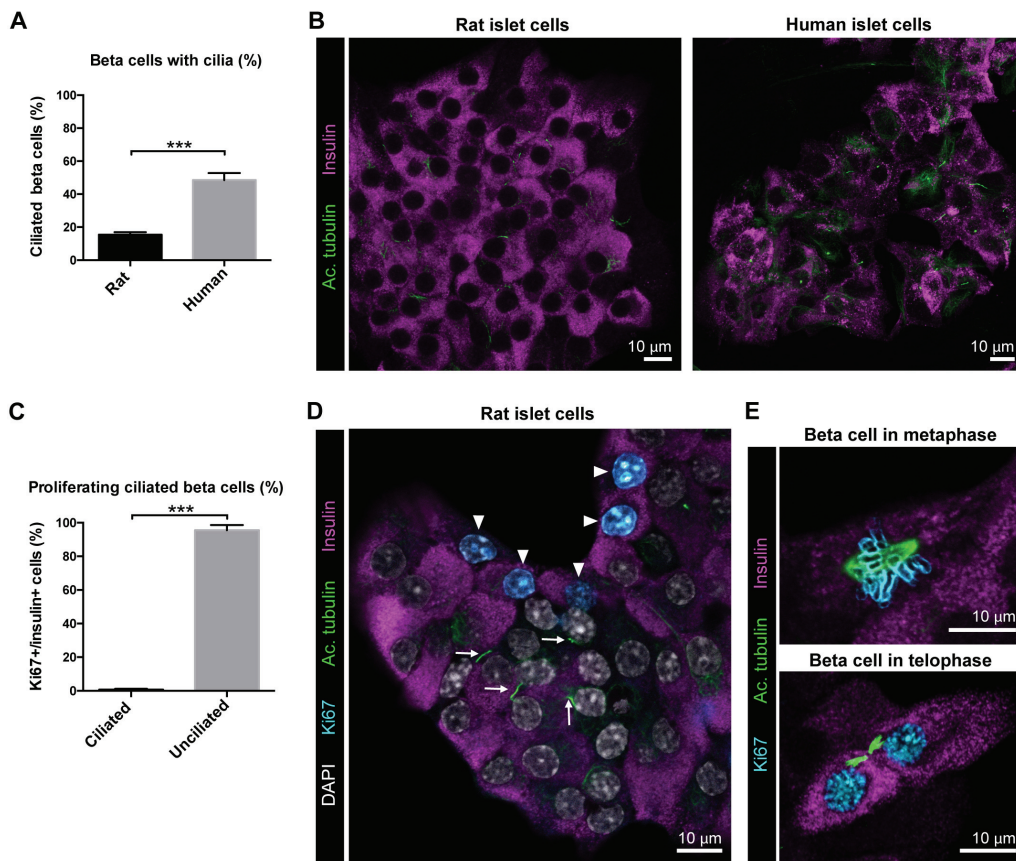
**Figure 7. Presence of primary cilia inversely correlates with beta cell proliferation.**
(**A**) Percentage of insulin-positive beta cells with primary cilia in rat and human islet monolayer cultures. Mean ± SEM ($n$ = 10 random image fields from each of two different donors). Statistical analysis by Student's $t$-test (*** $p < 0.001$). (**B**) Representative confocal images of rat and human islet cells immunostained for insulin and the cilia marker acetylated alpha tubulin. (**C**) Percentage of proliferating beta cells positive for both Ki67 and insulin with and without primary cilia in rat islet cells. Mean ± SEM ($n$ = 10 random image fields per group). Statistical analysis by Student's $t$-test (*** $p < 0.001$). (**D**) A representative confocal image showing unciliated proliferating Ki67-positive rat insulin-positive cells (arrowheads) and a group of Ki67-negative beta cells with cilia (arrows). (**E**) Confocal images showing the localization of acetylated tubulin during metaphase and telophase in mitotic beta cells.

We next asked if adaptation of a two-step protocol to drive cilia disassembly based on nutrient withdrawal and reintroduction (49) could be exploited as a mechanism to induce proliferation of primary beta cells (**Figure 8A**). Low glucose concentration causes islet cells to become more rounded, while high glucose culture medium causes the opposite effect, enhancing the adhesion and spreading of

primary islet cells (50). We tested the effect of high and low glucose on cell shape in our rat islet cell monolayer cultures and confirmed the dramatic effect on islet cell shape obtained by switching the glucose concentration from 11 mM to 5.5 mM (rounded cells) or from 5.5 mM to 11 mM (extended well adhered cells) (**Supplementary Figure 6** and results not shown). Cytoskeletal rearrangements, occurring when cells transition shape from rounded to extended highly-spread shape, have been shown to drive cilia reabsorption in human retinal cells and promote re-entry into the cell cycle (22). Furthermore, the ROCK inhibitor Y-27632, which induces a repositioning of the basal bodies below the nucleus, thus reducing ciliogenesis (22), has been reported to have mitogenic effects on beta cells (18). We employed a two-step protocol to induce beta cell rounding and elongate cilia, followed by a second step re-initiating cell spreading simultaneously with cilia disassembly. We focused these experiments on neonatal rat islet cell monolayer cultures due to the rarity of Ki67-positive beta cells in human islet monolayer cultures.

Neonatal rat islet cell monolayers were established in neuronal medium containing 11 mM glucose. After three days in culture, cells were subjected to serum and B27 starvation for 36 hours to induce ciliogenesis in either 5.5 mM or 11 mM glucose. To induce cilia disassembly, serum and B-27 were reintroduced and glucose concentration increased from 5.5 mM to 11 mM or from 11 mM to 17 mM in the presence or absence of the ROCK inhibitor Y-27632 (**Figure 8A, B**). Fluorescence analyses of cells at the different stages of the protocol revealed a rounding effect of serum and B-27 starvation in 11 mM glucose, which was reversed during the cilia disassembly phase (**Figure 8B**). Analyses of Ki67 expression at different stages of the protocol (**Figure 8C**), revealed ~6% of beta cells proliferating in the initial seeding phase. The percentage of proliferating cells decreased during the starvation phase but rebound during the cilia disassembly phase. Thus, increasing glucose from 11 mM to 17 mM following the starvation phase significantly

increased beta cell proliferation over the initial seeding with ~15% of beta cells being Ki67 positive. Addition of the ROCK inhibitor Y-27632 enhanced the proliferative effect slightly but not significantly to ~16% in this condition. Omitting the starvation step, failed to induce a significant increase in beta cell proliferation during the cilia disassembly phase. In cells subjected to starvation in 5.5 mM glucose, the rounding effect was much more pronounced than in 11 mM glucose (results not shown). Increasing the glucose concentration to 11 mM in the cilia disassembly step resulted in a non-significant increase in proliferation over the seeding phase. In this condition however, combining an increase in glucose concentration with addition of Y-27632 resulted in a significant increase in proliferation over the seeding phase with ~12% of beta cells being Ki67 positive (**Figure 8C**) suggesting that inhibition of ROCK may exert an influence on proliferation in a condition where the maximum effect of glucose is not exploited.

As serum starvation appeared to be a critical step in order to observe gains in beta cell proliferation from these stimuli, we asked whether the proliferative effects were connected with changes in cilia expression and/or length. Cilia parameters were analyzed at each step of the protocol for monolayer cultures subjected to 17 mM glucose and ROCK inhibitor following serum and B-27 starvation in 11 mM glucose (**Figure 8D**). Following initial seeding, primary cilia were expressed in ~15% of beta cells and average cilia length was ~3 μm. During starvation in 11 mM glucose, cilia expression increased to ~24% of beta cells and average cilia length increased to ~5 μm. Following re-introduction of serum and B-27, increasing glucose to 17 mM and adding ROCK inhibitor, cilia expression decreased to ~5% of beta cells and the remaining cilia length decreased to ~3 μm. The effects of the protocol on proliferation rate and cilia were mirrored in the overall beta cell density of the monolayers (**Figure 8E, F**). Initial seeding density was ~30,000 cells/cm$^2$ which decreased ~20,000 cell/cm$^2$ during starvation in 11 mM glucose. In the cilia disassembly phase, beta cell mass was significantly increased to ~70,000 cells/cm$^2$.

In summary, serum starvation caused cilia to grow, while induction of cilia disassembly caused cilia to resorb and beta cell proliferation to increase.
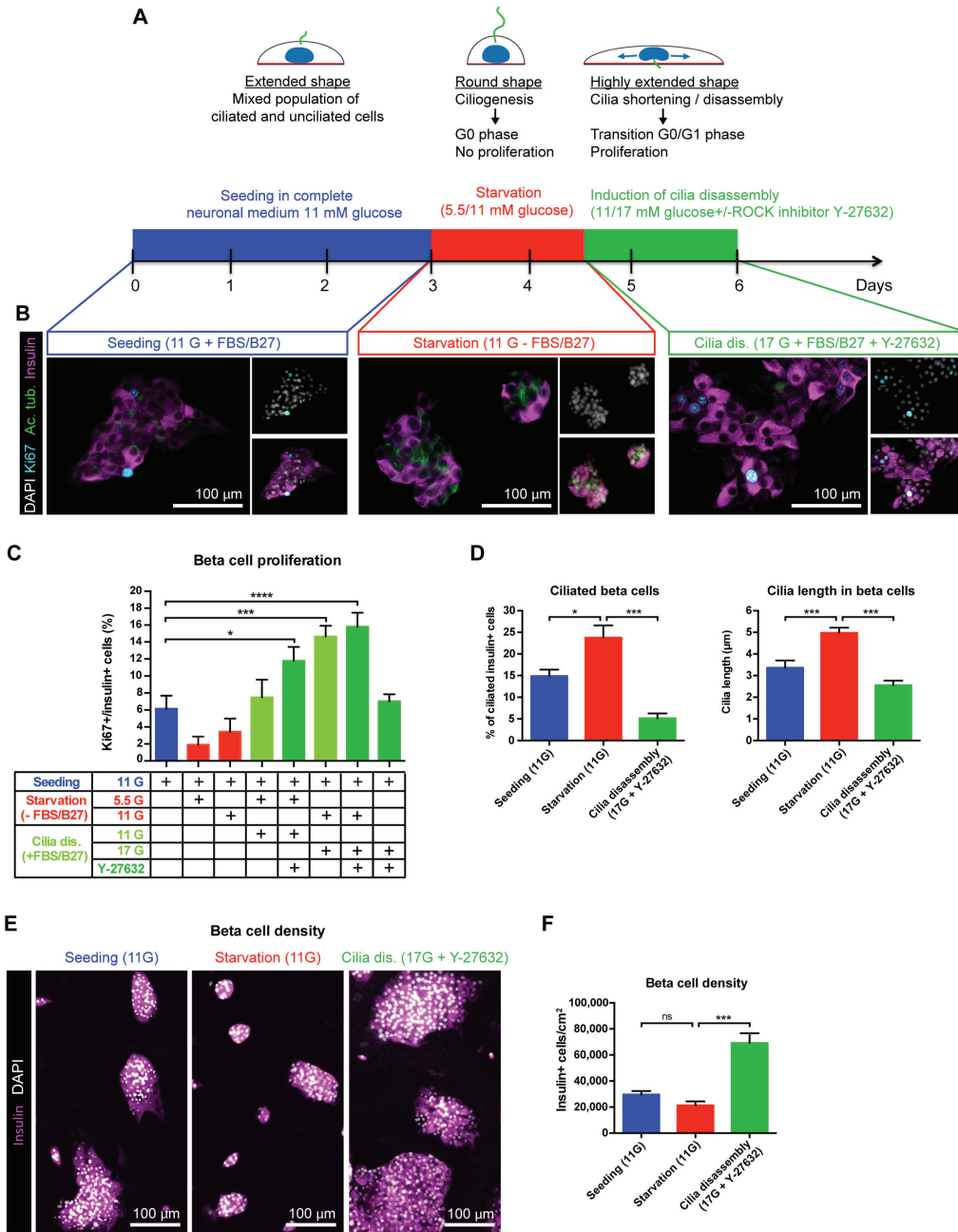


**Figure 8. Protocol for cilia disassembly stimulates beta cell proliferation.**
(**A**) Schematic representation of the protocol used for cilia disassembly in beta cells. Rat islet cell monolayers were established for 3 days in complete neuronal medium with 11mM glucose, and then exposed for 36 hours to serum starvation in either 5.5 mM or 11 mM glucose to stimulate rounding of cells and ciliogenesis. Extension of cells and cilia disassembly was induced through re-addition of FBS/B-27 combined with raising the glucose concentration from 5.5 mM to 11 mM or from 11 mM to 17

mM with or without addition of the ROCK inhibitor Y-27632. (**B**) Representative fluorescence images of rat islet monolayer cells at the different stages of the protocol described in (**A**) and immunostained for DAPI, Ki67, acetylated tubulin and insulin (5.5G, 11G, 17G are abbreviations for 5.5, 11 and 17 mM glucose respectively). (**C**) Beta cell proliferation during different stages and permutations of the cilia disassembly protocol. Mean ± SEM ($n$ = 10 random image fields per group). Statistical analysis by one-way ANOVA (* $p < 0.05$, *** $p < 0.001$, **** $p < .0001$, Dunnett's pairwise comparisons relative to the Seeding condition). (**D**) Quantification of the percentage of ciliated beta cells and cilia length during different stages of the cilia disassembly protocol and using 11mM glucose during the starvation phase. Mean ± SEM ($n$ = 10-20 random image fields per group). Statistical analysis by one-way ANOVA (* $p < 0.05$, ** $p < 0.01$, *** $p < 0.001$, ns no statistical difference, Tukey's post-hoc pairwise comparisons). (**E**) Representative fluorescence images of rat islet monolayer cells at three different stages of the cilia disassembly protocol, immunostained for DAPI and insulin. (**F**) Quantitation of density of islet cell monolayers in three groups representing the different stages of the cilia disassembly protocol. All three groups in (**E**) and (**F**) were cultured for a total of 144 hours before counting of cells with media change in each at 72 and 108 hours. In the first group, cells were cultured in neuronal medium with 11 mM glucose for 144 hours. In the second group, cells were cultured in neuronal medium with 11 mM glucose for 108 hours and in the same medium without serum and B-27 for 36 hours. In the third group, cells were cultured in neuronal medium with 11 mM glucose for 72 hours, in the same medium without serum and B-27 for 36 hours and in neuronal medium with 17 mM glucose and ROCK inhibitor for 36 hours. All analyses were performed in triplicate. Data are representative of two independent experiments.

## 2.5   DISCUSSION

We have developed a simple method for two-dimensional culture of primary human and rat islet cells. Critically, it is the combination of neuronal culture medium containing B-27 supplement together with collagen IV (human) or laminin (rat) surface-coating which enable formation of well spread and robustly attached islet cell monolayers. B-27 supplement contains a cocktail of growth factors and antioxidants formulated to support the viability of central nervous system neurons. Several of the constituent components of B-27 including retinoic acid (51), insulin (52), and triiodothyronine (53), are known to support islet cell function and survival, while the B-27 components superoxide dismutase, glutathione and corticosterone may reduce cellular inflammation resulting from the stress of whole islet dispersal. While we have not systematically analyzed the relative importance of each individual component of

B-27, we observed that in concert this cocktail leads to greatly improved health of islet single cell cultures.

Pancreatic islet cells share many features with neurons including the secretion of neurotransmitters and expression of neurotransmitter receptors for auto and paracrine coordination of islet function (54,55). The commonly used islet culture medium RPMI 1640 contains high concentrations of neuroactive amino-acids, L-Glutamate, L-Aspartate, and L-Cysteine. These amino acid components give RPMI medium an excitatory neurotoxic effect resulting in poor viability of primary neurons (56). As islet cells also express high levels of neurotransmitter receptors (55), the amino acid content of RPMI may induce similar toxic effects on fragile dispersed islet cells. The use of a neuron-compatible culture medium such as Neurobasal Medium or MEM which are intentionally formulated without neuroactive amino acids (25) may improve islet cell viability.

Cell-ECM (40) and cell-cell (57,58) interactions are critical to islet viability and function. When whole islets are dispersed to individual cells these connections are lost and dispersed islet cells often have reduced or dysregulated calcium signaling and insulin-secretory capability (59). In the culture system we describe, cell-ECM and cell-cell interactions are partially restored through defined matrix coatings, which ligate beta cell integrin receptors, and through the tendency for seeded dissociated islet cells to coalesce into micro societies of clustered neighboring endocrine cells. We found that collagen IV surface coating preferentially supports human islet cell adhesion while laminin, and to a lesser extent HTB-9, surface coating preferentially support rat islet cell adhesion. The lack of adhesion of human islet cells on laminin and HTB-9 is consistent with laminin being a major constituent protein in HTB-9 extracellular matrix. This species-specific preferential adhesion for collagen IV or laminin is likely a reflection of differential expression of alpha-beta integrin pairings between human and rat islets (40) and may imply the existence of underlying species differences in islet cell-matrix architecture.

70

The analysis of calcium signals in our monolayer culture indicates that the beta cells maintain full responsiveness to glucose. Furthermore, the wavelike propagation of calcium signals across neighboring beta cells within the islet cell monolayers are consistent with the efficient establishment and maintenance of cell-cell contacts. Such cell-cell interactions are essential to obtain good nutrient activation of beta cells (58). Strikingly, the cells analyzed showed no calcium signals under resting conditions. The beta cell activation that immediately followed initiation of the glucose stimulus was dependent on the metabolic triggering pathway of insulin secretion as it was suppressed when using the ATP-dependent K+ channel opener diazoxide. The calcium data provide strong evidence for the functional robustness of beta cells in the present monolayer culture system. Finally, it should be noted that the effectiveness of adenovirus infection in these monolayer cultures was impressive. Such expression of transgene after adenovirus infection in the large majority of beta cells would be hard or impossible to achieve in intact three dimensional pancreatic islets.

The method for culturing islet monolayer cells allowed us to study primary cilia in beta cells and establish the existence of an inverse correlation between beta cell proliferation and ciliogenesis, a relationship that has been described previously for other cell types but not for primary beta cells. This result is highly significant because primary beta cells are particularly refractory in culture and do not easily proliferate. Here, we identified a cilia disassembly mechanism, which is tightly interconnected with cell cycle progression, to be an active driver of proliferation in primary beta cells. Our results suggest that protocols to rapidly induce spreading of beta cells on surfaces can be exploited in a straightforward manner to drive beta cell mass expansion while preserving differentiated phenotype. It is possible that this proliferation pathway has not been previously identified in islets because beta cells must be grown on two-dimensional surfaces to encourage a high degree of spreading. Rounded beta cells may be less susceptible to stimuli that increase spreading and cilia resorption in the confined three-dimensional environment of intact

islets than in two-dimensional monolayer culture. With further development, a method to induce ex vivo beta cell expansion without dedifferentiation may serve to generate large numbers of beta cells from cadaveric human islets for treatment of diabetes or for research purposes.

The advancement in monolayer islet cell culture enables the study of subcellular-resolution processes in highly functional primary islet endocrine cells by live-cell and super-resolution microscopy techniques that require cells to be adherent on thin glass surfaces for optimal performance. With such imaging capacities, islet biology studies performed in primary islet cells can now benefit from the full array of possibilities offered by the latest advancements in light microscopy, particularly the visualization of molecular interactions and biochemical events at the sub-organelle level.

## 2.6  CONTRIBUTION OF THE DOCTORAL CANDIDATE

The doctoral candidate initially developed the concept and design of neurons and pancreatic islet cell co-culture (2.3.1). Then, together with the co-first author E.A.P., she established the islet cell monolayer culture concept and design and performed the analysis of islet monolayer characterization (2.3.2 and 2.3.3). She developed the cilia disassembly-driven beta cell proliferation strategies and performed experiments and analysis for islet monolayer characterization and cilia disassembly-driven beta cell proliferation (2.3.6). She helped the lab technician M.P. with the isolation of rodent islets and immunostaining. She also contributed to the writing of the paper, together with the co-first author E.A.P. and the corresponding author and thesis advisor S.B.

## 2.7 SUPPLEMENTARY INFORMATION

**A**  Human islet cells, 7 days, No ARA-C    Hu islets cells, 7 days, ARA-C 3 mM



**B**  Human islet cells, 7 days, No ARA-C    Hu islets cells, 7 days, ARA-C 3 mM



**C**  Human islet cell monolayer purity
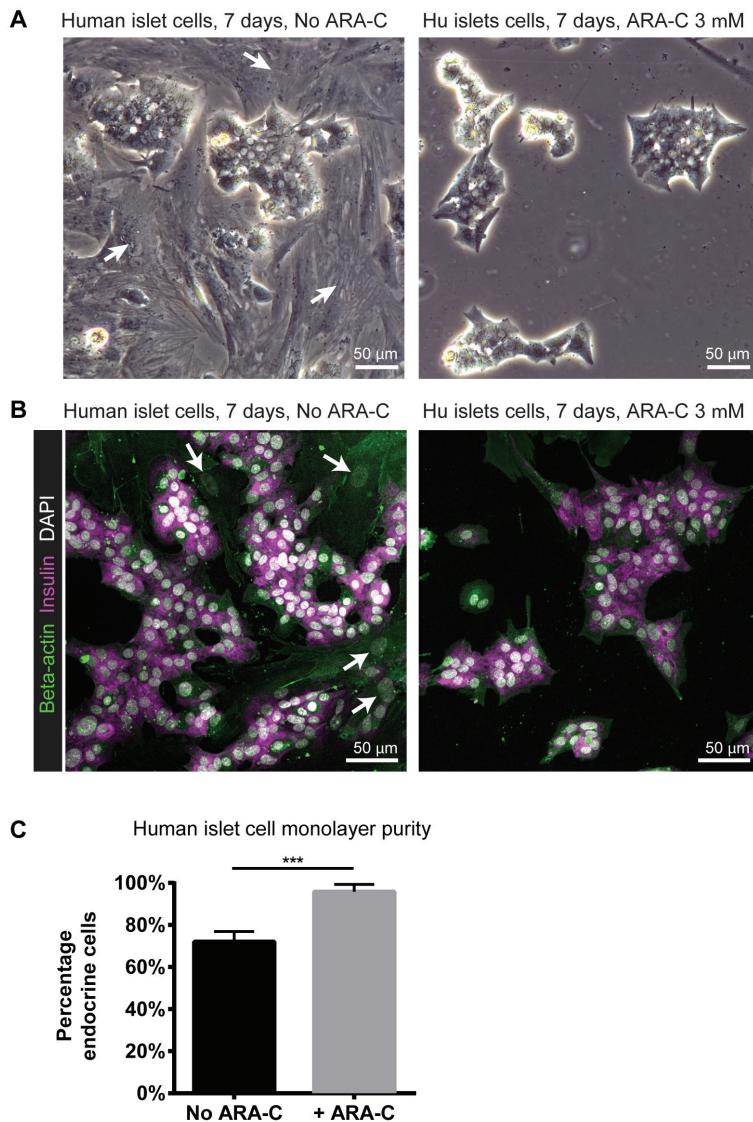


**Supplementary Figure 1. ARA-C-mediates elimination of fibroblast-like cells from human islet monolayers during culture for seven days on collagen IV-coated coverslips in neuronal medium.** (**A**) Transmitted light images showing human islet cells on collagen IV-coated coverslips treated or not with ARA-C (3 µM). Arrows indicate regions of fibroblast-like cells. (**B**) Confocal images of human islet cells treated or not with ARA-C (3 µM) and immunostained for β-actin and insulin. Nuclei were stained with DAPI. Arrows indicate regions of fibroblast-like cells. (**C**) Quantification of islet cell purity. Beta cells, constituting the majority of endocrine cells in the culture were identified based on insulin expression, while non-beta endocrine cells were identified by characteristic morphology similar to beta cells, easily distinguished from the much larger fibroblast-like cells. Mean ± SEM ($N$ = 6 random image fields per condition). Statistical analysis by Student's $t$-test (** p < 0.01).
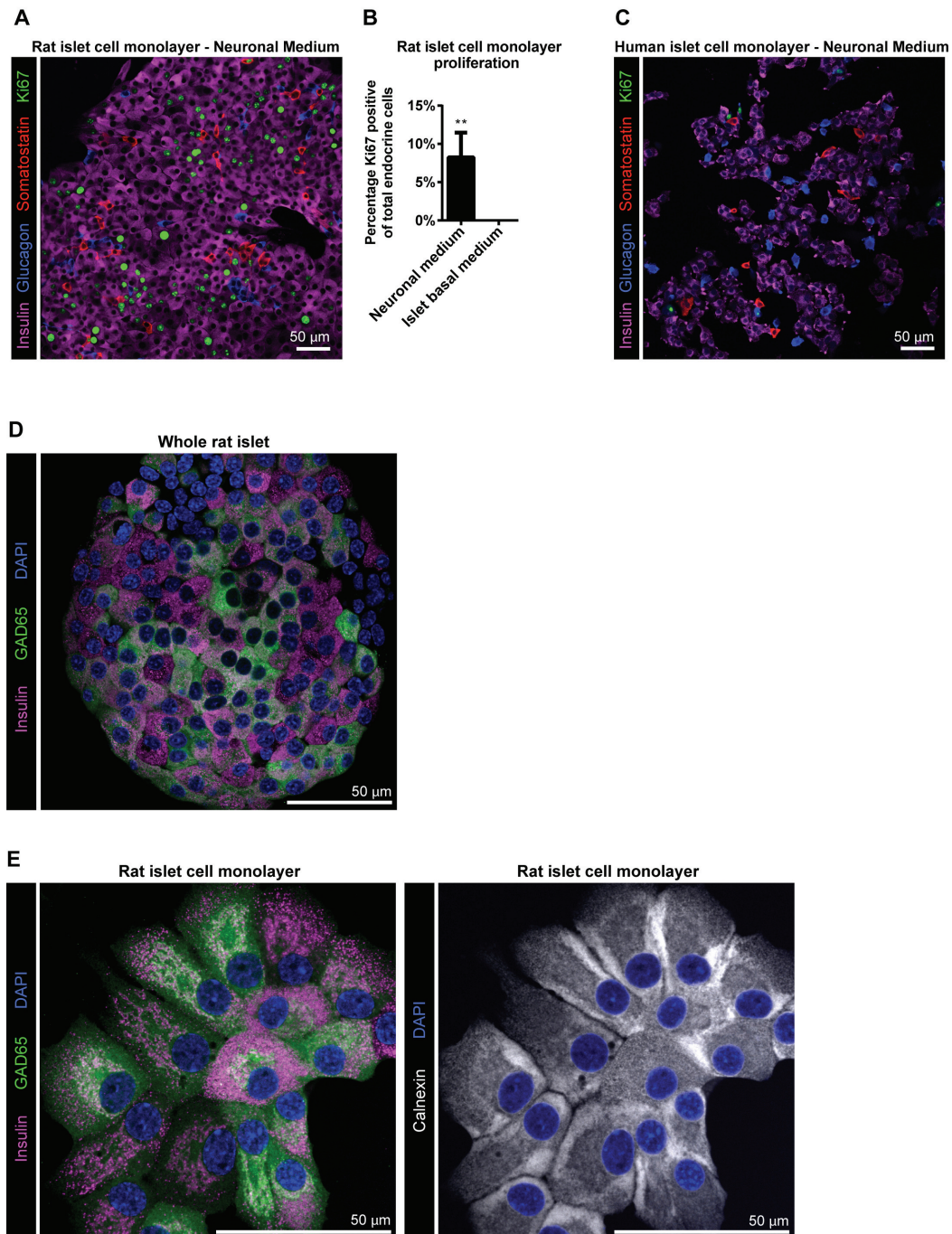
**Supplementary Figure 2**. Islet cell monolayer proliferation. (**A**) A representative confocal image of rat islet cells cultured for seven days on laminin-coated coverslips in neuronal medium and immunostained for insulin, glucagon, somatostatin and Ki67. (**B**) Quantification of the percentage of Ki67+ rat islet cells when cultured in neuronal medium compared to islet basal medium. Mean ± SEM. (N = 10 random image fields). Statistical analysis by Student's t-test (*** p < 0.001). (**C**) A representative confocal image of adult human islet cells from an 18-year-old donor, cultured for seven days on collagen IV-coated coverslips in neuronal medium and immunostained for insulin, glucagon, somatostatin and Ki67. (**D, E**) Representative confocal microscopy images of (**D**) a whole rat islet and (**E**) a rat islet cell monolayer immunostained for insulin, the neuroendocrine protein GAD65, or calnexin. Nuclei are stained by DAPI.

74
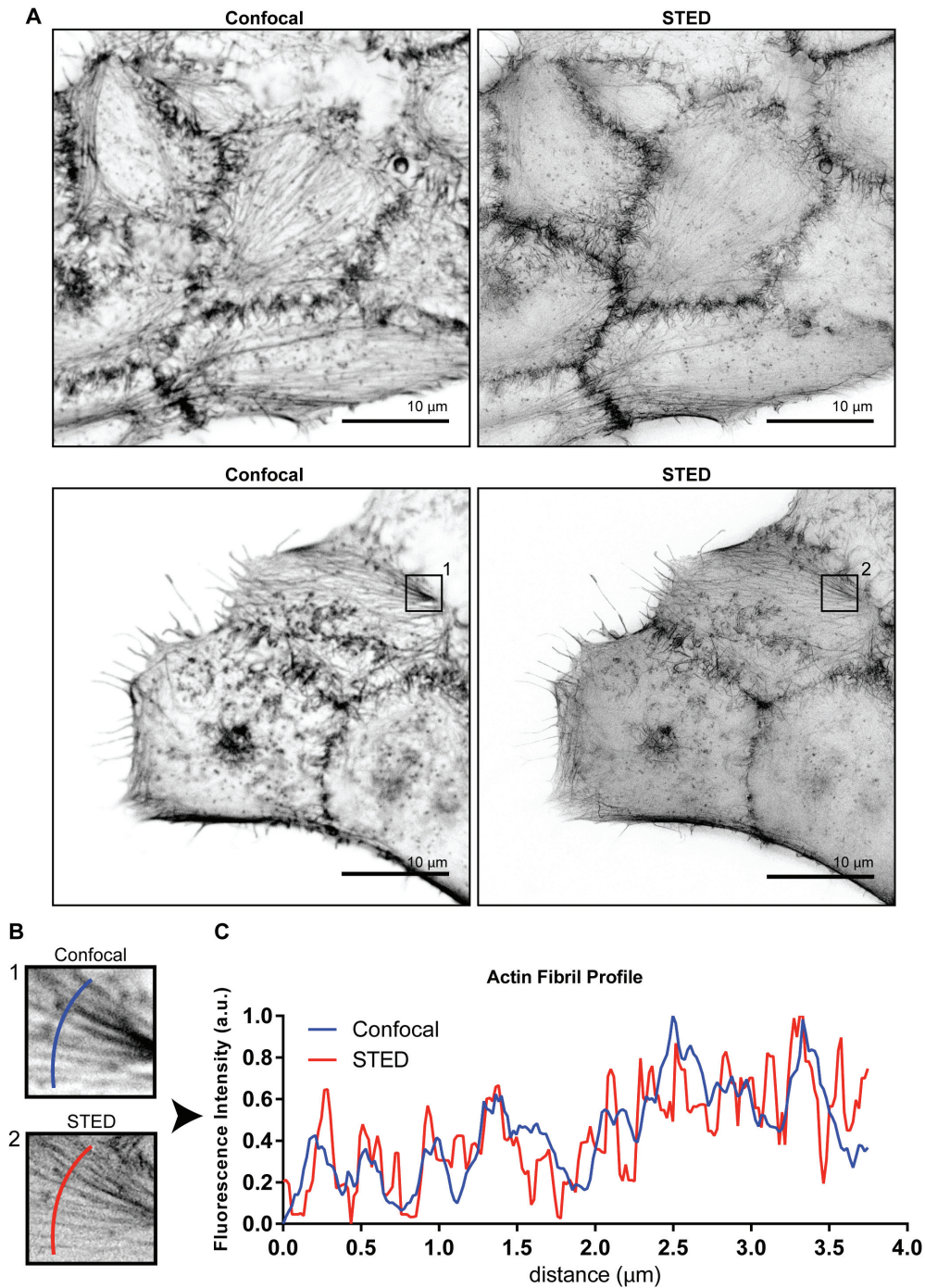
**Supplementary Figure 3**. **Confocal and STED super-resolution microscopy of the actin cytoskeleton in rat islet cell monolayers.**

(**A**) Representative images of rat islet cells stained with Alexa Fluor 488 phalloidin show high resolution structure of the beta cell cortical actin network. (**B**) Increased magnification of the bounded regions shown in the lower panels of (**A**). (**C**) Transverse fluorescence intensity profile measured across a group of actin filaments shown in (**B**) captured by STED and compared to confocal images.

TEM of rat islets



2 μm



1 μm
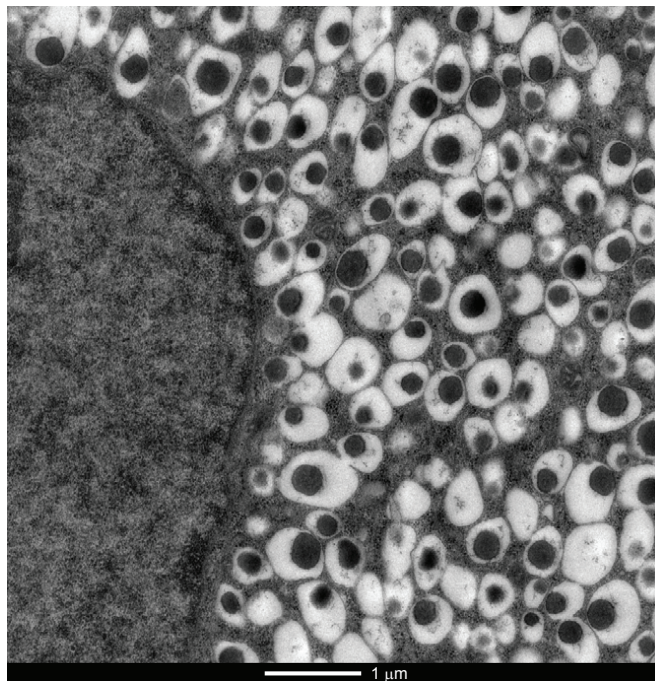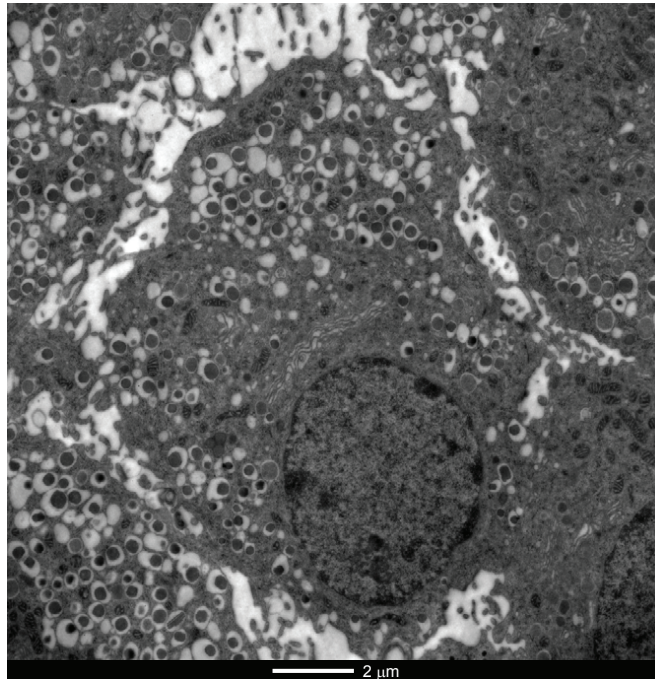
**Supplementary Figure 4**. **TEM of rat islets.**

Representative TEM images of whole rat islets used to measure the diameter of insulin granules in
Figure 6C.
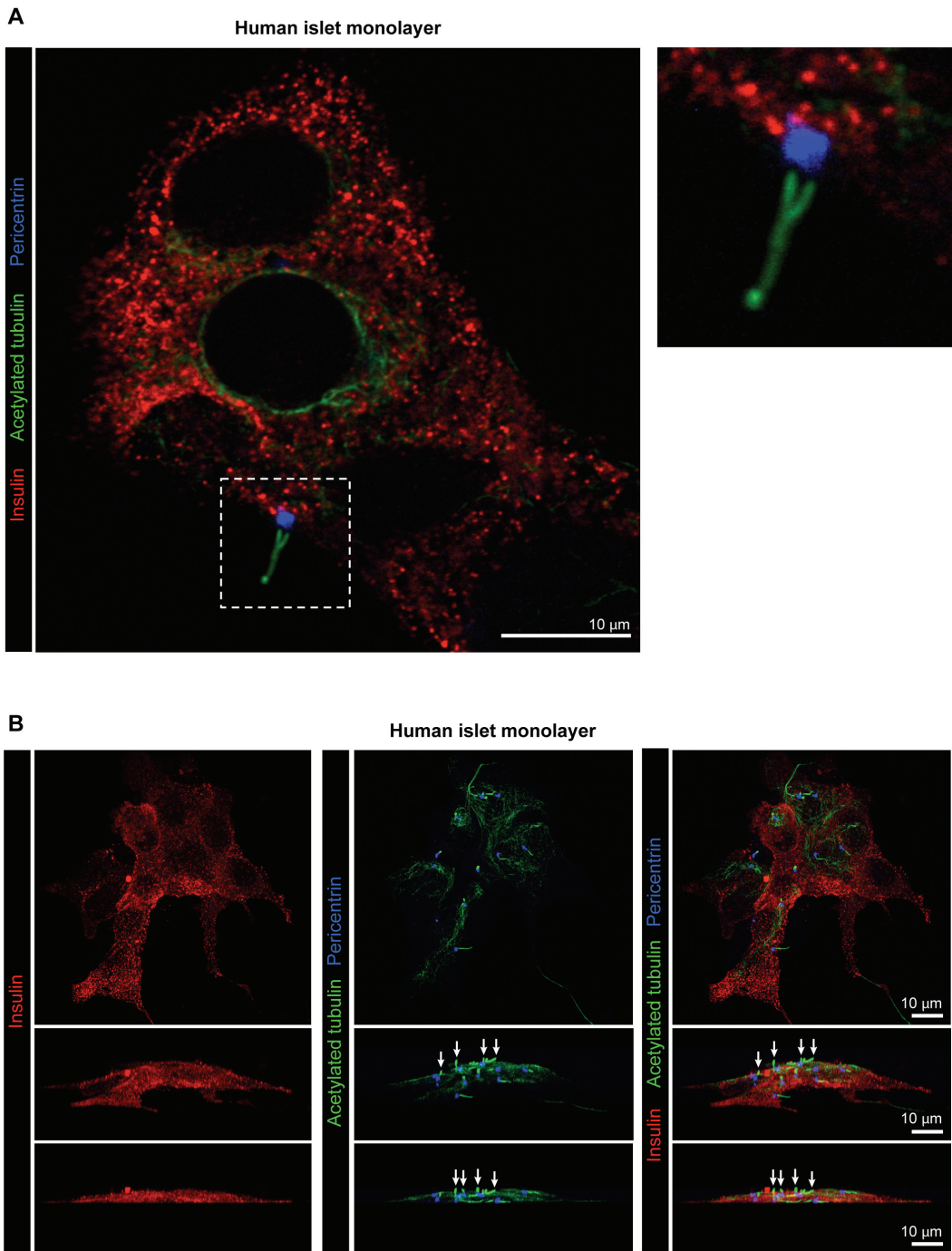
**Supplementary Figure 5**. **Confocal microscopy of primary cilia in human beta cells.**

(**A**) Left panel shows confocal analyses of primary human islet cells immunostained for insulin, the cilia marker acetylated alpha tubulin and the centrosomal protein pericentrin. Right panel, an increased magnification of the boxed region in the left panel, shows the localization of pericentrin at the base of a primary cilium originating from an insulin-expressing beta cell. (**B**) Three dimensional projections reconstructed from z-stacks obtained with confocal acquisitions of human islets cells immunostained for insulin, acetylated alpha tubulin and pericentrin. Arrows indicate individual cilia protruding from the apical side of human beta cells.

**Rat islet cells in 5.5 mM glucose**
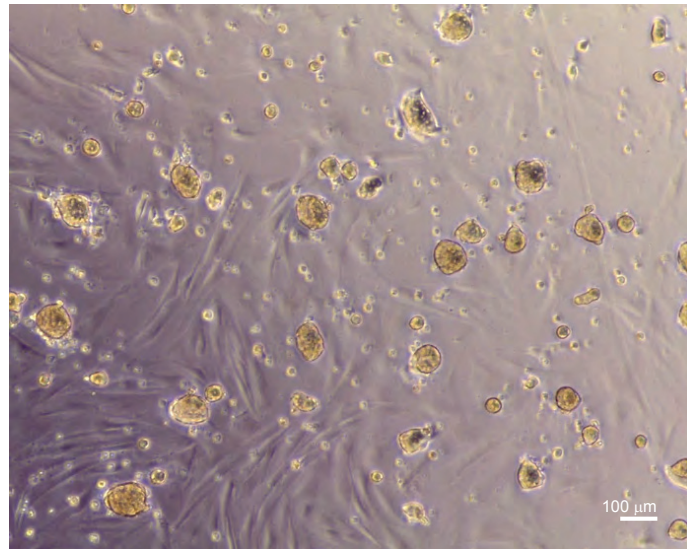


**Rat islet cells in 11 mM glucose**
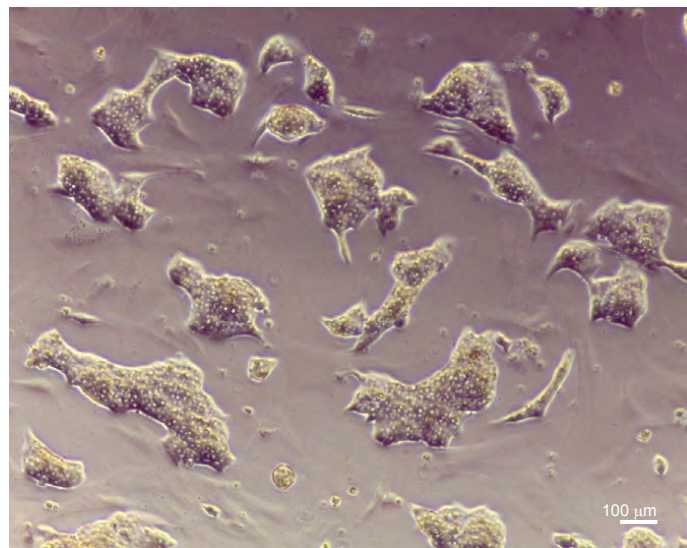


**Supplementary Figure 6**. **Glucose-dependent adhesion of rat islet cells.**

Representative transmitted light images of rat islet monolayer cells seeded on laminin coated glass for three days in neuronal medium containing 11 mM glucose and then switched to fresh neuronal medium containing either 5 mM or 11 mM glucose for 16 hours. The ability of cells to switch back and forth between rounded (5 mM glucose) vs a well spread (11 mM glucose) phenotype in response to a change in the glucose concentration was maintained for at least 3 days after the initial 3 day seeding period.

## 2.8  REFERENCES

1.  Bosco D, Meda P, Halban PA, Rouiller DG. Importance of cell-matrix interactions in rat islet beta-cell secretion in vitro: role of alpha6beta1 integrin. Diabetes 2000;49:233-243

2.  Hammar E, Parnaud G, Bosco D, Perriraz N, Maedler K, Donath M, Rouiller DG, Halban Pa. Extracellular matrix protects pancreatic β-cells against apoptosis: role of short- and long-term signaling pathways. Diabetes 2004;53:2034-2041

3.  Parnaud G, Bosco D, Berney T, Pattou F, Kerr-Conte J, Donath MY, Bruun C, Mandrup-Poulsen T, Billestrup N, Halban PA. Proliferation of sorted human and rat beta cells. Diabetologia 2008;51:91-100

4.  Huang B, Babcock H, Zhuang X. Breaking the diffraction barrier: super-resolution imaging of cells. Cell 2010;143:1047-1058

5.  Merglen A, Theander S, Rubi B, Chaffard G, Wollheim CB, Maechler P. Glucose sensitivity and metabolism-secretion coupling studied during two-year continuous culture in INS-1E insulinoma cells. Endocrinology 2004;145:667-678

6.  Minami K, Yano H, Miki T, Nagashima K, Wang CZ, Tanaka H, Miyazaki JI, Seino S. Insulin secretion and differential gene expression in glucose-responsive and -unresponsive MIN6 sublines. Am J Physiol Endocrinol Metab 2000;279:E773-781

7.  Lefebvre VH, Otonkoski T, Ustinov J, Huotari MA, Pipeleers DG, Bouwens L. Culture of adult human islet preparations with hepatocyte growth factor and 804G matrix is mitogenic for duct cells but not for beta-cells. Diabetes 1998;47:134-137

8.  Walpita D, Hasaka T, Spoonamore J, Vetere A, Takane KK, Fomina-Yadlin D, Fiaschi-Taesch N, Shamji A, Clemons PA, Stewart AF, Schreiber SL, Wagner BK. A human islet cell culture system for high-throughput screening. J Biomol Screen 2012;17:509-518

9.  Kaido T, Yebra M, Cirulli V, Rhodes C, Diaferia G, Montgomery AM. Impact of defined matrix interactions on insulin production by cultured human beta-cells: effect on insulin content, secretion, and gene transcription. Diabetes 2006;55:2723-2729

10. Kantengwa S, Baetens D, Sadoul K, Buck Ca, Halban Pa, Rouiller DG. Identification and characterization of alpha 3 beta 1 integrin on primary and transformed rat islet cells. Exp Cell Res 1997;237:394-402

11. Kanaani J, Cianciaruso C, Phelps Ea, Pasquier M, Brioudes E, Billestrup N, Baekkeskov S. Compartmentalization of GABA synthesis by GAD67 differs between pancreatic beta cells and neurons. PLoS One 2015;10:e0117130

12. Blum B, Roose AN, Barrandon O, Maehr R, Arvanites AC, Davidow LS, Davis JC, Peterson QP, Rubin LL, Melton DA. Reversal of beta cell de-differentiation by a small molecule inhibitor of the TGFβ pathway. eLife 2014;3:e02809

13. Gerdes JM, Christou-Savina S, Xiong Y, Moede T, Moruzzi N, Karlsson-Edlund P, Leibiger B, Leibiger IB, Ostenson CG, Beales PL, Berggren PO. Ciliary dysfunction impairs beta-cell insulin secretion and promotes development of type 2 diabetes in rodents. Nat Commun 2014;5:5308

14. Goto H, Inoko A, Inagaki M. Cell cycle progression by the repression of primary cilia formation in proliferating cells. Cell Mol Life Sci 2013;70:3893-3905

15. Nigg EA, Raff JW. Centrioles, centrosomes, and cilia in health and disease. Cell 2009;139:663-678

16. Wang P, Fiaschi-Taesch NM, Vasavada RC, Scott DK, Garcia-Ocana A, Stewart AF. Diabetes mellitus--advances and challenges in human beta-cell proliferation. Nat Rev Endocrinol 2015;11:201-212

17. Rulifson IC, Karnik SK, Heiser PW, Ten Berge D, Chen HN, Gu XY, Taketo MM, Nusse R, Hebrok M, Kim SK. Wnt signaling regulates pancreatic beta cell proliferation. Proc Natl Acad Sci U S A 2007;104:6247-6252

18. Aly H, Rohatgi N, Marshall CA, Grossenheider TC, Miyoshi H, Stappenbeck TS, Matkovich SJ, McDaniel ML. A novel strategy to increase the proliferative potential of adult human beta-cells while maintaining their differentiated phenotype. PLoS One 2013;8:e66131

19. Hobson A, Draney C, Stratford A, Becker TC, Lu D, Arlotto M, Tessem JS. Aurora Kinase A is critical for the Nkx6.1 mediated beta-cell proliferation pathway. Islets 2015;7:e1027854

20. Lancaster MA, Schroth J, Gleeson JG. Subcellular spatial regulation of canonical Wnt signalling at the primary cilium. Nat Cell Biol 2011;13:700-707

21. Chevrier V, Piel M, Collomb N, Saoudi Y, Frank R, Paintrand M, Narumiya S, Bornens M, Job D. The Rho-associated protein kinase p160ROCK is required for centrosome positioning. J Cell Biol 2002;157:807-817

22. Pitaval A, Tseng QZ, Bornens M, Thery M. Cell shape and contractility regulate ciliogenesis in cell cycle-arrested cells. J Cell Biol 2010;191:303-312

23. Pugacheva EN, Jablonski SA, Hartman TR, Henske EP, Golemis EA. HEF1-dependent Aurora A activation induces disassembly of the primary cilium. Cell 2007;129:1351-1363

24. Codazzi F, Di Cesare A, Chiulli N, Albanese A, Meyer T, Zacchetti D, Grohovaz F. Synergistic control of protein kinase Cgamma activity by ionotropic and metabotropic glutamate receptor inputs in hippocampal neurons. J Neurosci 2006;26:3404-3411

25. Brewer GJ, Torricelli JR, Evege EK, Price PJ. Optimized survival of hippocampal neurons in B27-supplemented neurobasal, a new serum-free medium combination. J Neurosci Res 1993;35:567-576

26. Schneider CA, Rasband WS, Eliceiri KW. NIH Image to ImageJ: 25 years of image analysis. Nat Methods 2012;9:671-675

27. JDRF nPOD Standard Operating Procedures: Immunopathology [article online], 2010. Available from http://www.jdrfnpod.org/for-investigators/standard-operating-procedures. Accessed 22 Feb 2016

28. Gustafsson MG, Shao L, Carlton PM, Wang CJ, Golubovskaya IN, Cande WZ, Agard DA, Sedat JW. Three-dimensional resolution doubling in wide-field fluorescence microscopy by structured illumination. Biophys J 2008;94:4957-4970

29. Tsuboi T, Rutter GA. Multiple forms of "kiss-and-run" exocytosis revealed by evanescent wave microscopy. Curr Biol 2003;13:563-567

30. Nagai T, Ibata K, Park ES, Kubota M, Mikoshiba K, Miyawaki A. A variant of yellow fluorescent protein with fast and efficient maturation for cell-biological applications. Nat Biotechnol 2002;20:87-90

31. Sbalzarini IF, Koumoutsakos P. Feature point tracking and trajectory analysis for video imaging in cell biology. J Struct Biol 2005;151:182-195

32. Palmer AE, Giacomello M, Kortemme T, Hires SA, Lev-Ram V, Baker D, Tsien RY. Ca2+ indicators based on computationally redesigned calmodulin-peptide pairs. Chem Biol 2006;13:521-530

33. Wiederkehr A, Szanda G, Akhmedov D, Mataki C, Heizmann CW, Schoonjans K, Pozzan T, Spat A, Wollheim CB. Mitochondrial matrix calcium is an activating signal for hormone secretion. Cell Metab 2011;13:601-611

34. Chang YC, Gottlieb DI. Characterization of the proteins purified with monoclonal antibodies to glutamic acid decarboxylase. J Neurosci 1988;8:2123-2130

35. Campbell-Thompson M, Wasserfall C, Kaddis J, Albanese-O'Neill A, Staeva T, Nierras C, Moraski J, Rowe P, Gianani R, Eisenbarth G, Crawford J, Schatz D, Pugliese A, Atkinson M. Network for Pancreatic Organ Donors with Diabetes (nPOD): developing a tissue biobank for type 1 diabetes. Diabetes Metab Res Rev 2012;28:608-617

36. Pugliese A, Yang M, Kusmarteva I, Heiple T, Vendrame F, Wasserfall C, Rowe P, Moraski JM, Ball S, Jebson L, Schatz DA, Gianani R, Burke GW, Nierras C,

Staeva T, Kaddis JS, Campbell-Thompson M, Atkinson MA. The Juvenile Diabetes Research Foundation Network for Pancreatic Organ Donors with Diabetes (nPOD) Program: goals, operational model and emerging findings. Pediatr Diabetes 2014;15:1-9

37. Rodriguez-Diaz R, Abdulreda MH, Formoso AL, Gans I, Ricordi C, Berggren PO, Caicedo A. Innervation patterns of autonomic axons in the human endocrine pancreas. Cell Metab 2011;14:45-54

38. Wang RN, Paraskevas S, Rosenberg L. Characterization of integrin expression in islets isolated from hamster, canine, porcine, and human pancreas. J Histochem Cytochem 1999;47:499-506

39. Diaferia GR, Jimenez-Caliani AJ, Ranjitkar P, Yang W, Hardiman G, Rhodes CJ, Crisa L, Cirulli V. β1 integrin is a crucial regulator of pancreatic β-cell expansion. Development 2013;140:3360-3372

40. Stendahl JC, Kaufman DB, Stupp SI. Extracellular matrix in pancreatic islets: relevance to scaffold design and transplantation. Cell Transplant 2009;18:1-12

41. Parnaud G, Hammar E, Rouiller DG, Armanet M, Halban PA, Bosco D. Blockade of beta1 integrin-laminin-5 interaction affects spreading and insulin secretion of rat beta-cells attached on extracellular matrix. Diabetes 2006;55:1413-1420

42. Banerjee M, Virtanen I, Palgi J, Korsgren O, Otonkoski T. Proliferation and plasticity of human beta cells on physiologically occurring laminin isoforms. Mol Cell Endocrinol 2012;355:78-86

43. Korpos E, Kadri N, Kappelhoff R, Wegner J, Overall CM, Weber E, Holmberg D, Cardell S, Sorokin L. The peri-islet basement membrane, a barrier to infiltrating leukocytes in type 1 diabetes in mouse and human. Diabetes 2013;62:531-542

44. Geron E, Boura-Halfon S, Schejter ED, Shilo BZ. The Edges of Pancreatic Islet beta Cells Constitute Adhesive and Signaling Microdomains. Cell Rep 2015;10:317-325

45. Cebecauer M, Heaslip AT, Nelson SR, Lombardo AT, Beck Previs S, Armstrong J, Warshaw DM. Cytoskeletal Dependence of Insulin Granule Movement Dynamics in INS-1 Beta-Cells in Response to Glucose. PLoS One 2014;9:e109082

46. Zhu X, Hu R, Brissova M, Stein RW, Powers AC, Gu G, Kaverina I. Microtubules negatively regulate insulin secretion in pancreatic β cells. Dev Cell 2015;34:656-668

47. Arous C, Halban PA. The skeleton in the closet: actin cytoskeletal remodeling in beta-cell function. Am J Physiol Endocrinol Metab 2015;309:E611-620

48. Schermelleh L, Carlton PM, Haase S, Shao L, Winoto L, Kner P, Burke B, Cardoso MC, Agard DA, Gustafsson MG, Leonhardt H, Sedat JW. Subdiffraction multicolor imaging of the nuclear periphery with 3D structured illumination microscopy. Science 2008;320:1332-1336

49. Plotnikova OV, Pugacheva EN, Golemis EA. Primary cilia and the cell cycle. Methods Cell Biol 2009;94:137-160

50. Bosco D, Gonelle-Gispert C, Wollheim CB, Halban PA, Rouiller DG. Increased intracellular calcium is required for spreading of rat islet beta-cells on extracellular matrix. Diabetes 2001;50:1039-1046

51. Brun PJ, Grijalva A, Rausch R, Watson E, Yuen JJ, Das BC, Shudo K, Kagechika H, Leibel RL, Blaner WS. Retinoic acid receptor signaling is required to maintain glucose-stimulated insulin secretion and beta-cell mass. FASEB J 2015;29:671-683

52. Johnson JD, Bernal-Mizrachi E, Alejandro EU, Han Z, Kalynyak TB, Li H, Beith JL, Gross J, Warnock GL, Townsend RR, Permutt MA, Polonsky KS. Insulin protects islets from apoptosis via Pdx1 and specific changes in the human islet proteome. Proc Natl Acad Sci U S A 2006;103:19575-19580

53. Aguayo-Mazzucato C, Zavacki AM, Marinelarena A, Hollister-Lock J, El Khattabi I, Marsili A, Weir GC, Sharma A, Larsen PR, Bonner-Weir S. Thyroid hormone

promotes postnatal rat pancreatic beta-cell development and glucose-responsive insulin secretion through MAFA. Diabetes 2013;62:1569-1580

54. Rodriguez-Diaz R, Menegaz D, Caicedo A. Neurotransmitters act as paracrine signals to regulate insulin secretion from the human pancreatic islet. J Physiol 2014;592:3413-3417

55. Marquard J, Otter S, Welters A, Stirban A, Fischer A, Eglinger J, Herebian D, Kletke O, Klemen MS, Stozer A, Wnendt S, Piemonti L, Kohler M, Ferrer J, Thorens B, Schliess F, Rupnik MS, Heise T, Berggren PO, Klocker N, Meissner T, Mayatepek E, Eberhard D, Kragl M, Lammert E. Characterization of pancreatic NMDA receptors as possible drug targets for diabetes treatment. Nat Med 2015;21:363-372

56. Choi DW, Mauluccigedde M, Kriegstein AR. Glutamate neurotoxicity in cortical cell-culture. J Neurosci 1987;7:357-368

57. Cabrera O, Berman DM, Kenyon NS, Ricordi C, Berggrern PO, Caicedo A. The unique cytoarchitecture of human pancreatic islets has implications for islet cell function. Proc Natl Acad Sci U S A 2006;103:2334-2339

58. Jaques F, Jousset H, Tomas A, Prost AL, Wollheim CB, Irminger JC, Demaurex N, Halban PA. Dual effect of cell-cell contact disruption on cytosolic calcium and insulin secretion. Endocrinology 2008;149:2494-2505

59. Benninger RK, Piston DW. Cellular communication and heterogeneity in pancreatic islet insulin secretion dynamics. Trends Endocrinol Metab 2014;25:399-406

# CHAPTER 3

# Aberrant accumulation of the diabetes autoantigen

# GAD65 in Golgi membranes in conditions of

# ER stress and autoimmunity

Adapted from the original manuscript

Edward A. Phelps, Chiara Cianciaruso, Iacovos P. Michael, Miriella Pasquier,

Jamil Kanaani, Rita Nano, Vanessa Lavallard, Nils Billestrup, Jeffrey A. Hubbell,

Steinunn Baekkeskov

## 3.1 ABSTRACT

Pancreatic islet beta cells are particularly susceptible to endoplasmic reticulum (ER) stress, which is implicated in beta cell dysfunction and loss during the pathogenesis of type 1 diabetes (T1D). The peripheral membrane protein GAD65 is an autoantigen in human T1D. GAD65 synthesizes GABA, an important autocrine and paracrine signaling molecule and a survival factor in islets. We show that ER stress in primary beta cells perturbs the palmitoylation cycle controlling GAD65 endomembrane distribution, resulting in aberrant accumulation of the palmitoylated form in *trans*-Golgi membranes. The palmitoylated form has heightened immunogenicity, exhibiting increased uptake by antigen presenting cells and T cell stimulation compared to the non-palmitoylated form. Similar accumulation of GAD65 in Golgi membranes is observed in human beta cells in pancreatic sections from GAD65 autoantibody positive individuals, who have not yet progressed to clinical onset of T1D, and T1D patients with residual beta cell mass and ongoing T cell infiltration of islets. We propose that aberrant accumulation of immunogenic GAD65

in Golgi membranes facilitates inappropriate presentation to the immune system following release from stressed and/or damaged beta cells, triggering autoimmunity.

## 3.2  INTRODUCTION

The GABA-synthesizing enzyme glutamic acid decarboxylase (GAD) exists in two isoforms, GAD65 and GAD67, encoded by different genes (1). The smaller isoform, GAD65, is an early target of autoimmunity in 70-80% of patients who develop T1D (2-4). Rat and human beta cells primarily express GAD65, while no GAD65 is detected at the protein level in mouse beta cells (5,6). Our understanding of how GAD65 becomes an autoantigen in T1D is limited due to the lack of this protein in beta cells of mice, and therefore an apparent lack of a significant role in the pathogenesis of diabetes in the highly studied NOD mouse model of T1D (7).

The GAD65 enzyme is synthesized in the cytosol as a hydrophilic cytosolic molecule, which undergoes hydrophobic post-translational modifications in the N-terminal domain to become membrane anchored (8-11). The first step of hydrophobic modifications is irreversible and results in a hydrophobic form that targets specifically to the cytosolic face of endoplasmic reticulum (ER) and *cis*-Golgi membranes, establishing an equilibrium between membrane and cytosolic pools (12). The second step of modifications, which include stabilization of membrane anchoring followed by a reversible double palmitoylation of cysteines 30 and 45 (10) by a Golgi localized protein acyl transferase (PAT) DHHC17 (also known as HIP14) (13), result in trapping of GAD65 in Golgi membranes, sorting to the *trans*-Golgi network (TGN) and targeting to an axonal vesicular pathway in route to synaptic vesicles in presynaptic clusters in neurons and to peripheral vesicles in beta cells (12,14,15). Palmitoylation is not required for anchoring of GAD65 to Golgi membranes but is critical for anterograde targeting of GAD65 from *cis*-Golgi to TGN membranes and post-Golgi peripheral vesicles (12). A depalmitoylation step by an acyl protein

thioesterase (APT) can release GAD65 from peripheral vesicle membranes and/or TGN membranes mediating retrograde trafficking back to Golgi membranes by a non-vesicular pathway. The protein can then enter a cycle of re-palmitoylation and de-palmitoylation (12). Palmitoylation is suggested to serve a critical function in regulating the rate of GABA synthesis in the presynaptic compartment of neurons (16,17).

Pancreatic beta cells have a well-developed, extensive, and highly active ER, reflecting their role in synthesizing and secreting large amounts of insulin. When the protein synthesis and secretion machinery becomes overloaded, either due to a high physiological demand on a limited number of cells or from exogenous stressors such as inflammation or a diet high in fatty acids, the accumulation of unfolded and improperly folded proteins transiting through the ER results in the cell experiencing a state of ER stress (18). Beta cells are highly sensitive to ER stress, which is implicated in the pathogenesis of T1D (19-22). It has been proposed that the initiation of autoimmunity against the beta cell follows an initial period of prolonged beta cell ER stress and apoptosis, induced by inflammatory cytokines secreted by early invading immune cells as well as the beta cells themselves (19,23).

Here we report a dramatic effect of ER stress on the subcellular distribution of the T1D autoantigen GAD65 in primary rat and human beta cells and accumulation of a more highly immunogenic palmitoylated form in Golgi membranes. A similar accumulation is detected in pancreatic sections of human GAD65 autoantibody positive individuals and T1D patients.

## 3.3  METHODS

### 3.3.1  Cell cultures

INS-1E rat insulinoma cells (24) were cultured in RPMI 1640 with GlutaMAX, 10% FBS, 1% Penicillin/Streptomycin (P/S), 1 mM sodium pyruvate, 10 mM HEPES, and 50 μM β-mercaptoethanol. The DR4 (DRA1*0101, DRB1*0401) positive human EBV-transformed B cell line Priess (25) was cultured in IMDM GlutaMAX medium with 10% FBS, and 1% P/S. A DR4 (DRA1*0101, DRB1*0401) restricted mouse T cell hybridoma cell line T33.1, recognizing the GAD65 aa 274-286 epitope (GAD65$^{274-286}$) (26), was cultured in RPMI 1640 with GlutaMAX, 10% FBS, 1% P/S, and 0.1% β-mercaptoethanol. Primary rat hippocampal neurons were prepared from 2- to 3-day-old Sprague Dawley rats as described by Codazzi et al (27).

### 3.3.2  Islet culture

Rat islets isolated from P5 Sprague Dawley rats as previously described (15) were cultured in RPMI 1640, 10% FBS, and 1% P/S at 37°C, 5% $CO_2$. Human islets were cultured in CMRL 1066 with 2 mM L-Glutamine, 25 mM HEPES, 10% FBS, and 1% P/S at 25°C, 5% $CO_2$.

### 3.3.3  Islet single cell cultures

Rat or human islets dissociated into single cells by digestion with trypsin-EDTA were cultured at 50,000 cells/well on laminin-coated Thermanox coverslips (Nunc) or 100,000 cells/well on Fluorodishes (World Precision Instruments) in MEM, 11 mM glucose, 5% FBS, 1 mM Sodium Pyruvate, 10 mM HEPES, 1X B-27 (Gibco), and 1% P/S at 37°C, 5% $CO_2$.

### 3.3.4 Human pancreatic sections

Human pancreatic sections were obtained from the Juvenile Diabetes Research Foundation (JDRF) Network for Pancreatic Organ Donors with Diabetes (nPOD) tissue bank (28; 29). Sections were obtained from 8 autoantibody negative healthy donors with normal islets (Supplementary Table 1), 8 potentially prediabetic individuals positive for GAD65 autoantibodies (GADA+) (Supplementary Table 2), and 8 autoantibody positive T1D patients, including 6 who were GADA+ (Supplementary Table 3). Donors were selected to have remaining insulin positive beta cells to enable analyses of the subcellular localization of GAD65. Furthermore, we sought to include individuals, who were reported by nPOD as positive for CD3+ T cell infiltration and/or insulitis (Supplementary Tables 2 and 3). Insulitis is defined by nPOD as the presence of 6 or more CD3+ T cells immediately adjacent to or within 3 or more islets of a defined minimum size in pancreatic sections (30).


### 3.3.5 Immunofluorescence staining

Human pancreas sections were deparaffinized followed by acidic-pH heat-mediated antigen retrieval. Cultures of single pancreatic islet cells were fixed with 4% PFA. Samples were blocked and permeabilized in PBS + 0.3% Triton X-100, 10% goat or donkey serum. Primary antibodies (CHOP, Santa Cruz, sc-575, 1:100; GAD6, mouse monoclonal antibody against C-terminus of GAD65 (31), 1:1000; N-GAD65 mAb, mouse monoclonal antibody against N-terminus of GAD65 (32), 1:300; Giantin, Abcam, ab24586, 1:1000; Insulin, Linco 4011-01, 1:10,000; Insulin, Abcam, ab14042, 1:2,000; CD3, Dako M7254, 1:30) were incubated overnight at 4°C in PBS + 0.3% Triton X-100, 1% goat or donkey serum. Alexa Fluor conjugated secondary antibodies (Molecular Probes) were incubated at 1:200 dilution in PBS + 0.3% Triton X-100 for 30 min at room temperature.

### 3.3.6  Image capture, analysis, and quantification

Samples were imaged on a Zeiss LSM700 confocal microscope with 63x/1.40 NA Plan-Apochromat oil-immersion objective for single islet cells and 40x/1.30 NA Plan-Apochromat oil-immersion objective for pancreatic tissue sections. All images for quantification within a single experiment were captured with the same laser power and detector gain. The ratio of GAD65 mean fluorescence intensity in the Golgi compartment and post-Golgi vesicles compared to the rest of the cytosol was calculated with a custom ImageJ macro. Individual beta cells in a given field of view were identified and outlined by hand. For each cell, the macro automatically defined a region of interest (ROI) outlining the Golgi compartment, identified by giantin co-stain or by characteristic morphology and brightness thresholding of GAD65 stain, and GAD65+ vesicles, identified by brightness thresholding of GAD65+ bright puncta. A second ROI defined the remainder of the cell, excluding the Golgi, GAD65+ vesicles, and nucleus. GAD65 Golgi accumulation was reported as the ratio of mean fluorescence intensity (MFI) for the two ROIs.

### 3.3.7  SDS-PAGE and Western Blotting

Gel electrophoresis was performed with the NuPAGE system (Invitrogen) with transfer onto PVDF membranes with the iBlot 2.0 (Life Technologies) device. Membranes were blocked with Odyssey Blocking Buffer (LI-COR Biosciences), incubated in primary antibody (GAD1701, a custom antibody against C-terminus of GAD67 that reacts equally well with GAD65 and GAD67 (5), 1:5000) overnight at 4°C, and detected with secondary antibody IRDye 800CW (LI-COR Biosciences). Blots were imaged on the LI-COR Odyssey scanner.

### 3.3.8 Treatment of cells to induce ER stress

Sodium palmitate (1 mM) (Sigma-Aldrich) was conjugated to fatty-acid-free BSA (0.17 mM) (Calbiochem) in 150 mM NaCl pH 7.4 for 1 h. Stock palmitate-BSA (1 mM palmitate, 0.17 mM BSA) was added to culture media to achieve a final palmitate concentration of either 0.1 mM or 0.5 mM. A stock solution of BSA (0.17 mM BSA) without palmitate was added to the control (untreated) wells. Thapsigargin (Invitrogen) was used at a final concentration of 2 µM. Rat IFNγ and rat IL-1β (R&D Systems) were used at a final concentration of 10 U/ml for each.

### 3.3.9 Fluorescence recovery after photobleaching imaging and analysis

Fluorescence recovery after photobleaching (FRAP) experiments were performed on a Zeiss LSM700 confocal microscope with environmental stage at 512x512 pixel resolution, 1% laser power and 1.94 s frame interval. GAD65-GFP fluorescence in the Golgi compartment of transfected cells, treated or not to induce ER stress, was bleached with 50% laser power. Time-stacks of GAD65-GFP fluorescence recovery in the Golgi compartment were double normalized for percentage of initial intensity and whole cell photobleaching in ImageJ. Two-phase and single-phase association curves were plotted in Graphpad Prism to obtain half-time of recovery.

### 3.3.10 S-acylation resin-assisted capture (Acyl Rac) palmitoylation assay

Acyl-RAC on recombinant human GAD65 (rhGAD65, FIRS Laboratories, RSR) was performed as described by Forrester, et al. (33).

### 3.3.11 Uptake of GAD65-488 by Priess Cells

rhGAD65 was depalmitoylated overnight by treatment with 200 mM HA and labeled with DyLight 488 NHS Ester (Thermo Fisher Scientific). Palmitoylated or depalmitoylated GAD65-488 was incubated at 10 µg/ml with 50,000 Priess cells/well in 96-well plates. Cells were stained with LIVE/DEAD® Aqua (Molecular Probes) and analyzed by Cyan Flow Cytometer (Beckman Coulter) and FlowJo software.

### 3.3.12 Activation of GAD65-specific T cells

Unmodified rhGAD65 containing native palmitate modifications or HA-treated depalmitoylated GAD65 were incubated overnight with 50,000 Priess cells/well at 2 µg/ml in 96-well plates. GAD65 loaded Priess cells were then incubated for 24 h with 30,000 T33.1 T cells. IL2 secretion was analyzed by ELISA kit (eBioscience).

### 3.3.13 Plasmids

Generation of GAD65-GFP and GAD65(C30,45A)-GFP was described previously (11,12,14). INS-1E and primary rat islet cells were transfected by Lipofectamine 2000 (Invitrogen).

### 3.3.14 Statistics

Means among three or more groups were compared by analysis of variance (ANOVA) in GraphPad Prism 6 software. If deemed significant, Tukey's post-hoc pairwise comparisons were performed. Means between two groups were compared using Student's *t*-test. A confidence level of 95% was considered significant.

### 3.3.15 Ethical approval

Animals were used under EPFL animal regulation guidelines and an IACUC approved protocol. Human islets were received from the University Hospital of Geneva and San Raffaele Scientific Institute, Milan through the European Consortium for Islet Transplantation (ECIT) islets for basic research program ECIT and were approved by the Institutional Review Board of the University Hospital of Geneva (CER Nr. 05–028) and by the Ethics Committee of the San Raffaele Scientific Institute of Milan (IPF002-2014). Human pancreatic sections obtained via the nPOD tissue bank, University of Florida, Gainesville, FL, USA were harvested from cadaveric organ donors by certified organ procurement organizations partnering with nPOD in accordance with organ donation laws and regulations and classified as "Non-Human Subjects" by the University of Florida Institutional Review Board (28,29). EPFL grants permit for the use of human material as long as the provider can certify that the samples were obtained according to local laws and regulations, as well as good practices in the country were they were collected.

## 3.4 RESULTS

### 3.4.1 ER stress results in accumulation of GAD65 in the Golgi compartment

Primary rat and human beta cells derived from dissociated whole islets were cultured as monolayers on coverslips to allow for high-resolution confocal microscopy. The monolayer islet cells were fixed and immunostained for insulin, GAD65, and the Golgi marker giantin (**Figure 1**). As previously reported (15), GAD65 is detected diffuse in the cytosol as well as in Golgi membranes and post-Golgi vesicles in beta cells. Insulin is detected in distinct large dense core vesicles (LDCVs).

92
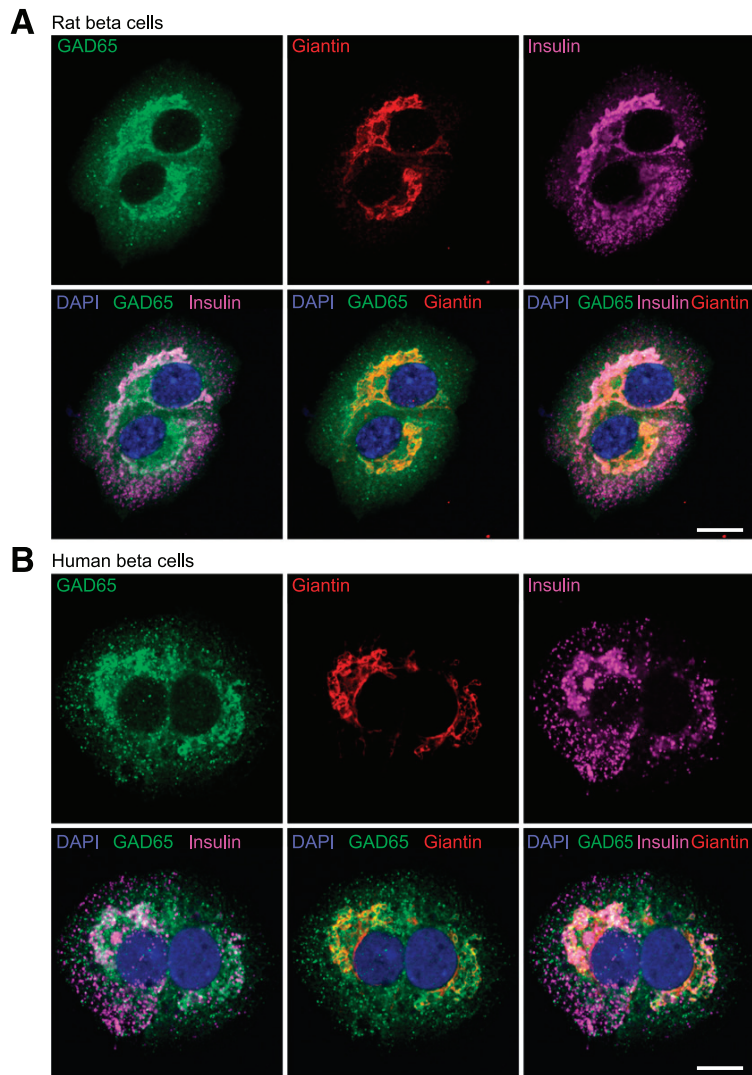
**Figure 1**. **Confocal analyses of GAD65 localization in primary beta cells.**

(**A**) Primary rat beta cells immunostained for GAD65 and giantin (Golgi) show a subcellular distribution of GAD65 in the cytosol and the Golgi compartment. Apart from the Golgi compartment, GAD65 is localized to vesicles, which are distinct from insulin granules. The confocal images are representative of similar analyses of 7 independent isolations of rat islets. Scale bar 10 μm. (**B**) Immunostaining of primary human beta cells for GAD65, giantin, and insulin reveals localization of GAD65 in the Golgi compartment as well as in peripheral vesicles distinct from insulin containing vesicles. The confocal images are representative of similar analyses of independent isolations of human islets from 4 donors. Scale bar 10 μm.

To induce mild ER stress, primary islet cell monolayers were subjected to a 48 h time course of low levels (10 U/ml) of the inflammatory cytokines IL-1β and IFNγ or overnight treatment with the saturated fatty acid palmitate (500 μM) (**Figure 2**), both of which have been previously shown to trigger ER stress in beta cells (34-36). Cells

were also treated for 8 h with thapsigargin, which is a potent ER stress inducing agent (37) (**Figure 2**). We monitored ER stress by nuclear translocation of CHOP, a multifunctional transcription factor in the ER stress response (**Figure 2**).

The different treatment conditions resulted in varying degrees of ER stress as shown by the timeframe until nuclear translocation of CHOP, indicating that the different treatment conditions affected the cells with variable strength and specificity. While incubation with thapsigargin or palmitate induced CHOP activation at 8 and 18 h respectively, CHOP activation was detected at 48 h (but not 24 h) of cytokine treatment (**Figure 2**). Notably, all three treatment conditions resulted in a marked increase in the Golgi-localization of GAD65 (**Figure 2**). Accumulation of GAD65 in Golgi membranes during palmitate induced ER stress was also observed in primary human beta cells and in another cell type expressing GAD65, primary rat hippocampal GABA-ergic neurons (**Supplementary Figure 1**).
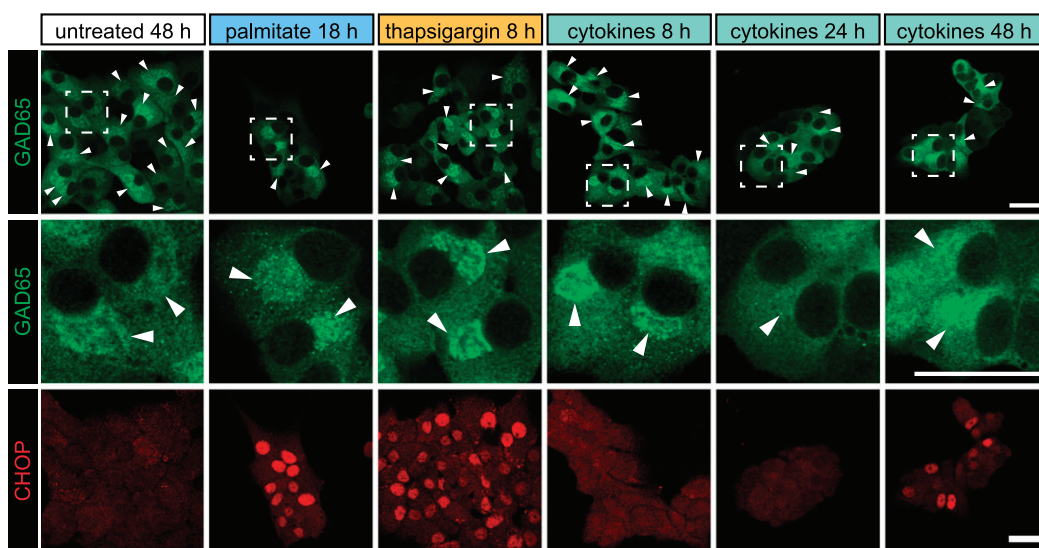


**Figure 2. Activation of ER stress pathways in beta cells by thapsigargin, palmitate, or inflammatory cytokines.**

Primary rat beta cells were treated with palmitate (500 µM, 18 h), thapsigargin (2 µM, 8 h), or cytokines (10 U/ml, 8, 24, or 48 h) to induce ER stress and immunostained for GAD65 (top two panels) and CHOP (bottom panel). GAD65 positive Golgi compartments are indicated by arrowheads. For all three treatment modules, GAD65 expression in the Golgi compartment becomes noticeably brighter. Middle panels show increased magnification of framed regions in the top panels. The confocal images are representative of similar analyses of 6 independent isolations of rat islets. Scale bars 10 µm.

Accumulation of GAD65 in the Golgi compartment during induction of ER stress by either palmitate or thapsigargin was confirmed by co-staining for the Golgi marker giantin (**Figure 3A, Supplementary Figure 1A-C**) but Golgi structures are also clearly identifiable by GAD65 localization in both beta cells and neurons (12,15,38). Quantification following a two hour incubation with either palmitate or thapsigargin revealed a significant accumulation of GAD65 in the Golgi compartment (**Figure 3B, Supplementary Figure 1D**).
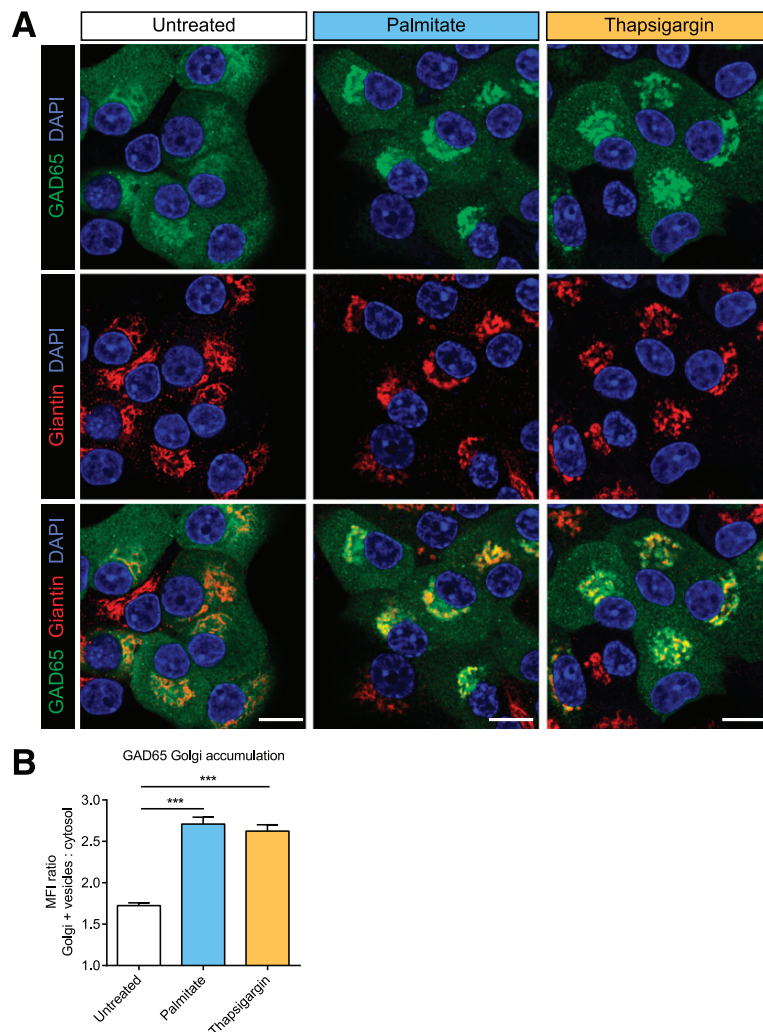


**Figure 3. Treatment of beta cells with palmitate or thapsigargin promotes Golgi accumulation of GAD65.**
(**A**) Primary rat beta cells were treated with palmitate (500 µM, 2 h) or thapsigargin (2 µM, 2 h) to induce ER stress and immunostained for GAD65 and Giantin. Scale bars 10 µm. (**B**) Image quantification of GAD65 accumulation in the Golgi compartment reported as the ratio of MFI for GAD65 in the Golgi compartment and GAD65-positive vesicles to MFI for GAD65 in the rest of the cell excluding the

nucleus. Results are presented as mean ± SEM (n = 39-43 beta cells from 8 image fields analyzed per condition. Cells positive for giantin and negative for GAD65 represent non-beta islet cells). Data were analyzed using one-way ANOVA followed by Tukey's multiple comparisons test (** $P < 0.001$). Analyses of accumulation of GAD65 in Golgi membranes in rat beta cells, human beta cells, and rat hippocampal neurons incubated with palmitate for 2 h is shown in Supplementary Figure 1.

The time course of accumulation of GAD65 in Golgi membranes during palmitate induced ER stress was studied further. Rat islet cell monolayers were treated with 100 µM or 500 µM of palmitate for 10 min, 2 h, and 18 h and immunostained for CHOP, GAD65, and insulin (**Figure 4, Supplementary Figure 2**). Golgi accumulation of GAD65 occurred almost immediately upon addition of palmitate and was clearly visible at 10 min (**Figure 4A, Supplementary Figure 2A**). The strong Golgi accumulation of GAD65 persisted at 2 h and was still visible at 18 h, although the intensity began to fade coinciding with activation of CHOP (**Figure 4C,D**). Quantification of GAD65 membrane accumulation showed a statistically significant increase in the ratio of MFI for GAD65 in the Golgi compartment for cells incubated for 10 min and 2 h in 100 or 500 µM palmitate (**Figure 4B**). Across all conditions and time points there were no notable changes in the subcellular localization of insulin (**Supplementary Figure 2B**). Taken together the results indicate that induction of ER stress results in aberrant accumulation of GAD65 in the Golgi compartment.
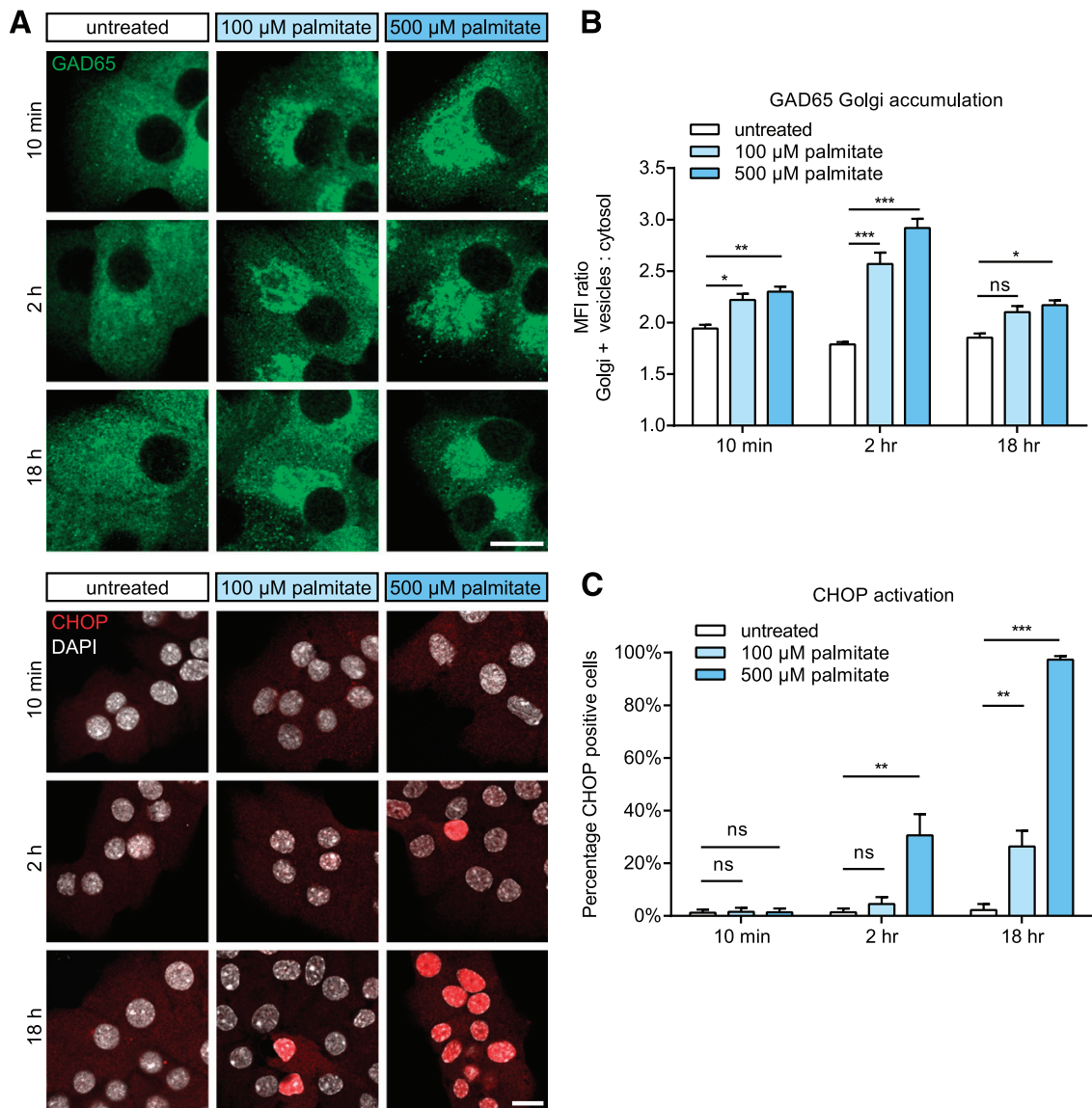
**Figure 4. Time course of Golgi accumulation of GAD65 upon palmitate treatment.**

(**A**) Confocal analyses of monolayer cultures of primary rat beta cells  treated or not with 100 µM palmitate, or 500 µM palmitate for 10 min, 2 h, and 18 h respectively. Fixed cells were immunostained for GAD65 and CHOP. Scale bar 10 µm. (**B**) Image quantification of GAD65 accumulation in the Golgi compartment reported as the ratio of MFI for GAD65 in the Golgi and GAD65-positive vesicles to MFI for GAD65 in the rest of the cell excluding the nucleus. Results are presented as mean ± SEM ($n$ = 28-45 cells from 4-5 image fields analyzed per condition). Data were analyzed using two-way ANOVA followed by Tukey's multiple comparisons test (* $P < 0.05$, ** $P < 0.01$ and *** $P < 0.001$). (**C**) Image quantification of CHOP positive nuclei as a percentage of total nuclei. Results are presented as mean ± SEM ($n$ = 4-10 image fields analyzed per condition). Data were analyzed using two-way ANOVA followed by Tukey's multiple comparisons test (* $P < 0.05$, ** $P < 0.01$ and *** $P < 0.001$). Corresponding lower magnification images of primary beta rat beta cells stained for GAD65 and insulin are shown in Supplementary Figure 2.

### 3.4.2 Palmitoylation is required for GAD65 accumulation in the Golgi compartment during ER stress

The distribution of GAD65 between ER/*cis*-Golgi and TGN/vesicular membranes is controlled by its palmitoylation/depalmitoylation/repalmitoylation cycle. While palmitoylation of cysteines 30 and 45 is not required for firm anchoring of GAD65 to Golgi membranes, it is critical for its anterograde trafficking from *cis*-Golgi to TGN membranes and targeting to post-Golgi vesicles (12). We assessed whether a palmitoylation-deficient mutant of GAD65 was capable of accumulating in the Golgi compartment in beta cells undergoing ER stress. Primary rat beta cells were transfected with either wild-type (WT) GAD65-GFP or palmitoylation deficient GAD65(C30,45A)-GFP, and treated with palmitate or thapsigargin for 1 h to induce ER stress. Cells were imaged live by confocal microscopy and the images were measured for MFI of GAD65-GFP in the Golgi compartment (**Figure 5**). ER stress induced by palmitate or thapsigargin significantly increased the fraction of WT GAD65-GFP in Golgi and vesicle membranes, while palmitoylation-deficient GAD65(C30,45)-GFP was unaffected (**Figure 5**). Thus, Golgi accumulation of GAD65 in response to ER stress is restricted to palmitoylation competent GAD65.
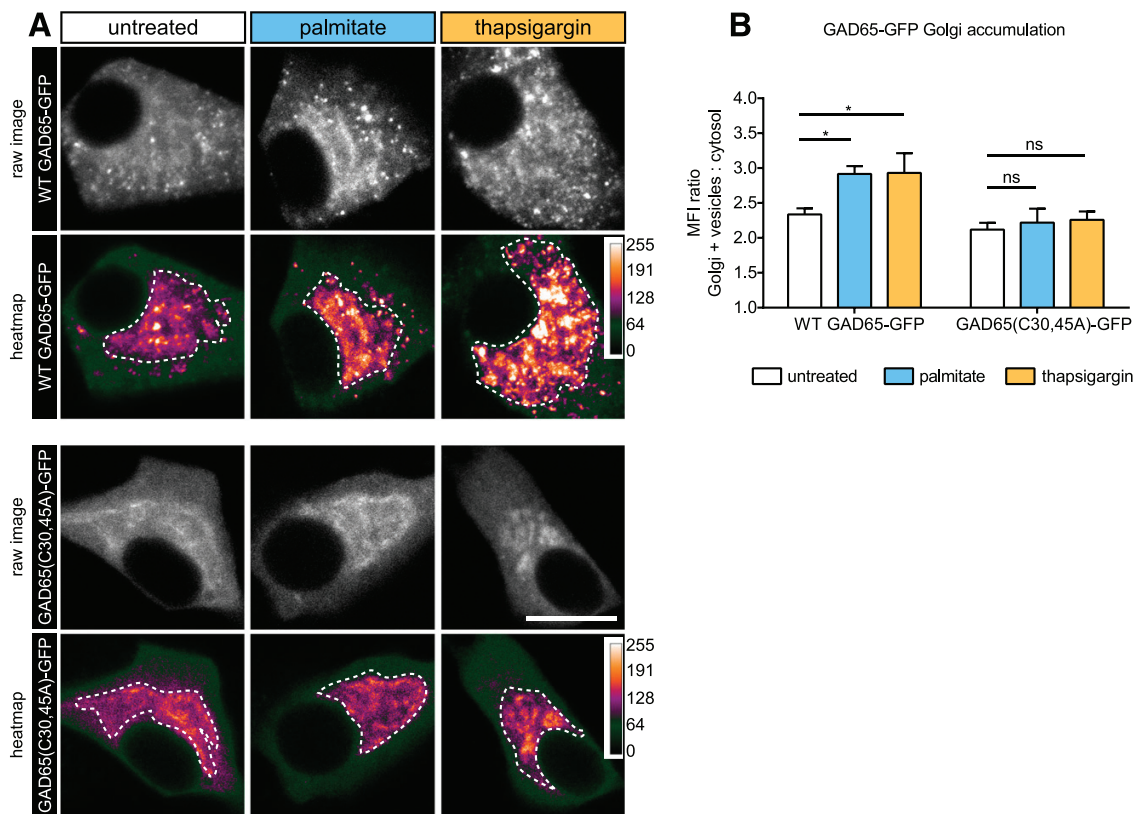
**Figure 5. Palmitoylation is required for Golgi accumulation of GAD65.**
(**A**) Primary rat beta cells were transfected with either WT GAD65-GFP or the palmitoylation deficient mutant GAD65(C30,45A)-GFP and imaged live following a 1 h treatment with palmitate (500 μM) or thapsigargin (2 μM) to induce ER stress. Images are also displayed with a heat-map to highlight the increase in Golgi and vesicle brightness. Golgi regions are indicated with a dashed outline. Scale bar 10 μm. (**B**) Image quantification of GAD65 accumulation in the Golgi compartment expressed as the ratio of MFI for GAD65 in the Golgi and GAD65-positive vesicles to MFI for GAD65 in the rest of the cell excluding the nucleus. Results are presented as mean ± SEM ($n$ = 6-10 cells analyzed per condition). Data were analyzed using one-way ANOVA followed by Tukey's multiple comparisons test (* $P < 0.05$).

### 3.4.3 Recovery of wild-type but not palmitoylation-deficient GAD65 in the Golgi compartment after photobleaching is inhibited during ER stress

We next assessed the effect of ER stress on the kinetics of replenishment of WT GAD65-GFP as well as the palmitoylation deficient mutant GAD65(C30,45A)-GFP into Golgi membranes following irreversible photobleaching. We previously reported that the fluorescence recovery after photobleaching (FRAP) of WT GAD65-GFP in Golgi membranes involves two pools of the protein, a rapid pool and a slow

pool (12). The rapid Golgi replenishment pool represents the non-palmitoylated form of GAD65, which has undergone the first step of hydrophobic modifications resulting in weak on/off membrane association. The second and slower replenishment pool represents palmitoylation competent GAD65, which, following anterograde vesicular trafficking to the TGN and periphery, can undergo depalmitoylation and non-vesicular retrograde trafficking back to Golgi membranes. INS-1E cells (**Figure 6A-D**) and primary rat islet cells (**Supplementary Figures 3,4**) were subjected to irreversible photobleaching of the Golgi compartment. Recovery of GAD65-GFP in Golgi membranes was recorded for untreated cells and for cells pre-treated with palmitate (**Figure 6, Supplementary Figure 3**) or thapsigargin (**Supplementary Figure 4**) for 1 hour to induce early-stage ER stress. Analysis of the data was performed using non-linear regression, assuming one or multiple pools of replenishing protein. Induction of ER stress significantly impaired the Golgi replenishment kinetics of WT GAD65-GFP in INS-1E cells treated with palmitate (**Figure 6C,D**) and in primary islet cells treated with either palmitate (**Supplementary Figure 3**) or thapsigargin (**Supplementary Figure 4**). In contrast, the Golgi replenishment kinetics of palmitoylation deficient GAD65(C30,45A)-GFP was similar for both untreated and treated cells (**Figure 6C,D, Supplementary Figures 3,4**). Calculations of half time of recovery of the rapid and slow pools of WT GAD65-GFP, revealed that while the half time of recovery of the rapid pool replenishing the Golgi was minimally or not affected, the half time of recovery of the slow pool was increased 3-4 fold (**Figure 6C,D, Supplementary Figures 3,4**). The results of these experiments indicate that ER stress, whether induced by palmitate or thapsigargin, inhibits and perturbs the palmitoylation cycle of WT GAD65-GFP.
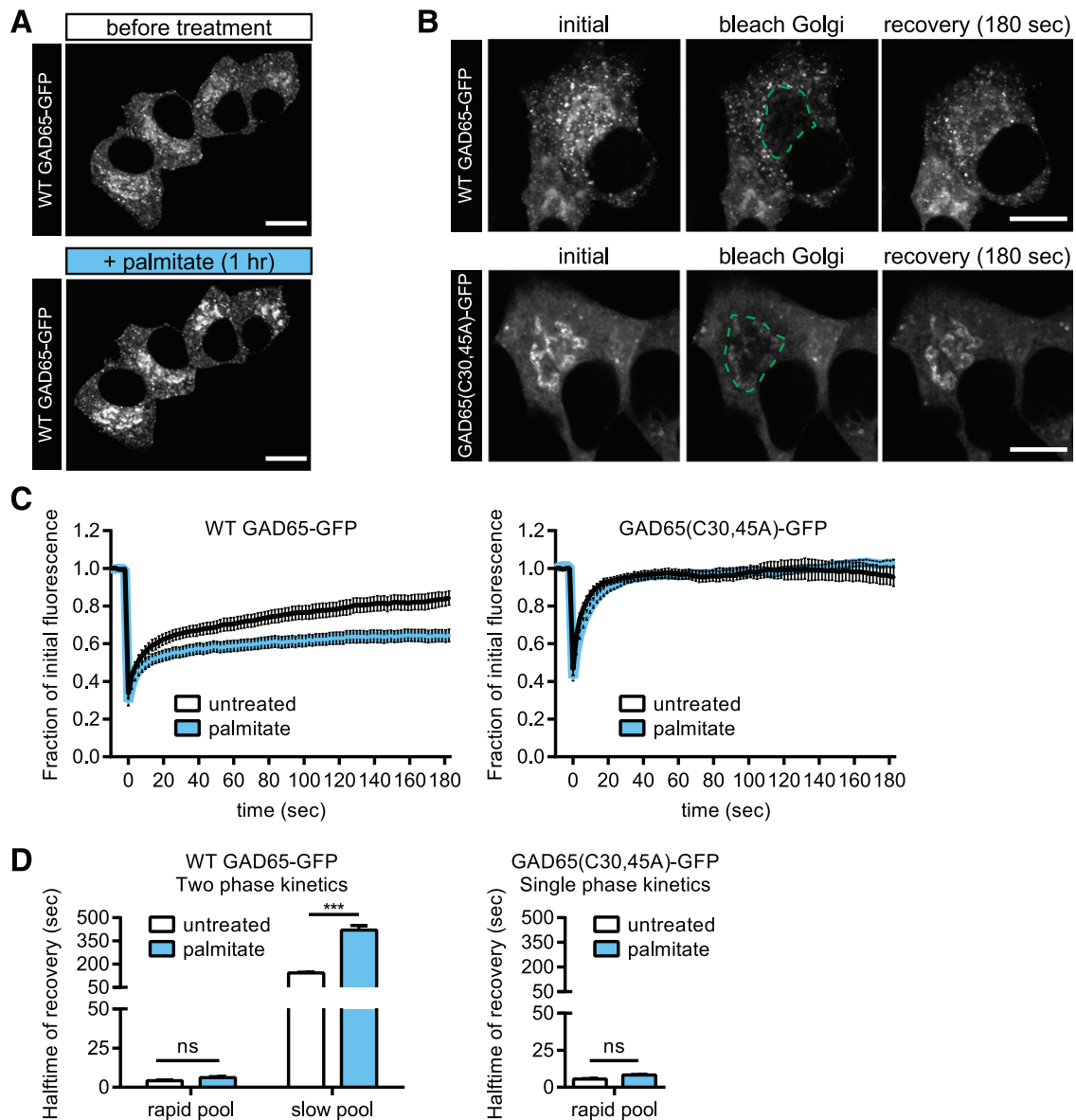
**Figure 6. Fluorescence recovery after photobleaching in the Golgi of WT but not palmitoylation-deficient GAD65 is inhibited during ER stress.**

(**A**) Live cell images of INS-1E cells transfected with GAD65-GFP before and after treatment with palmitate (500 µM) for 1 h show accumulation of GAD65-GFP in the Golgi. Scale bar 10 µm. (**B**) Representative images from FRAP analyses of INS-1E cells expressing either WT GAD65-GFP or palmitoylation-deficient GAD65(C30,45A)-GFP. The entire Golgi compartment was photobleached and recovery of fluorescence was followed by live cell imaging. Scale bar 10 µm. (**C**) Kinetics of fluorescence recovery after bleaching the entire Golgi-associated pool of WT GAD65-GFP or GAD65(C30,45A) in INS-1E cells pretreated or not with palmitate for 1 h. Results from a representative experiment are presented as mean ± SEM (*n* = 10 cells per condition). (**D**) Calculated halftimes of Golgi fluorescence recovery in INS-1E cells following photobleaching. WT GAD65-GFP exhibits two-phase recovery kinetics corresponding to a rapid as well as a slow recovery pool, while palmitoylation-deficient

GAD65(C30,45A)-GFP exhibits single-phase recovery kinetics corresponding to a rapid recovery pool. Results are presented as the mean halftime of recovery ± SEM $(n$ = 3 independent experiments, 10 cells per experiment). Data were analyzed by Student's $t$-test comparing the halftime parameter between the association curve fits of the combined data set from three independent experiments (*** P < .001). FRAP analyses of GAD65 Golgi recovery in primary rat beta cells treated with palmitate or thapsigargin are shown in Supplementary Figure 3 and Supplementary Figure 4, respectively.

### 3.4.4 Uptake and processing of GAD65 by antigen presenting B lymphocytes is enhanced by palmitoylation

Given that modification of peptides and proteins by palmitoylation may enhance their immunogenicity (39), we assessed whether the palmitoylation state of GAD65 has an effect on its uptake by antigen presenting cells (APCs) and/or activation of T cells in an APC / T-cell co-culture assay. Recombinant human GAD65 produced in yeast was depalmitoylated by thiol-acyl cleavage with hydroxylamine (HA), and depalmitoylation was confirmed biochemically by the S-acylation resin-assisted capture (Acyl-RAC) assay (33) (**Figure 7A**). Analyses of uptake of DyLight-488 labeled palmitoylated and non-palmitoylated GAD65 by the HLA-DR4 (DRB1*0401) positive human B-cell line Priess revealed a 2.5 fold increase in uptake of palmitoylated compared to the de-palmitoylated GAD65 (**Figure 7B**). Furthermore, Priess cells were loaded with palmitoylated or depalmitoylated GAD65 and used as APCs to stimulate the GAD65 specific HLA-DR4 (DRB1*0401)-restricted murine T-cell hybridoma line T33.1 that recognizes the GAD65[274-286] epitope. In this APC / T cell co-culture assay, presentation of palmitoylated GAD65 induced a 3-fold higher secretion of IL-2 by T33.1 cells compared to the depalmitoylated protein (**Figure 7C**). Taken together, the results indicate that palmitoylation facilitates uptake and processing of GAD65 by APCs resulting in increased antigen-specific stimulation of T cells. Thus the palmitoylated form of GAD65 that accumulates in Golgi during ER stress has higher immunogenicity, consistent with a possible role of ER stress in activating autoreactive T cells in T1D.
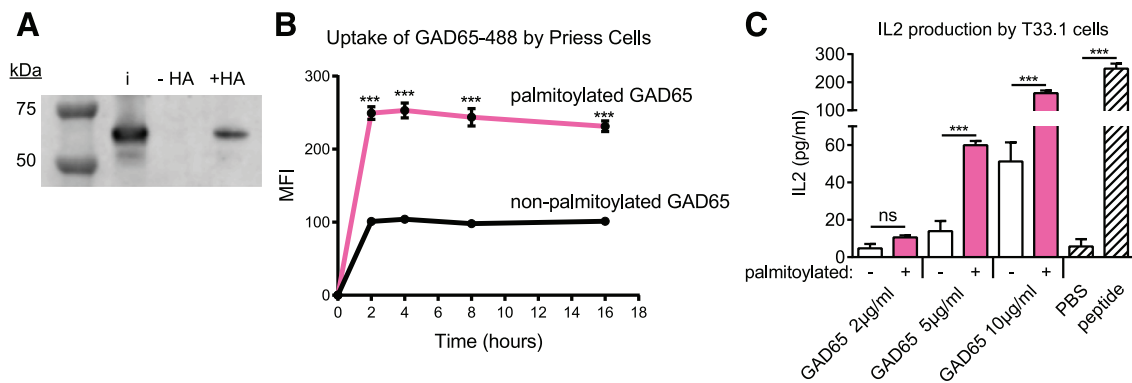
**Figure 7. Palmitoylation confers increased immunogenicity upon GAD65.**

(**A**) Recombinant human GAD65 produced in yeast was shown to be palmitoylated by the S-acylation resin-assisted capture (Acyl-RAC) assay. Free thiols in recombinant GAD65 were capped with methyl methanethiosulfonate (MMTS) followed by cleavage of palmitate-thiol modifications with hydroxylamine (HA), pulldown with a thiol-reactive pyridyl-disulfide agarose resin, and detection by Western blot. Lanes: i =input, positive control of unmodified recombinant GAD65; -HA = negative control without HA resulting in no palmitate cleavage and no protein pulldown; +HA = HA added with palmitate groups cleaved and protein recovered by thiol-reactive pulldown. (**B**) Time course of uptake of equimolar amounts of DyLight-488 labeled palmitoylated or depalmitoylated (HA cleaved) recombinant GAD65 by MHC-class II DR4 positive human Priess B-cell APCs measured by flow cytometry. Results are presented as mean ± SEM (*n* = 3 experimental replicates). Data were analyzed by two-way ANOVA followed by Tukey's multiple comparisons test (*** $P < 0.001$). (**C**) Priess cells were loaded with equimolar amounts of palmitoylated or depalmitoylated GAD65 (HA cleaved) and tested for stimulation of the DR4 restricted GAD65-specific T33.1 T-cell hybridoma cells by IL-2 secretion measured by ELISA. Results are presented as mean ± SEM (*n* = 3 experimental replicates). Data were analyzed by two-way ANOVA followed by Tukey's multiple comparisons test (*** $P < 0.001$).

### 3.4.5  GAD65 accumulates in the Golgi compartment in human beta cells during progression of T1D autoimmunity

We addressed the question whether the experimental accumulation of GAD65 in the Golgi compartment induced by treatment with ER stressors in vitro is of relevance for human diabetes. Human pancreatic sections provided by the nPOD tissue bank (28; 29) representing 8 healthy donors (**Supplementary Table 1**), 8 potentially prediabetic individuals positive for GAD65 autoantibodies (GADA+)

(**Supplementary Table 2**), and 8 T1D patients with residual beta cell mass (**Supplementary Table 3**) were immunostained for GAD65, giantin, insulin, glucagon and the pan-T cell marker CD3 (**Figure 8A-D**). In five of eight GADA+ individuals and seven of eight T1D patients, the GAD65 signal in beta cell Golgi membranes compared to cytosol was higher than one standard deviation above the mean for healthy control individuals where GAD65 immunostaining was mostly uniform (**Figure 8E, Supplementary Tables 1-3**, last column). Staining of serial sections for the pan-T cell marker, CD3 (**Figure 8A**), confirmed peri- and intra-islet infiltrating T cells in islets from three of eight GADA+ individuals as well as in six of eight T1D patients (**Figure 8A** and results not shown). Examination of the nPOD-provided patient information (**Supplementary Tables 1-3**) for individual donors revealed that the highest Golgi accumulation observed in the pre-diabetic GADA+ group was from a single autoantibody positive (GADA+) 2.2-year-old child expressing the HLA-class II T1D susceptibility haplotype DR4, DQ8 (**Supplementary Table 2**) showing infiltrates of CD3-positive T cells in and around islets (**Figure 8A**, nPOD 6090) but not meeting the nPOD insulitis criteria (**Supplementary Table 2**). This child may represent a case of a young, genetically susceptible individual in the early stages of autoimmunity associated with development of T1D. The lowest Golgi accumulation in the GADA+ group was observed in a 31-year-old, single autoantibody positive (GADA+) individual with normal islet morphology and no insulitis (**Supplementary Table 2**, nPOD 6181). The highest Golgi accumulation observed in the T1D group was observed in a double autoantibody positive (GADA+ and mIAA+) 11-year-old individual expressing the T1D HLA-class II susceptibility haplotypes DR3, DQ2 and DR4, DQ8 and with ongoing insulitis (**Supplementary Table 3**) (30) as confirmed by our CD3 immunostaining (**Figure 8A**, nPOD 6265). Taken together, the results suggest that aberrant accumulation of GAD65 in Golgi membranes may correlate with active islet autoimmunity in human T1D.
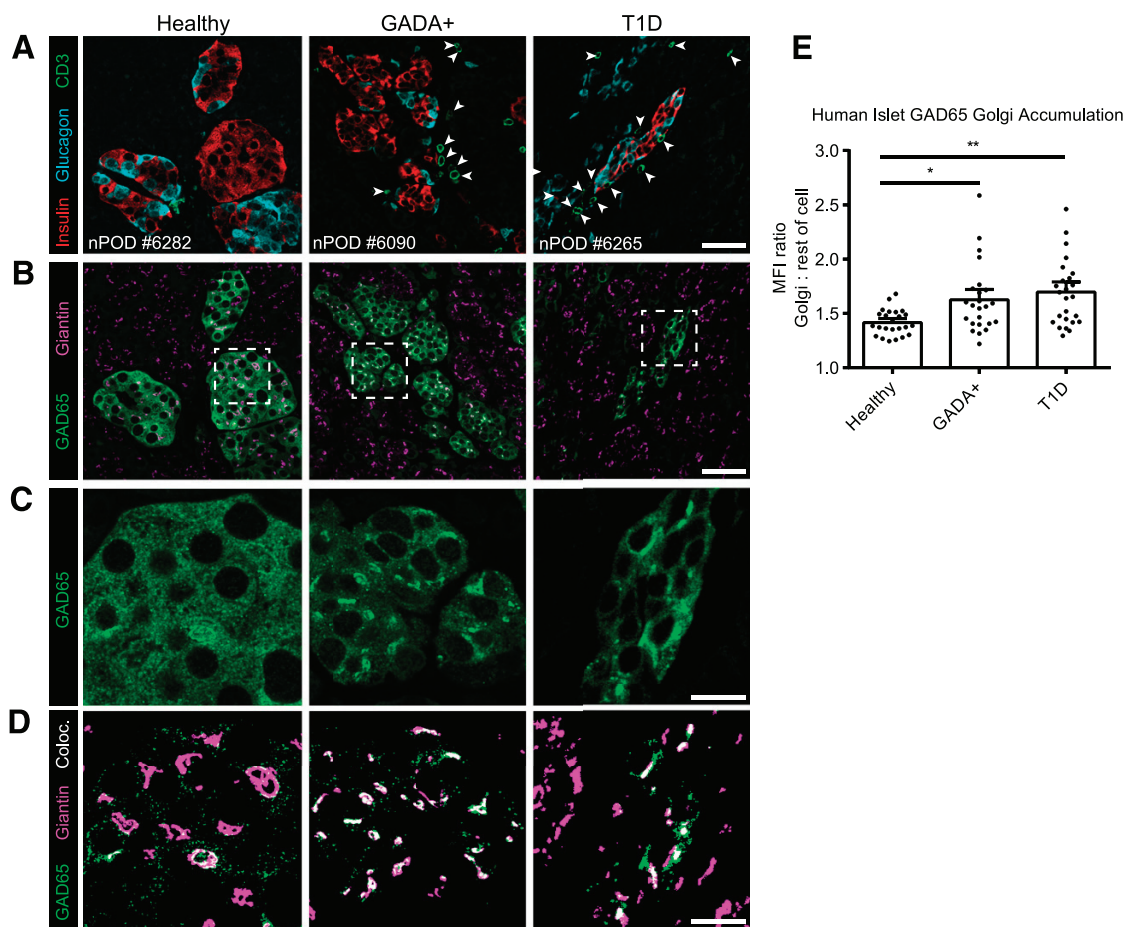
**Figure 8. Confocal analyses of islets in paraffin sections of human pancreas from healthy, non-diabetic GAD65 autoantibody positive, or T1D with residual beta cell mass.**

(**A**) Immunostaining of human pancreatic sections for insulin, glucagon or CD3 from the indicated nPOD case numbers. Arrowheads indicate CD3+ T-cells. Scale bar 50 μm. (**B**) The same human islet from a serial section, immunostained for GAD65 and giantin. Scale bar 50 μm. (**C**) Increased magnification of GAD65 staining in the framed region shown in (*B*). Scale bar 10 μm. (**D**) Thresholded binary images of the same region in (*C*) show the colocalization between giantin (Golgi) and the bright GAD65 signal. Scale bar 10 μm. (**E**) Image quantification of GAD65 accumulation in the Golgi compartment in 3 representative islets from 8 individuals per donor category, reported as the ratio of MFI for GAD65 in the Golgi of beta cells to MFI for GAD65 in the rest of the cell excluding the nucleus. Results are presented as scatter dot plots overlaying the mean ± SEM (*n* = 24 islets from 8 donors). Data were analyzed by one-way ANOVA followed by Tukey's multiple comparisons test (* P < 0.05, ** P < 0.01). The average GAD65 Golgi accumulation calculated per individual as well as demographic information for healthy, GADA+, and T1D donors is listed in Supplementary Tables 1-3.

105

## 3.5 DISCUSSION

In this study, we show that treatment of islet cell cultures by three separate regimens known to induce ER stress in beta cells results in accumulation of GAD65 in Golgi membranes. Importantly, analysis of human pancreatic tissue sections revealed significant accumulation of GAD65 in beta cell Golgi membranes in GADA+ potentially pre-diabetic individuals and in T1D patients with residual beta cell mass. Thus, aberrant accumulation of GAD65 in Golgi membranes is observed both in beta cells in culture undergoing experimentally-induced ER stress as well as in beta cells of individuals experiencing active beta cell autoimmunity.

We have shown earlier that palmitoylation of GAD65 results in anterograde trafficking from *cis*-Golgi to TGN membranes (12). The evidence presented in this study shows that only WT GAD65 but not palmitoylation deficient GAD65(C30,45A) accumulates in Golgi membranes during ER stress. This increase of GAD65 in Golgi membranes is consistent with the accumulated protein representing the palmitoylated form of GAD65 in TGN membranes, suggesting that the palmitoylation cycle of GAD65 significantly slows down during induction of ER stress. This retardation in transport likely affects the control of GAD65 distribution between peripheral vesicle membranes, where the majority of GAD65 enzymatic functional activity is believed to take place, and Golgi membranes, which may serve as a sorting station for this protein. We therefore propose that perturbation in the regulation GAD65 membrane distribution by ER stress may have negative consequences for GABA synthesis and secretion. GABA serves as an important signaling molecule and survival/growth factor in islets of Langerhans (40).

The mechanisms by which cytokines, palmitate, and thapsigargin induce ER stress in beta cells may differ (34). One commonality between the three different treatments is that each is implicated in dysregulation of calcium homeostasis (41). Both inflammatory cytokines and thapsigargin have been shown to induce beta cell ER stress through downregulation or inhibition of the sarco/endoplasmic reticulum

Ca$^{2+}$ ATPase, resulting in elevation of cytosolic calcium concentrations and depletion of ER Ca$^{2+}$ stores (42). Palmitate is reported to induce ER stress through lipotoxic signaling pathways mediating a block in ER uptake of Ca$^{2+}$ and a sustained depletion of ER Ca$^{2+}$ stores (35,43). The idea that dysregulation of ER/cytosolic Ca$^{2+}$ concentrations is involved in Golgi accumulation of GAD65 is supported by the fact that a similar effect could be achieved by strongly depolarizing cells by abruptly elevating extracellular glucose or KCl concentration (Phelps, Cianciaruso, and Baekkeskov unpublished results). While it is currently unknown how a change in calcium homeostasis could affect membrane trafficking of GAD65, it is of note that earlier studies have suggested modulation of the affinity of GAD65 to liposome membranes by calcium ion concentration (44). Interestingly, there is evidence to suggest that palmitate treatment of insulinoma cells alters the lipid composition of endomembranes and specifically disrupts lipid raft microdomains (45), a dynamic hub for palmitoylated proteins (46). It is of note that distribution of H-Ras into lipid rafts is regulated by its palmitoylation/depalmitoylation cycle (47), which shares similarities with the acylation cycle of GAD65 (16). Thus, it is possible that alterations in lipid raft composition are part of the mechanism involved in perturbation of GAD65 trafficking and accumulation in Golgi membranes.

Parallel to the important role of GAD65 as the highly regulated and the only GABA synthesizing enzyme in human beta cells, it can assume a detrimental role as a major target of autoimmunity associated with pancreatic human beta cell destruction and development of T1D in genetically susceptible individuals (2). The autoantigenicity of GAD65 is in stark contrast to the highly homologous GAD67 isoform, which is not an independent autoantigen. GAD67 primarily differs from GAD65 in the N-terminal domain (48) that mediates hydrophobic post-translational modifications, membrane anchoring, palmitoylation and trafficking of GAD65 (12), suggesting that this region is integral to the susceptibility of GAD65 to become a pathogenic auto-antigen. GAD67 does not undergo hydrophobic modifications (49)

and can only be targeted to membranes by piggy-backing onto other proteins (15,38).

Our data show that compared to depalmitoylated GAD65, palmitoylated GAD65 induces a significantly stronger effector T-cell response by the T cell hybridoma T33.1, which recognizes GAD65$^{274-286}$ in the context of DR4, a T1D MHC-class II susceptibility haplotype. Palmitoylation of peptide epitopes has been shown to enhance immunogenicity of autoimmune epitopes in experimental autoimmune encephalomyelitis (50) and in synthetic peptide vaccines (51). Palmitoylation of a protein increases its avidity for binding to membranes. The uptake of palmitoylated GAD65 by the DR4-positive human B-cell line Priess was significantly enhanced compared to non-palmitoylated GAD65. We posit that the increase in uptake, conferred by palmitoylation, may involve enhanced binding to the surface of Priess cells resulting in increased uptake by endocytosis and enhanced targeting to late endosomes for proteolytic processing and presentation to T cells in the context of MHC-class II antigens (reviewed in (52)). Palmitoylation of GAD65 may also affect antigen unfolding and proteolysis and alter the hierarchy of peptides displayed to CD4+ T cells. The T33.1 hybridoma reporter cell line is clonally restricted to a single MHC-class II binding epitope, GAD65$^{274-286}$, which is distant from the palmitoylated cysteine residues in GAD65, aa 30 and 45. Therefore, the possibility of palmitoylation increasing the MHC-class II binding affinity of this epitope can be excluded in our experimental system. Rather, we suggest that increased stimulation of T33.1 cells reflects a quantitative increase in the levels of the GAD65$^{274-286}$ epitope available for binding to DR4 in late endosomes and elevated expression on the surface of Priess cells. If palmitoylated GAD65, which has accumulated in TGN during ER stress, is released by distressed or dying beta cells and encountered by APCs, its heightened immunogenicity compared to non-palmitoylated GAD65 may stimulate autoimmunity in genetically predisposed individuals. An important agenda for future studies will be to elucidate the mechanisms by which palmitoylated, immunogenic GAD65 is

released from beta cells undergoing ER stress, as well as the determinants of that stress, which the results presented herein suggest could be key factors in the mechanism that results in autoimmunity to GAD65 associated with development of type I diabetes.

## 3.6  CONTRIBUTION OF THE DOCTORAL CANDIDATE

The doctoral candidate helped in the design and realization of the experiments of ER stress induction by cytokines, thapsigargin and palmitate in pancreatic beta cells (3.3.1). She performed the experiments of uptake and presentation of the palmitoylated and non-palmitoylated forms of GAD65 by B lymphocytes to autoreactive T cells (3.3.4). She helped with the acquisition of the immunostaining analyses on the nPOD tissue sections (3.3.5). She helped the lab technician M.P. with the isolation of rodent islets and immunostaining. She provided her contribution in writing a section of the manuscript describing experiments directly performed by her (3.3.4).

A  Rat beta cells

B  Human beta cells

C  Rat neurons

D  GAD65 Golgi Accumulation
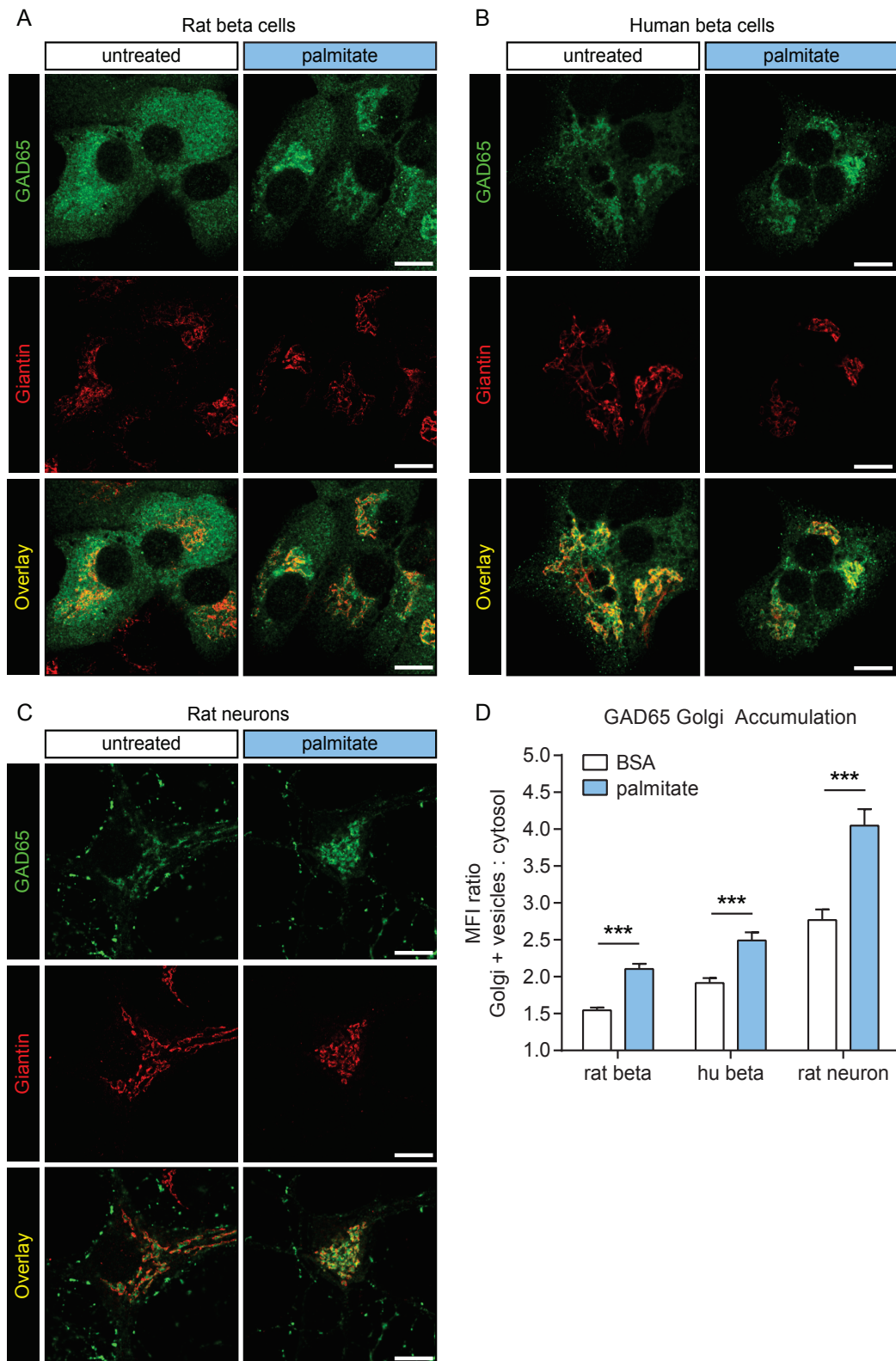
**Supplementary Figure 1. Accumulation of GAD65 in Golgi membranes during palmitate induced ER stress in rat and human beta cells and in rat neurons.**

(**A**) Rat beta cells, (**B**) human beta cells, or (**C**) rat neurons were left untreated or treated with palmitate (500 µM) for 2 h. Fixed cells were immunostained for GAD65 and giantin (Golgi). Scale bar 10 µm. (**D**) Image quantification of GAD65 accumulation in the Golgi compartment expressed as the ratio of MFI for GAD65 in the Golgi and GAD65-positive vesicles to MFI for GAD65 in the rest of the cell excluding the nucleus. Results are presented as mean ± SEM (*n* = 30-63 cells analyzed per condition for rat beta cells, *n* = 24-38 cells analyzed per condition for human beta cells, *n* = 15-17 cells analyzed per condition for rat neurons). Data were analyzed using Student's *t*-test (*** P < 0.001).
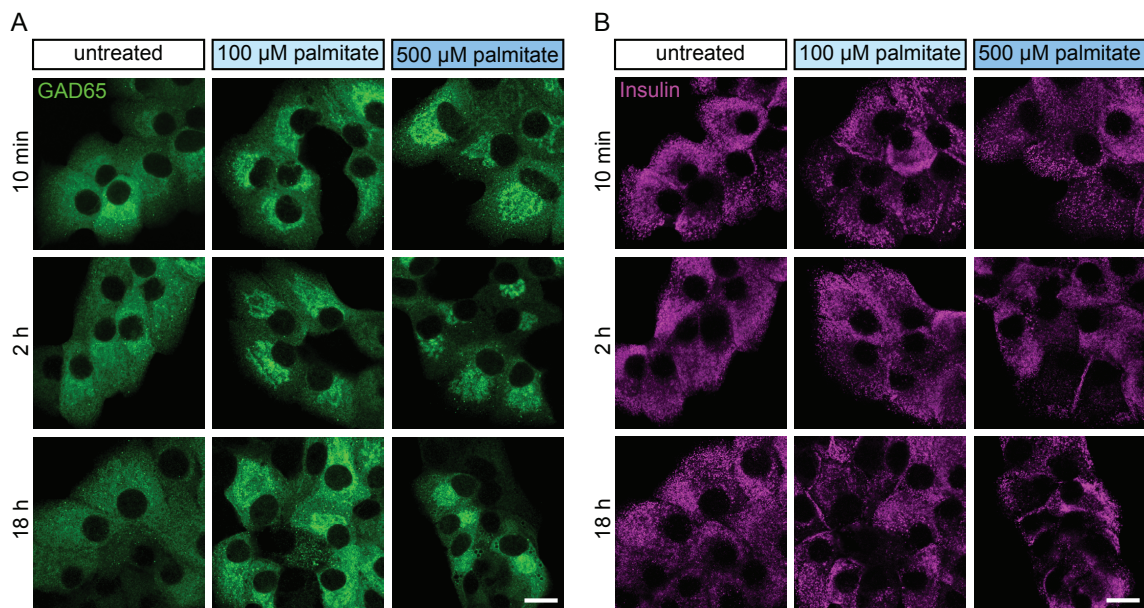


**Supplementary Figure 2. Time course of Golgi accumulation of GAD65 upon palmitate treatment.**
Confocal analyses of monolayer cultures of primary rat beta cells left untreated or treated with 100 µM palmitate or 500 µM palmitate for 10 min, 2 h, and 18 h respectively. Fixed cells were immunostained for GAD65, insulin, and CHOP. Staining for CHOP and higher magnification GAD65 images of the framed regions in the left panel are shown in Figure 4. Scale bars 10 µm.
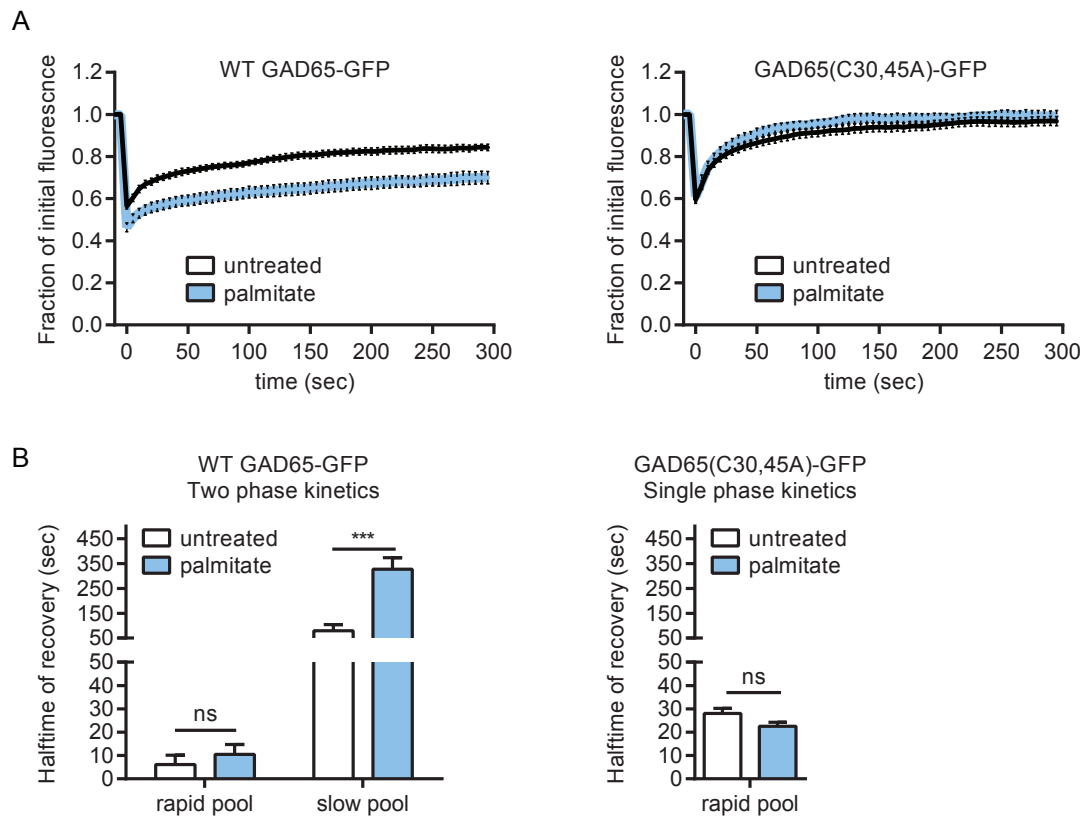
**Supplementary Figure 3. Fluorescence recovery after photobleaching in the Golgi of WT but not palmitoylation-deficient GAD65 is inhibited during palmitate-induced ER stress.**

(**A**) Kinetics of fluorescence recovery after bleaching the entire Golgi-associated pool of WT GAD65-GFP or GAD65(C30,45A) in primary rat beta cells pretreated or not with palmitate (500 µM) for 1 h. Results are presented as mean ± SEM (*n* = 9-15 cells per condition). (**B**) Halftimes of Golgi fluorescence recovery in primary rat beta cells. Results are presented as the mean ± SEM (*n* = 9-15 cells per condition). Data were analyzed by Student's *t*-test comparing the halftime parameter between association curve fits (* P < 0.05, *** P < 0.001).
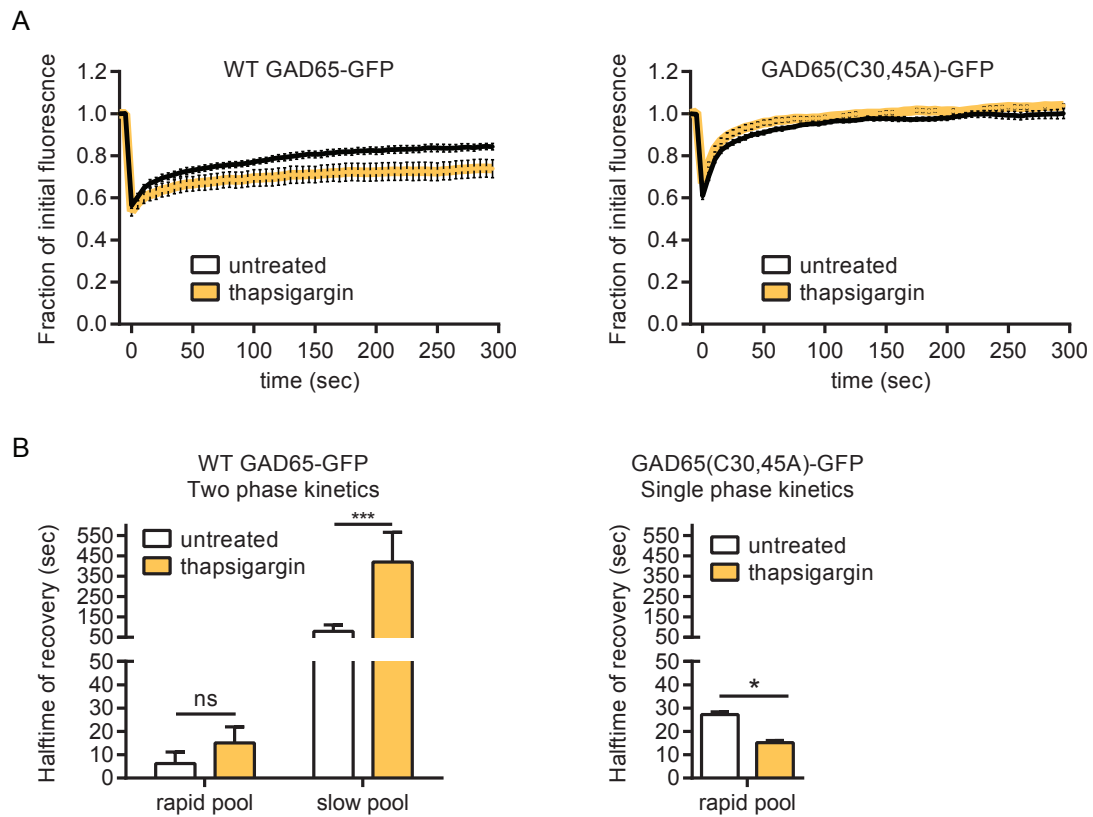
**Supplementary Figure 4. Fluorescence recovery after photobleaching in the Golgi of WT but not palmitoylation-deficient GAD65 is inhibited during thapsigargin-induced ER stress.**

(**A**) Kinetics of fluorescence recovery after bleaching the entire Golgi-associated pool of WT GAD65-GFP or GAD65(C30,45A) in primary rat beta cells pretreated or not with thapsigargin (2 µM) for 1 h. Results are presented as mean ± SEM (*n* = 6-10 cells per condition). (**B**) Halftimes of Golgi fluorescence recovery in primary rat beta cells. Results are presented as the mean ± SEM (*n* = 6-10 cells per condition). Data were analyzed by Student's *t*-test comparing the halftime parameter between association curve fits (* P < 0.05, *** P < 0.001).

| nPOD CaseID | Donor Type | AutoAb | Age (years) | Diabetes Duration (years) | Gender | Ethnicity | C-peptide (ng/ml) | BMI | Cause of Death | nPOD histopathology notes | HLA | Golgi : Cell MFI ratio * |
|---|---|---|---|---|---|---|---|---|---|---|---|---|
| 6096 | No diabetes | Negative | 16 | n/a | Female | African American | 2.97 | 18.8 | Head Trauma | Ins+/Gluc+ normal islets. | DRB1*0302,1503 DQA1*0102,0401 DQB1*0402,0602 | 1.56 |
| 6164 | No diabetes | Negative | 0.03 | n/a | Male | Caucasian | not provided | 16.5 | Anoxia | Ins+/Gluc+ normal islets. | DRB1*0301,0301 DQA1*0501,0501 DQB1*0201,0201 | 1.55 |
| 6162 | No diabetes | Negative | 22.7 | n/a | Male | African American | 7.61 | 28.9 | Head Trauma | Ins+/Gluc+ normal islets. | DRB1*1303,1602 DQA1*0102,0501 DQB1*0301,0502 | 1.45 |
| 6289 | No diabetes | Negative | 19 | n/a | Male | African American | 8.05 | 38.3 | Head Trauma | Ins+/Gluc+ normal islets. | DRB1*0411,0701 DQA1*0201,0301 DQB1*0202,0302 | 1.44 |
| 6112 | No diabetes | Negative | 6.3 | n/a | Female | Hispanic | 5.11 | 18.4 | Head Trauma | Ins+/Gluc+ normal islets. | DRB1*0407,1302 DQA1-0102,0301 DQB1*0301,0501 | 1.37 |
| 6178 | No diabetes | Negative | 24.5 | n/a | Female | Caucasian | 4.55 | 27.5 | Anoxia | Ins+/Gluc+ normal islets. | DRB1*0401,1501 DQA1*0102,0301 DQB1*0301,0602 | 1.36 |
| 6282 | No diabetes | Negative | 14 | n/a | Male | Caucasian | 6.83 | 41.9 | Head Trauma | Ins+/Gluc+ normal islets. | DRB1*1301,1501 DQA1*0102,0103 DQB1*0602,0603 | 1.32 |
| 6168 | No diabetes | No serum available | 51 | n/a | Male | Hispanic | not provided | 25.2 | Cerebrovascular/ Stroke | Ins+/Gluc+ normal islets. | DRB1*0103,0404 DQA1*0101,0301 DQB10302,0501 | 1.27 |

* Cases are arranged from highest to lowest GAD65 MFI ratio for GAD65 in the Golgi compartment to the rest of the cell

**Supplementary Table 1**. Demographic and patient information for JDRF nPOD human pancreatic sections from non-diabetic donors. Donor information obtained from the nPOD online pathology database. Data shown in the last column are from this study.

| nPOD CaseID | Donor Type | AutoAb | Age (years) | Diabetes Duration (years) | Gender | Ethnicity | C-peptide (ng/ml) | BMI | Cause of Death | nPOD histopathology notes | HLA | Golgi : Cell MFI ratio * |
|---|---|---|---|---|---|---|---|---|---|---|---|---|
| 6090 | Autoab positive | GADA+ | 2.2 | n/a | Male | Hispanic | 5.34 | 18.8 | Head Trauma | Ins+/Gluc+ islets, numerous. CD3+ infiltrates throughout exocrine tissue. | DRB1*0404,1501 DQA1*0102,0301 DQB1*0302,0602 | 2.11 |
| 6310 | Autoab positive | GADA+ | 28 | n/a | Female | Hispanic | 10.54 | 23.9 | Anoxia | Ins+/Gluc+ islets, numerous, some hyperplastic. Low grade insulitis, periphery and foci. | DRB1*0701,1102 DQA1*0201,0501 DQB1*0202,0319 | 1.84 |
| 6123 | Autoab positive | GADA+ | 23.2 | n/a | Female | Caucasian | 2.01 | 17.6 | Head Trauma | Ins+/Gluc+ islets, various sizes. | DRB1*0801,1101 DQA1*0401,0501 DQB1*0301,0402 | 1.75 |
| 6314 | Autoab positive | GADA+ | 21 | n/a | Male | Caucasian | 1.49 | 23.8 | Head Trauma | Ins+/Gluc+ islets, numerous, several large islets (200-400um). Insulitis not observed. | DRB1*0103,0401 DQA1*0101,0301 DQB1*0301,0501 | 1.59 |
| 6147 | Autoab positive | GADA+ | 23.8 | n/a | Female | Caucasian | 3.19 | 32.9 | Head Trauma | Ins+/Gluc+ normal islets. | DRB1*0401,0802 DQA1*0301,0401 DQB1*0301,0402 | 1.54 |
| 6267 | Autoab positive | GADA+ IA-2A+ | 23 | n/a | Female | Caucasian | 16.59 | 23.5 | Anoxia | Ins+/Gluc+ normal islets. Insulitis found in all regions. | DRB1*0401,0404 DQA1*0301,0301 DQB1*0302,0302 | 1.48 |
| 6197 | Autoab positive | GADA+ IA-2A+ | 22 | n/a | Male | African American | 17.48 | 28.2 | Head Trauma | Ins+/Gluc+ islets, plentiful. Insulitis (rare). | DRB1*0302,0701 DQA1*0201,0401 DQB1*0202,0402 | 1.41 |
| 6181 | Autoab positive | GADA+ | 31.9 | n/a | Male | Caucasian | 0.6 | 21.9 | Head Trauma | Ins+/Gluc+ normal islets. | DRB1*0101,0401 DQA1*0101,0301 DQB1*0302,0501 | 1.29 |

* Cases are arranged from highest to lowest GAD65 MFI ratio for GAD65 in the Golgi compartment to rest of the cell

**Supplementary Table 2.** Demographic and patient information for JDRF nPOD human pancreatic sections from GADA+ donors who have not yet progressed to clinical type 1 diabetes. Donor information obtained from the nPOD online pathology database. Data shown in the last column are from this study.

| nPOD CaseID | Donor Type | AutoAb | Age (years) | Diabetes Duration (years) | Gender | Ethnicity | C-peptide (ng/ml) | BMI | Cause of Death | nPOD histopathology notes | HLA | Golgi : Cell MFI ratio * |
|---|---|---|---|---|---|---|---|---|---|---|---|---|
| 6265 | T1D | GADA+ mIAA+ | 11 | 8 | Male | Caucasian | 0.06 | 12.9 | Cerebrovascular/Stroke | Ins+/Gluc+ islets-rare with remainder insulin-negative. Insulitis present. | DRB1*0301,0401 DQA1*0301,0501 DQB1*0201,0302 | 2.28 |
| 6088 | T1D | GADA+ IA-2A+ ZnT8A+ mIAA+ | 31.2 | 5 | Male | Caucasian | <0.05 | 27 | Head Trauma | Ins+/Gluc+ islets (much decreased). Insulitis present. | DRB1*0101,0301 DQA1*0101,0501 DQB1*0201,0501 | 1.80 |
| 6245 | T1D | GADA+ IA-2A+ | 22 | 7 | Male | Caucasian | <0.05 | 23.2 | Head trauma | Ins+ (reduced frequency)/Gluc+ islets, some pseudoatrophic (gluc+ only). Possible insulitis. | DRB1*0301,0405 DQA1*0301,0501 DQB1*0201,0302 | 1.70 |
| 6211 | T1D | GADA+ IA-2A+ ZnT8A+ mIAA+ | 24 | 4 | Female | African American | <0.05 | 24.4 | Anoxia | Ins+(reduced)/Gluc+ islets, numerous. | DRB1*0405,1201 DQA1*0301,0501 DQB1*0301,0302 | 1.70 |
| 6195 | T1D | GADA+ IA-2A+ ZnT8A+ mIAA+ | 19.2 | 5 | Male | Caucasian | <0.05 | 23.7 | Head Trauma | Ins+ (rare)/Gluc+ islets. Insulitis present in a small number of islets. | DRB1*0401,1501 DQA1*0102,0301 DQB1*0302,0602 | 1.58 |
| 6046 | T1D | IA-2A+ ZnT8A+ | 18.8 | 8 | Female | Caucasian | <0.05 | 25.2 | Anoxia | Ins+/Gluc+ islets in occ. lobule, other lobules/entire blocks ins-/gluc+ islets. Insulitis present. | DRB1*0101,0401 DQA1*0101,0301 DQB1*0302,0501 | 1.55 |
| 6084 | T1D | mIAA+ | 14.2 | 4 | Male | Caucasian | <0.05 | 26.3 | Anoxia | Ins+/Gluc+ islets in lobules with moderate to severe adipose infiltrates. Very irregular islets. | DRB1*0301,0401 DQA1*0301,0501 DQB1*0201,0302 | 1.53 |
| 6049 | T1D | GADA+ mIAA+ | 15 | 10 | Female | African American | <0.05 | 20.8 | Anoxia | Ins-/Gluc+ (majority) islets with rare Ins+ islets. | DRB1*0404,0901 DQA1*0301,0301 DQB1*0201,0302 | 1.44 |

* Cases are arranged from highest to lowest GAD65 MFI ratio for GAD65 in the Golgi compartment to rest of the cell

**Supplementary Table 3.** Demographic and patient information for JDRF nPOD human pancreatic sections from type 1 diabetic donors. Donor information obtained from the nPOD online pathology database. Data shown in the last column are from this study.

## 3.8 REFERENCES

1. Erlander MG, Tillakaratne NJK, Feldblum S, Patel N, Tobin AJ. Two genes encode distinct glutamate decarboxylases. Neuron 1991;7:91-100

2. Baekkeskov S, Aanstoot HJ, Christgau S, Reetz A, Solimena M, Cascalho M, Folli F, Richter-Olesen H, De Camilli P. Identification of the 64K autoantigen in insulin-dependent diabetes as the GABA-synthesizing enzyme glutamic acid decarboxylase. Nature 1990;347:151-156

3. Baekkeskov S, Landin M, Kristensen JK, Srikanta S, Bruining GJ, Mandrup-Poulsen T, de Beaufort C, Soeldner JS, Eisenbarth G, Lindgren F, et al. Antibodies to a 64,000 Mr human islet cell antigen precede the clinical onset of insulin-dependent diabetes. J Clin Invest 1987;79:926-934

4. Atkinson MA, Maclaren NK, Scharp DW, Lacy PE, Riley WJ. 64,000 Mr autoantibodies as predictors of insulin-dependent diabetes. Lancet 1990;335:1357-1360

5. Kim J, Richter W, Aanstoot HJ, Shi Y, Fu Q, Rajotte R, Warnock G, Baekkeskov S. Differential expression of GAD65 and GAD67 in human, rat, and mouse pancreatic islets. Diabetes 1993;42:1799-1808

6. Petersen JS, Russel S, Marshall MO, Kofod H, Buschard K, Cambon N, Karlsen AE, Boel E, Hagopian WA, Hejnaes KR, et al. Differential expression of glutamic acid decarboxylase in rat and human islets. Diabetes 1993;42:484-495

7. Kash SF, Condie BG, Baekkeskov S. Glutamate decarboxylase and GABA in pancreatic islets: lessons from knock-out mice. Horm Metab Res 1999;31:340-344

8. Christgau S, Schierbeck H, Aanstoot HJ, Aagaard L, Begley K, Kofod H, Hejnaes K, Baekkeskov S. Pancreatic beta cells express two autoantigenic forms of glutamic acid decarboxylase, a 65-kDa hydrophilic form and a 64-kDa amphiphilic

form which can be both membrane-bound and soluble. J Biol Chem 1991;266:23516

9. Christgau S, Aanstoot HJ, Schierbeck H, Begley K, Tullin S, Hejnaes K, Baekkeskov S. Membrane anchoring of the autoantigen GAD65 to microvesicles in pancreatic beta-cells by palmitoylation in the NH2-terminal domain. J Cell Biol 1992;118:309-320

10. Shi Y, Veit B, Baekkeskov S. Amino acid residues 24-31 but not palmitoylation of cysteines 30 and 45 are required for membrane anchoring of glutamic acid decarboxylase, GAD65. J Cell Biol 1994;124:927-934

11. Kanaani J, El-Husseini AE, Aguilera-Moreno A, Diacovo JM, Bredt DS, Baekkeskov S. A combination of three distinct trafficking signals mediates axonal targeting and presynaptic clustering of GAD65. J Cell Biol 2002;158:1229-1238

12. Kanaani J, Patterson G, Schaufele F, Lippincott-Schwartz J, Baekkeskov S. A palmitoylation cycle dynamically regulates partitioning of the GABA-synthesizing enzyme GAD65 between ER-Golgi and post-Golgi membranes. J Cell Sci 2008;121:437-449

13. Huang K, Yanai A, Kang R, Arstikaitis P, Singaraja RR, Metzler M, Mullard A, Haigh B, Gauthier-Campbell C, Gutekunst CA, Hayden MR, El-Husseini A. Huntingtin-interacting protein HIP14 is a palmitoyl transferase involved in palmitoylation and trafficking of multiple neuronal proteins. Neuron 2004;44:977-986

14. Kanaani J, Diacovo MJ, El-Husseini AE, Bredt DS, Baekkeskov S. Palmitoylation controls trafficking of GAD65 from Golgi membranes to axon-specific endosomes and a Rab5a-dependent pathway to presynaptic clusters. J Cell Sci 2004;117:2001-2013

15. Kanaani J, Cianciaruso C, Phelps EA, Pasquier M, Brioudes E, Billestrup N, Baekkeskov S. Compartmentalization of GABA Synthesis by GAD67 Differs between Pancreatic Beta Cells and Neurons. PLoS One 2015;10:e0117130

16. Baekkeskov S, Kanaani J. Palmitoylation cycles and regulation of protein function (Review). Mol Membr Biol 2009;26:42-54

17. Fukata Y, Fukata M. Protein palmitoylation in neuronal development and synaptic plasticity. Nat Rev Neurosci 2010;11:161-175

18. Oakes SA, Papa FR. The role of endoplasmic reticulum stress in human pathology. Annu Rev Pathol 2015;10:173-194

19. Eizirik DL, Cardozo AK, Cnop M. The role for endoplasmic reticulum stress in diabetes mellitus. Endocr Rev 2008;29:42-61

20. Marhfour I, Lopez XM, Lefkaditis D, Salmon I, Allagnat F, Richardson SJ, Morgan NG, Eizirik DL. Expression of endoplasmic reticulum stress markers in the islets of patients with type 1 diabetes. Diabetologia 2012;55:2417-2420

21. Engin F, Yermalovich A, Nguyen T, Hummasti S, Fu W, Eizirik DL, Mathis D, Hotamisligil GS. Restoration of the unfolded protein response in pancreatic beta cells protects mice against type 1 diabetes. Sci Transl Med 2013;5:211ra156

22. Song B, Scheuner D, Ron D, Pennathur S, Kaufman RJ. Chop deletion reduces oxidative stress, improves beta cell function, and promotes cell survival in multiple mouse models of diabetes. J Clin Invest 2008;118:3378-3389

23. Eizirik DL, Colli ML, Ortis F. The role of inflammation in insulitis and beta-cell loss in type 1 diabetes. Nat Rev Endocrinol 2009;5:219-226

24. Merglen A, Theander S, Rubi B, Chaffard G, Wollheim CB, Maechler P. Glucose sensitivity and metabolism-secretion coupling studied during two-year continuous culture in INS-1E insulinoma cells. Endocrinology 2004;145:667-678

25. Jaume JC, Parry SL, Madec AM, Sonderstrup G, Baekkeskov S. Suppressive effect of glutamic acid decarboxylase 65-specific autoimmune B lymphocytes on processing of T cell determinants located within the antibody epitope. J Immunol 2002;169:665-672

26. Wicker LS, Chen SL, Nepom GT, Elliott JF, Freed DC, Bansal A, Zheng S, Herman A, Lernmark A, Zaller DM, Peterson LB, Rothbard JB, Cummings R, Whiteley PJ. Naturally processed T cell epitopes from human glutamic acid decarboxylase identified using mice transgenic for the type 1 diabetes-associated human MHC class II allele, DRB1*0401. J Clin Invest 1996;98:2597-2603

27. Codazzi F, Di Cesare A, Chiulli N, Albanese A, Meyer T, Zacchetti D, Grohovaz F. Synergistic control of protein kinase Cgamma activity by ionotropic and metabotropic glutamate receptor inputs in hippocampal neurons. J Neurosci 2006;26:3404-3411

28. Campbell-Thompson M, Wasserfall C, Kaddis J, Albanese-O'Neill A, Staeva T, Nierras C, Moraski J, Rowe P, Gianani R, Eisenbarth G, Crawford J, Schatz D, Pugliese A, Atkinson M. Network for Pancreatic Organ Donors with Diabetes (nPOD): developing a tissue biobank for type 1 diabetes. Diabetes Metab Res Rev 2012;28:608-617

29. Pugliese A, Yang M, Kusmarteva I, Heiple T, Vendrame F, Wasserfall C, Rowe P, Moraski JM, Ball S, Jebson L, Schatz DA, Gianani R, Burke GW, Nierras C, Staeva T, Kaddis JS, Campbell-Thompson M, Atkinson MA. The Juvenile Diabetes Research Foundation Network for Pancreatic Organ Donors with Diabetes (nPOD) Program: goals, operational model and emerging findings. Pediatr Diabetes 2014;15:1-9

30. Campbell-Thompson M, Fu A, Kaddis JS, Wasserfall C, Schatz DA, Pugliese A, Atkinson MA. Insulitis and beta-Cell Mass in the Natural History of Type 1 Diabetes. Diabetes 2016;65:719-731

31. Chang YC, Gottlieb DI. Characterization of the proteins purified with monoclonal antibodies to glutamic acid decarboxylase. J Neurosci 1988;8:2123-2130

32. Hampe CS, Lundgren P, Daniels TL, Hammerle LP, Marcovina SM, Lernmark A. A novel monoclonal antibody specific for the N-terminal end of GAD65. J Neuroimmunol 2001;113:63-71

33. Forrester MT, Hess DT, Thompson JW, Hultman R, Moseley MA, Stamler JS, Casey PJ. Site-specific analysis of protein S-acylation by resin-assisted capture. J Lipid Res 2011;52:393-398

34. Kharroubi I, Ladriere L, Cardozo AK, Dogusan Z, Cnop M, Eizirik DL. Free fatty acids and cytokines induce pancreatic beta-cell apoptosis by different mechanisms: role of nuclear factor-kappaB and endoplasmic reticulum stress. Endocrinology 2004;145:5087-5096

35. Cunha DA, Hekerman P, Ladriere L, Bazarra-Castro A, Ortis F, Wakeham MC, Moore F, Rasschaert J, Cardozo AK, Bellomo E, Overbergh L, Mathieu C, Lupi R, Hai T, Herchuelz A, Marchetti P, Rutter GA, Eizirik DL, Cnop M. Initiation and execution of lipotoxic ER stress in pancreatic beta-cells. J Cell Sci 2008;121:2308-2318

36. Brozzi F, Nardelli TR, Lopes M, Millard I, Barthson J, Igoillo-Esteve M, Grieco FA, Villate O, Oliveira JM, Casimir M, Bugliani M, Engin F, Hotamisligil GS, Marchetti P, Eizirik DL. Cytokines induce endoplasmic reticulum stress in human, rat and mouse beta cells via different mechanisms. Diabetologia 2015;58:2307-2316

37. Bertolotti A, Zhang Y, Hendershot LM, Harding HP, Ron D. Dynamic interaction of BiP and ER stress transducers in the unfolded-protein response. Nat Cell Biol 2000;2:326-332

38. Kanaani J, Kolibachuk J, Martinez H, Baekkeskov S. Two distinct mechanisms target GAD67 to vesicular pathways and presynaptic clusters. J Cell Biol 2010;190:911-925

39. Pfender NA, Grosch S, Roussel G, Koch M, Trifilieff E, Greer JM. Route of uptake of palmitoylated encephalitogenic peptides of myelin proteolipid protein by antigen-presenting cells: importance of the type of bond between lipid chain and peptide and relevance to autoimmunity. J Immunol 2008;180:1398-1404

40. Soltani N, Qiu H, Aleksic M, Glinka Y, Zhao F, Liu R, Li Y, Zhang N, Chakrabarti R, Ng T, Jin T, Zhang H, Lu WY, Feng ZP, Prud'homme GJ, Wang Q. GABA exerts protective and regenerative effects on islet beta cells and reverses diabetes. Proc Natl Acad Sci U S A 2011;108:11692-11697

41. Marre ML, James EA, Piganelli JD. Beta cell ER stress and the implications for immunogenicity in type 1 diabetes. Frontiers in cell and developmental biology 2015;3:67

42. Cnop M, Welsh N, Jonas JC, Jorns A, Lenzen S, Eizirik DL. Mechanisms of pancreatic beta-cell death in type 1 and type 2 diabetes: many differences, few similarities. Diabetes 2005;54:S97-107

43. Marmugi A, Parnis J, Chen X, Carmichael L, Hardy J, Mannan N, Marchetti P, Piemonti L, Bosco D, Johnson P, Shapiro JAM, Cruciani-Guglielmacci C, Magnan C, Ibberson M, Thorens B, Valdivia HH, Rutter GA, Leclerc I. Sorcin links pancreatic β-Cell lipotoxicity to ER Ca2+ stores. Diabetes 2016;65:1009-1021

44. Covarrubias M, Tapia R. Calcium-dependent binding of brain glutamate decarboxylase to phospholipid vesicles. J Neurochem 1978;31:1209-1214

45. Boslem E, Weir JM, MacIntosh G, Sue N, Cantley J, Meikle PJ, Biden TJ. Alteration of endoplasmic reticulum lipid rafts contributes to lipotoxicity in pancreatic beta-cells. J Biol Chem 2013;288:26569-26582

46. Levental I, Lingwood D, Grzybek M, Coskun U, Simons K. Palmitoylation regulates raft affinity for the majority of integral raft proteins. Proc Natl Acad Sci U S A 2010;107:22050-22054

47. Agudo-Ibanez L, Herrero A, Barbacid M, Crespo P. H-ras distribution and signaling in plasma membrane microdomains are regulated by acylation and deacylation events. Mol Cell Biol 2015;35:1898-1914

48. Bu DF, Erlander MG, Hitz BC, Tillakaratne NJ, Kaufman DL, Wagner-McPherson CB, Evans GA, Tobin AJ. Two human glutamate decarboxylases, 65-kDa GAD and 67-kDa GAD, are each encoded by a single gene. Proc Natl Acad Sci U S A 1992;89:2115-2119

49. Kanaani J, Lissin D, Kash SF, Baekkeskov S. The hydrophilic isoform of glutamate decarboxylase, GAD67, is targeted to membranes and nerve terminals independent of dimerization with the hydrophobic membrane-anchored isoform, GAD65. J Biol Chem 1999;274:37200-37209

50. Greer JM, Denis B, Sobel RA, Trifilieff E. Thiopalmitoylation of myelin proteolipid protein epitopes enhances immunogenicity and encephalitogenicity. J Immunol 2001;166:6907-6913

51. Beekman NJ, Schaaper WM, Tesser GI, Dalsgaard K, Kamstrup S, Langeveld JP, Boshuizen RS, Meloen RH. Synthetic peptide vaccines: palmitoylation of peptide antigens by a thioester bond increases immunogenicity. J Pept Res 1997;50:357-364

52. Blum JS, Wearsch PA, Cresswell P. Pathways of antigen processing. Annu Rev Immunol 2013;31:443-473

# CHAPTER 4

# Primary human and rat beta cells release the intracellular autoantigens GAD65, IA-2 and proinsulin in exosomes together with cytokine-induced enhancers of immunity

Adapted from the original manuscript

Chiara Cianciaruso, Edward A. Phelps, Miriella Pasquier, Romain Hamelin, Davide Demurtas, Mohamed Alibashe Ahmed, Lorenzo Piemonti, Sachiko Hirosue, Melody Swartz, Michele De Palma, Jeffrey A. Hubbell, Steinunn Baekkeskov

## 4.1  ABSTRACT

The target autoantigens in several organ-specific autoimmune diseases, including type 1 diabetes (T1D), are intracellular membrane proteins, whose initial encounter with the immune system is poorly understood. Here we propose a new model for how these proteins can initiate autoimmunity. We found that rat and human pancreatic islets release the intracellular beta cell autoantigens in human T1D, GAD65, IA-2 and proinsulin, in exosomes, which are taken up by and activate dendritic cells. Accordingly, anchoring of GAD65 to exosome-mimetic liposomes strongly boosted antigen presentation and T cell activation in the context of the human type 1 diabetes susceptibility haplotype HLA-DR4. Cytokine-induced ER stress enhanced exosome secretion by beta cells, induced exosomal release of the immunostimulatory chaperones calreticulin, Gp96 and ORP150 and increased exosomal stimulation of antigen presenting cells. We propose that stress-induced

exosomal release of intracellular autoantigens and immunostimulatory chaperones may play a role in initiation of autoimmune responses in T1D.

## 4.2  INTRODUCTION

Type 1 diabetes (T1D) in humans is an autoimmune disease characterized by circulating autoantibodies, lymphocytic infiltration of pancreatic islets of Langerhans, and cell-specific destruction of beta cells, leading to insulin deficiency (1). Prior to lymphocytic infiltration, physiological islet abnormalities have been described in the non-obese diabetic (NOD) mouse model of T1D, including upregulation of inflammatory cytokines (1) and increased endoplasmic reticulum (ER) stress in beta cells (2). Furthermore, the importance of ER stress and the beneficial effects of restoring organelle function have been reported (3).

Two main target autoantigens in human T1D, GAD65 (4) and IA-2 (5) are rare intracellular membrane proteins in beta cells. Circulating autoantibodies to these proteins are an early marker of beta cell autoimmunity in man and can be used together with HLA-Class II haplotyping to detect individuals at risk long before clinical onset of disease (6). The mechanisms by which these intracellular autoantigens are initially recognized by the immune system, taken up by antigen presenting cells (APCs), and presented to self-reactive T cells have, however, not been clarified. A third autoantigen, insulin, constitutes ~50% of beta cell proteins and is released by regulated exocytosis of secretory granules (7). There is evidence that epitopes in proinsulin, the uncleaved prohormone form of insulin, escape immune tolerance in T1D (7,8).

MIN6 and INS-1 insulinoma cells, derived from a mouse and rat beta cell tumor, respectively, have been reported to release extracellular vesicles (EVs), including exosomes (9). Exosomes are small-diameter (30-150 nm) biologically active vesicles that are secreted in the extracellular space by most cell types,

following the formation of multivesicular bodies (MVBs) in the late endosomal pathway and their fusion with the plasma membrane (10).

Exosomes can display immunostimulatory and immunoregulatory functions (11). In the context of T1D, exosomes from MIN6 cells were reported to stimulate autoreactive NOD T cells (9) and marginal zone-like B cells that accumulate in the pancreas of prediabetic NOD mice (12). In addition, islet-associated mesenchymal stem cell-like cells were shown to produce immunostimulatory exosomes that activated autoreactive T and B cells in NOD mice (13). We and others have been unable to detect expression of the GAD65 protein in mouse islet cells and in insulinoma cells (14-16) and neither GAD65 nor IA-2 appear to be required for development of T1D in the NOD mouse (17,18).

Here we have isolated exosomes from primary human and rat islets, which, differently from insulinoma cells and mouse islets, express GAD65 in addition to IA-2 and insulin. We present the characterization of flotillin1, CD9, and CD81-containing exosomes and report the release of GAD65, IA-2 and proinsulin/insulin therein. We further show that cytokine-induced ER stress results in increased release of exosomes decorated with inflammatory proteins that may promote beta cell autoimmunity.

## 4.3  METHODS

### 4.3.1  Islets and cell cultures

Rat islets were isolated from P5 Sprague Dawley rats (18) and from HLA-DR4+/+ NOD mice (19) and cultured as previously described (18). DR4^{+/+}NOD mice were obtained from Dr. Grete Sønderstrup, Stanford University. These mice are homozygous for the human T1D MHC-class II susceptibility haplotype DRA1*0101, DRB1*0401 (hereafter referred to as DR4) and express DR4 antigens as well as human CD4 in lymphoid cells, and human proinsulin in pancreatic β cells. The mice are negative for expression of murine MHC-class II IA and IE antigens (20). They do not develop T1D. Human islets, received through the European Consortium for Islet Transplantation (ECIT) Islets for Basic Research Program, were obtained from six non-diabetic donors, four males and two females, age 36-59 years with a body mass index of 20-29 kg/m$^2$. The causes of death were stroke (3 donors), cerebral bleeding (1 donor) and cardiac arrest (1 donor). Humans islets (95-100% purity) were cultured in Connaught Medical Research Laboratories 1066 (CMRL) medium with 2 mM L-Glutamine, 25 mM Hepes and 10% FBS. Monolayer cultures were derived from whole islets dispersed into single cells and seeded on Thermanox-coverslips (ThermoFisher Scientific) coated with HTB-9 cell-derived extracellular matrix (21). Bone marrow dendritic cells (BMDC) were isolated from HLA-DR4+/+ NOD mice (22) and cultured for 8 days with RPMI 1640 GlutaMAX medium with 11 mM glucose, 10% FBS, 1% Antibiotic-Antimycotic and GM-CSF (200 µg /ml, PeproTech). INS-1E cells (23) were cultured in RPMI 1640 GlutaMAX with 10% FBS, 1% P/S, 1 mM sodium pyruvate, 10 mM Hepes and 50 µM β-mercaptoethanol. MIN6 cells (24) were cultured in DMEM GlutaMAX medium with 25 mM glucose, 15%FBS, 1% P/S and 70 µM β-mercaptoethanol. HTB-9 cells were cultured in RPMI 1640 GlutaMAX medium with 10% FBS and 1% P/S. The DR4 (DRA1*0101, DRB1*0401) positive human

EBV-transformed B cell line Priess (25) was cultured in Iscove's Modified Dulbecco's Medium GlutaMAX medium (IMDM) with 10% FBS and 1% P/S and used for antigen presentation.

### 4.3.2 Exosome isolation

Rat islets, human islets, INS-1E or Priess cells were seeded in exosome-depleted medium (26). Supernatant was collected every two or three days. For comparative analyses of exosomes released with and without cytokines, rat and human islets were divided into cell culture dishes (500 islets each) and rat IL1β (10U/ml) and IFNγ (10U/ml) (R&D Systems) or human IL1β (20U/ml) and IFNγ (10 U/ml) (R&D Systems) added to half of the plates. This concentration of cytokines has been shown to result in a very mild form of ER stress in beta cells (18). Culture media were collected and replaced with fresh media with or without cytokines every two days for a total of six days. Islets were counted after each replacement of medium: the total loss of islets in medium with and without cytokines was ≤20% and ≤5% respectively for rat islets at the end of the collection period. Trypan blue staining of islets cells following dispersion of islet samples in trypsin/EDTA revealed robust viability of cells with and without cytokines throughout the collection period (**Supporting Figures 1A and 2A**).

Exosomes from culture media were isolated by differential centrifugation (26). In brief, media were centrifuged at 300xg for 10 min to remove live cells, followed by 2,000xg for 10 min to remove dead cells followed by centrifugation at 10,000xg for 35 min at 4°C to remove cell debris, large vesicles and heavy membranes, including Golgi membranes, lysosomes and apoptotic bodies. Supernatants were transferred to a new tube and centrifuged at 110,000xg for 70 min at 4°C to isolate exosomes. The resulting pellet was re-suspended, washed in 35 ml PBS to eliminate serum and

secreted proteins and re-centrifuged. The final pellet was re-suspended in 50-100 µl of PBS and stored at -80°C.

### 4.3.3 Transmission Electron Microscopy

Exosomes or liposomes (15 µl, at different dilutions in PBS) were applied to carbon-coated 400 mesh grids (Canemco-Marivac), negatively stained with 2% uranyl acetate, and images obtained with a transmission electron microscope (Tecnai Spirit, FEI Company).

### 4.3.4 Nanoparticle Tracking Analysis

Exosomes and liposomes (1:1,000 in PBS) were analyzed using a Nanoparticle Tracking Analyses (NTA) instrument NS300 (NanoSight, Malvern Instruments Ltd.). Five measurements of 60 seconds were recorded consecutively for each sample and a 532 nm laser diode source was used to analyze fluorescence of Bodipy-labeled exosomes.

### 4.3.5 Proteomics

EV preparations (5 µg protein) from untreated or cytokine-treated rat islets, untreated human islets, or INS-1E cells were analyzed by liquid chromatography tandem mass spectrometry (LC-MS/MS). Briefly, each sample was digested in solution as previously described (27). Peptides were desalted using StageTips and dried in a vacuum concentrator. For LC-MS/MS analysis, resuspended peptides were separated by reverse phase chromatography on a Dionex Ultimate 3000 RSLC nano UPLC system connected in-line with an Orbitrap Elite (ThermoFisher Scientific). Database search was performed using Mascot 2.5 (Matrix Science) and SEQUEST in Proteome Discoverer v.1.4. against a human or rat Uniprot protein database. Data

were further processed and inspected in Scaffold™ 4.2.1 (Proteome Software). Normalized quantitative values were utilized to compare the protein profile in exosomes from three different preparations of untreated and cytokine-treated rat islets. The normalization scheme in Scaffold adjusts the sum of the selected quantitative value for all proteins in the list within each MS sample to a common value: the average of the sums of all MS samples present in the experiment. This is achieved by applying a scaling factor for each sample to each protein or protein group adjusting in this way the selected value to a normalized "Quantitative Value". Normalized quantitative values were utilized to compare the protein profile in exosomes from untreated and cytokine-treated rat islets. For proteomic detection of GAD65 and IA-2, exosomal proteins were separated by SDS-PAGE (Invitrogen). Proteins were eluted from gel slices corresponding to the relative mobility of GAD65 and IA-2 and subjected to LC-MS/MS analyses (27).

### 4.3.6  SDS-PAGE and Western Blot analysis

Cell lysates were prepared by resuspending pellets of 200 islets or $2 \times 10^6$ INS-1E or MIN6 cells in 200 µl of RIPA buffer (Sigma) and incubating on ice for 20 minutes followed by centrifugation at 13,000xg for 20 minutes at 4°C and collection of the supernatant. Brain extracts from P5 rats were obtained by collagenase D (Roche) digestion on a 40 µm cell strainer. After centrifugation at 600xg for 5 minutes at 4°C, the pellet was resuspended in 1 ml RIPA buffer and processed as described above. The BCA protein assay kit (ThermoFisher Scientific) was used to measure the protein concentration of cell extracts. A total of 5-15 µg protein per lane was analyzed SDS-PAGE and Western Blotting as described (18). Recombinant human GAD65 used for standard was from FIRS Laboratories RSR. Primary antibodies used were: GAD1701 (rabbit anti-GAD65/GAD67) (14) 1:5000, rabbit anti-flotillin1 (donated by G. Van der Goot) 1:2000, mouse anti-CD9 antibody (Santa Cruz, sc-

13118) 1:100, 76F-B4 (mouse anti-IA-2, donated by E. Bonifacio) (28) 1:20, mouse anti-beta actin (Sigma, A1978) 1:2000, chicken anti-Calreticulin (Abcam, ab14234) 1:1000, rabbit anti-Gp96 (Abcam, ab13509) 1:1000, mouse anti-PDI (BD Transduction Laboratories, 610947) 1:500 and mouse anti-Alix (Cell Signaling, 2171) 1:1000.

### 4.3.7 Quantitation of insulin in exosomes by ELISA

EVs from human or rat islets were lysed in PBS+1% Triton and subjected to serial dilutions prior to quantitative analyses using ELISA kits for human or rat insulin and proinsulin (Mercodia).

### 4.3.8 Immunofluorescence

Single islet cells were fixed with 4% PFA and blocked/permeabilized in PBS+0.3% Triton, 10% goat or donkey serum. The primary antibodies mouse anti-GAD65 (15) 1:1000, sheep anti-TGN38 (Biorad, AHP499) 1:100, rabbit anti-flotillin1 1:200, rabbit anti-CHOP (Santa Cruz, sc-575) 1:100, guinea pig anti-insulin (Linco, 4011-01) 1:1000 and rabbit anti-CD81 (Sigma, SAB3500454) 1:300 were incubated overnight at 4°C in PBS+0.3% Triton, 5% goat/donkey serum. Alexa Fluor-conjugated secondary antibodies (Life Technologies) were incubated at 1:200 in PBS+0.3% Triton for 30 min at RT. Coverslips were mounted with Prolong Gold antifade reagent with or without DAPI (Life Technologies). Samples were imaged on a Zeiss LSM700 confocal microscope and images processed in ImageJ.

### 4.3.9 Treatment and transfections of islet monolayer cultures

Rat islet cells were incubated with rat cytokines (IFNγ and IL1β, 10 U/ml each) for 4, 8 or 24 hours.

Transfection with the MAGT1-GFP plasmid (29) and GFP-Rab11 WT plasmid (30) were performed using Lipofectamine™2000 (Life Technologies). Cell labeling using BODIPY®TR-Ceramide (Life Technologies) was done according to the manufacturers protocol.

### 4.3.10  Uptake of islet-exosomes by antigen presenting cells

Rat islet-exosomes (10 ng protein/ml) were labeled with 5 µM of BODIPY®TR-Ceramide (Life Technologies) in PBS for 30 min at RT (31), followed by two PBS washes and ultracentrifugations at 110,000xg for 70 min at 4°C.

Bodipy-labeled exosomes (20-25 µg protein/ml) were incubated with 100,000 DR4^{+/+} BMDCs or Priess cells labeled with 0.5 µM carboxyfluorescein succinimidyl ester (CFSE) (Life Technologies). Uptake was analyzed on a Zeiss LSM700 confocal microscope with a stage-mounted incubation chamber at 37°C, 5%$CO_2$. Cells collected at the end of the experiment were blocked with anti-mouse CD16/32 (BioLegend, 101302) 1:200, stained with LIVE/DEAD® Violet (Life Technologies) and CD11c-APC antibody (eBioscience, 17-0114-82) 1:800, and analyzed by BD™LSRII Flow Cytometer (BD Biosciences) and FlowJo software.

### 4.3.11  Immunostimulation of BMDCs by islet-derived exosomes

Rat and human islet-EVs (40 and 50 µg protein/ml) were incubated for 24 hours with 50,000 DR4^{+/+}BMDCs. PBS and CpG-A (5 µg/ml, ODN1585, InvivoGen) were used as negative and positive controls respectively. Concentrations of TNFα, IL6 and IL1β in the cell supernatant were measured by ELISA (eBioscience).

### 4.3.12 Preparation of GAD65-liposomes mimicking exosomes

Liposomes were prepared according to the protocol by Masserini et al. (32). Ganglioside GM3, cholesterol and sphingomyelin (Avanti Polar Lipids Inc.) were dissolved in chloroform-methanol (2:1 v/v) in a molar ratio of 8:1:1. After rehydration of the lipid film in PBS, liposomes were size-selected by extrusion through 100 nm nucleopore track-etched membranes (Whatman) using a Lipex$^{TM}$ extruder (Northern Lipids Inc.). Endotoxin-free recombinant human GAD65 (1 mg/ml) produced in yeast (rhGAD65) (FIRS Laboratories RSR) was incubated with liposomes ($1x10^{11}$ particles/ml), in a total volume of 100 µl, at RT for 2h, and purified by ultracentrifugation (100,000xg for 70 minutes) to remove unbound protein. Anchoring of GAD65 to liposome membranes can be easily achieved due to the presence of hydrophobic post-translational modifications including a double palmitoylation (33). The BCA protein assay kit (ThermoFisher Scientific) was used to analyze the concentration of GAD65 conjugated to liposomes.

### 4.3.13 Immunogenicity of GAD65-liposomes

To test antigenicity of free GAD65 compared to liposome-conjugated GAD65, free rhGAD65 protein and GAD65-liposomes were incubated for 24 hours with 50,000 DR4$^{+/+}$ NOD BMDCs. DR4 (DRA1*0101, DRB1*0401) restricted T33.1 T cells were added and incubation continued overnight. PBS or empty liposomes (in equivalent amount to the highest concentration of GAD65-liposomes used in the assay) were used as negative controls and 0.5 µg/ml GAD$_{274-286}$ peptide (GenScript) was used as a positive control. IL2 secretion by T cells was analyzed by ELISA.

### 4.3.14 Statistical analyses

Means among three or more groups were compared by analysis of variance (ANOVA) in GraphPad Prism 6. If deemed significant, Tukey's post-hoc pairwise

comparisons were performed. Means between two groups were compared using Student's *t*-test. A confidence level of 95% was considered significant.

### 4.3.15 Ethical approval

Animals were used under EPFL animal regulation guidelines and an IACUC approved protocol. Human islets were received from University Hospital of Geneva and San Raffaele Scientific Institute, Milan, through ECIT, and approved by the Institutional Review Board of Geneva University Hospital (CER Nr. 05–028) and the Ethics Committee of San Raffaele Institute (IPF002-2014).

### 4.3.16 Acknowledgments and funding

## 4.4  RESULTS

### 4.4.1  Rat and human pancreatic islets release the GAD65, IA-2 and insulin/proinsulin autoantigens in EVs with characteristics of exosomes

EVs were isolated from primary rat and human pancreatic islet cells and the rat insulinoma cell line INS-1E by differential centrifugations of culture supernatants (26). Transmission electron microscopic (TEM) analysis of EVs from rat and human islets demonstrated the presence of vesicles with size and shape compatible with those of exosomes (34) (**Figure 1A**). Nanoparticle-tracking analysis (NTA) indicated a uniform size distribution, with a major peak at 143±5 nm and 139±5 nm for rat and human EVs respectively (**Figure 1B**), similar to the size of exosomes from neural stem cells (34).

The proteome of EVs from rat or human islets and INS-1E cells were analyzed by LC-MS/MS and found to contain proteins previously identified in exosomes from other cell types (**Supplementary Table 1**). Those included flotillin1, which appears to control sorting of specific proteins toward MVB destined for exosomal secretion (35), the tetraspanins CD9 and CD81, which may play a critical role in mediating protein loading and inclusion into endosomal membranes and exosomes (36,37) while Alix and CD63 were not detected. Furthermore, Rab11, Rab27a, Rab27b and Rab35, which are implicated in the biogenesis of exosomes (38,39), and Rab1, which is involved in vesicle trafficking from ER to Golgi intermediate membranes (40), were detected in islet EVs together with the autoantigen proinsulin/insulin

130

(**Supplementary Table 1**). As shown in **Figure 1C**, insulin was an integral part of islet exosomes, rather than a contamination from secreted insulin and accounted for 7-8% of human- and 2-3% of rat-islet exosome proteins as measured by ELISA (**Figure 1D**). Proinsulin constituted ~12% and ~0.5% of total insulin in human and rat islet exosomes respectively (**Figure 1D**). The rare beta cell autoantigens GAD65 and IA-2 were not detected in islet-EVs by LC-MS/MS of total islet cells. GAD65 and IA-2 are difficult to detect by LC-MS/MS likely due to their hydrophobicity and poor peptide ionization. However, both proteins were detected in human islet exosomes following pre-purification by SDS-PAGE and elution of gel slices in their mobility range (**Supporting Figure 3**).

We next analyzed expression of GAD65 and IA-2 and the exosomal markers flotillin1 and CD9 by Western blotting (WB) of islet EVs and compared with expression in total islet lysates. These analyses unequivocally identified the autoantigens GAD65 and IA-2 in both human and rat EVs (**Figure 1E, F, Supplementary Figure 1A and 1B**). Human islets only express the GAD65 isoform, while rat islets primarily express the GAD65 isoform but also the non-autoantigenic isoform GAD67, which can form heterodimers with GAD65 and become membrane bound in rat islet beta cells (15). Both isoforms were detected in rat islet exosomes (**Figure 1E, Supplementary Figure 1A**). In contrast to a previous report (9), GAD65 was not detected in lysates of the mouse insulinoma cell line MIN6. Furthermore, as reported previously (14-16), only GAD67 but not GAD65 was detected in mouse islet and rat INS-1E cells (**Supplementary Figure 1A**). The ratio of GAD65 in exosomes and total lysates was approximately 1:2 in human islets and 1:5 in rat islets (**Figure 1E**). Since approximately half of total beta cell GAD65 is firmly membrane-anchored (41), the concentration ratio of GAD65 in EVs vs total beta cell membranes was ~1:1 for human and ~2:5 for rat. The transmembrane IA-2 autoantigen of 68-70 kD (28) was detected in human and rat islet-exosomes (**Figure 1F, Supplementary Figure**

**1B)**; the concentration ratio between exosomes and total islet lysate was ~1:2 for IA-2 in human and ~1:6 in rat islets (**Figure 1F**).

The WB analyses revealed a 25-fold enrichment of the exosomal marker flotillin1 in EVs from both human and rat pancreatic islets compared to islet lysates (**Figure 1G**). CD9 was detected in human islet-EVs on WB but was not enriched over lysates (**Figure 1G**). The exosome marker Alix was detected in islet lysates and EVs from INS-1E cells, but was below detection limit in islet-EVs (**Supplementary Figure 1C**), consistent with the notion that in islet cells, flotillin1-, CD9- and CD81-positive exosomes represent a population of exosomes distinct from and more abundant than Alix-, syndecan/syntenin- and CD63-positive exosomes (42).

Together, the results suggest that human and rat pancreatic islets release EVs presenting characteristics of flotillin1-, CD9- and CD81-positive exosomes. Importantly, islet-exosomes contain the GAD65, IA-2 and insulin/proinsulin autoantigens associated with development of T1D in humans.
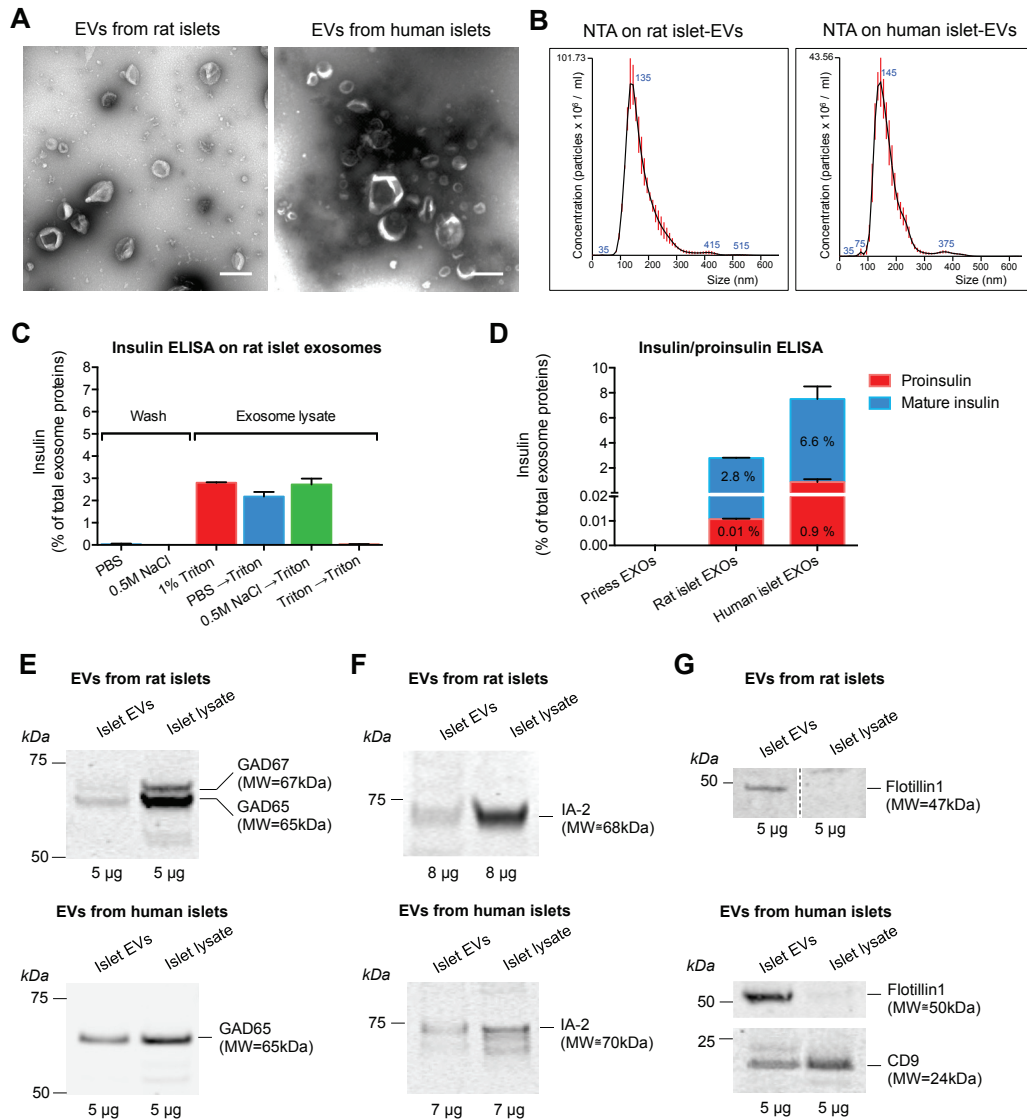
**Figure 1. Human and rat islets release extracellular vesicles, mainly exosomes, containing the exosomal markers flotillin1 and CD9 and the beta cell autoantigens GAD65, IA-2 and proinsulin/insulin.**

(**A**) EM analysis of rat and human islet extracellular vesicles (EVs) with "cup-shaped" morphology and 30–200 nm in diameter, with an average size of 120 nm, in both rat and human preparations. Vesicle sizes were estimated by measuring the diameters of 20 exosomes in five different fields. While some vesicles are larger (150-200 nm), the main constituents of the EV preparations are exosomes (30-150 nm). Scale bars: 200 nm. (**B**) Particle-size distribution of EVs from rat and human islets using nanoparticle tracking analyses. Data are representative of n = 3 independent experiments. (**C**) Aliquots of purified rat islet-exosomes were resuspended in PBS, PBS supplemented with NaCl to a final concentration of 0.5 M, or PBS containing 1% Triton X-100 and incubated for 1h followed by sedimentation at 110,000xg for 1h. Pellets were extracted in PBS/1% Triton X-100 and supernatants were subjected to serial dilutions and analyzed for insulin/proinsulin by ELISA. Insulin is only released from exosomes by detergent suggesting that is an integral part of exosomes rather than a contaminant from islet cell culture media. Analyses were performed in technical triplicates. Results are reported as mean ± SD. (**D**) Insulin/proinsulin content of human and rat islet-exosomes measured by ELISA after

extraction in PBS containing 1% Triton X-100. Data for human insulin/proinsulin are shown as mean ± SD of 3 independent experiments. Data for rat insulin/proinsulin are reported as mean ± SD for the triplicate rat islet EV lysates shown in (**C**). Data are representative of 3 independent experiments. (**E-G**) Western blot analyses of (**E**) GAD65, (**F**) IA-2 and (**G**) CD9 and flotillin1 expression in total lysates or EV preparations of rat and human islets. Human islets only express the GAD65 isoform of GAD, while rat islets express both GAD65 and the non-autoantigenic isoform GAD67. The results shown are representative of 2-5 independent experiments.

## 4.4.2  Trafficking of the autoantigen GAD65 to EVs may involve a pathway from the Golgi compartment to MVB via the perinuclear recycling endosome compartment

We investigated whether there is a convergence between pathways for exosome formation and the known intracellular trafficking of GAD65, which would facilitate loading of the autoantigen into EVs/exosomes.

Two pathways have been proposed for sorting membrane proteins to MVBs and exosomes. The first involves endocytosis of plasma membrane proteins and transport through early endosomes to late endosomes (LEs) and MVBs (10). The second involves transport from the *trans* Golgi network (TGN) to recycling endosomes and LE/MVB (31,38). Firmly membrane-anchored GAD65 is primarily localized to the TGN and peripheral vesicles in beta cells but is not detected at the plasma membrane (33,43). Furthermore, the transmembrane protein IA-2 and proinsulin/insulin are processed in the ER and Golgi prior to targeting to the membrane and lumen of insulin secretory granules respectively which is where proinsulin undergoes the final processing to insulin prior to regulated secretion (7).

We explored the possibility that islet beta cells form MVBs and exosomes using the TGN pathway, and asked whether GAD65 can be detected along this route. The small GTP-binding protein Rab11 is localized in the perinuclear endosomal recycling compartment (ERC) and is implicated in the control of trafficking to and from this compartment (44). Moreover, Rab11 is implicated in the exosomal biogenesis pathway originating at the TGN (38) and appears to promote the fusion of MVBs with

the plasma membrane to release exosomes (45). We, therefore, assessed the possible colocalization of Rab11 with GAD65 and the TGN marker TGN38 in rat islet cells expressing GFP-Rab11a. As reported previously (43), GAD65 colocalized with the TGN38 marker protein in the TGN (**Figure 2A, arrowheads**). Furthermore, GAD65 and GFP-Rab11a colocalized in the perinuclear ERC, as well as in a few smaller vesicular structures close to the surface of beta cells (**Figure 2A, arrows**). Colocalization between GAD65 and the exosomal marker flotillin1 was detected in beta cells both in vesicle-like compartments in proximity to the Golgi compartment as well as in the periphery of the cell (**Figure 2B, arrows**). Similarly, the exosomal marker CD81 and insulin/proinsulin colocalized extensively in vesicles budding off from the TGN (**Figure 2C, arrows**) or localized in the periphery (**Figure 2C, arrowheads**).

Laulagnier et al. (31) found that a population of exosomes released by RBL-2H3 cells is characterized by lipid composition similar to that of Golgi membranes and preferably absorbs a fluorescent Bodipy-Ceramide stain used for labeling of Golgi membranes. We confirmed that Bodipy-Ceramide specifically labels the Golgi compartment in rat islet cells (**Figure 2D**). We assessed the efficiency and specificity of Bodipy-Ceramide labeling of rat islet-exosomes using NTA. No significant differences were detected in the vesicle size distribution between the light scattering and the fluorescence acquisition settings (**Figure 2E**), suggesting that the labeling procedure indeed targets exosomes. Thus the lipid composition of islet-exosomes may resemble that of the Golgi, suggesting that in primary islet cells, a sizable fraction of MVBs may originate from Golgi membranes.

Taken together, the results support the notion of an exosome biogenesis pathway for beta cell autoantigens that originates in the TGN. For GAD65, the pathway appears to pass through the ERC and involve Rab11.
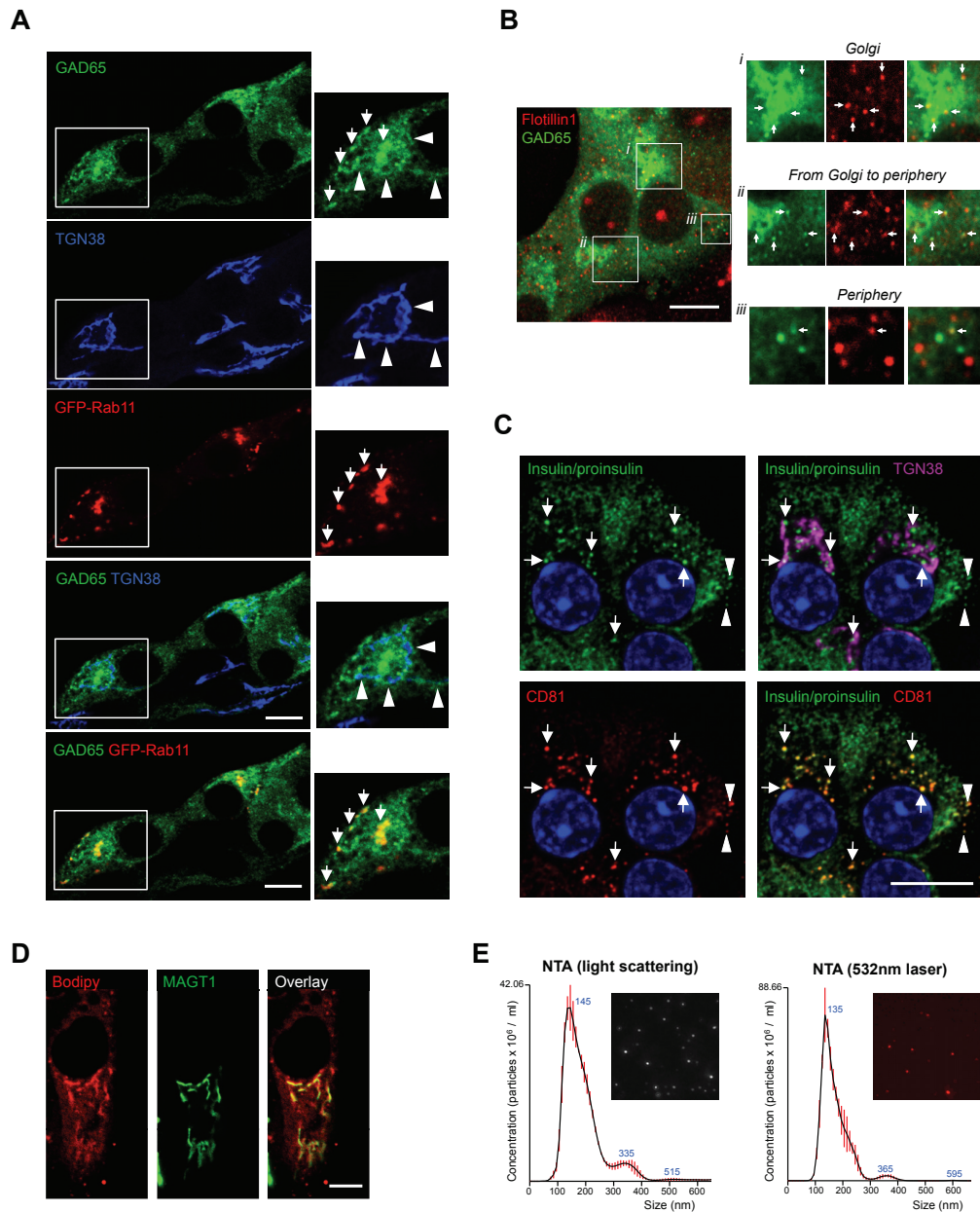
**Figure 2. Analyses of a putative pathway for biogenesis of beta cell EVs from the *trans*-Golgi network.**

(**A**) Confocal analyses of primary rat islet cells transfected with GFP-Rab11 and immunostained for GAD65 (green) and the *trans*-Golgi marker TGN38 (blue) revealing colocalization of GAD65 and TGN38 (arrowheads), minimal colocalization of TGN38 and GFP-Rab11, and colocalization of GAD65 and GFP-Rab11 (arrows) in the perinuclear endosomal recycling compartment close to the Golgi region and in vesicular structures in the cell periphery. (**B**) Confocal analyses of immunostaining of primary human islet cells for GAD65 (green), the exosomal marker flotillin1 (red) reveals colocalization in vesicular structures in proximity to (i) the Golgi compartment, (ii) between Golgi and peripheral structures and (iii) in the periphery close to the plasma membrane. (**C**) Confocal analyses of immunostaining of primary rat islet cells for insulin/proinsulin (green), the exosomal marker CD81 (red) and TGN38 (magenta) reveals co-localization of CD81 and insulin/proinsulin in vesicles budding off the Golgi compartment (arrows) and localized in the periphery (arrowheads). Nuclei are stained in blue with DAPI.

(**D**) Primary rat islet cells transfected with a plasmid encoding the Golgi protein MAGT1-GFP and incubated with Bodipy-Ceramide for 30 minutes reveal specific staining of lipids in Golgi membranes by the Bodipy-Ceramide dye. (**E**) Nanoparticle tracking analyses of Bodipy-Ceramide labeled rat islet-exosomes reveal a uniform size distribution with a major peak at 137±5 nm similar to that determined with no fluorescence filter, suggesting that the labeling procedure is effective and exosome-specific.
All scale bars are 10 µm.

### 4.4.3 Uptake of islet-EVs results in stimulation of HLA-DR4^{+/+}dendritic cells

We next assessed the ability of professional APCs to take up islet-EVs. Incubation of Bodipy-labeled islet-exosomes with bone marrow-derived dendritic cells (BMDCs) from HLA-DR4^{+/+} transgenic mice (**Figure 3A, 3B, Supplementary Figure 2A and 2C**) and the DR4^{+/+} human Priess B cell line (**Supplementary Figure 2B and 2D**) revealed an efficient and rapid uptake within 2-3 hours, as shown by fluorescent microscopy and flow cytometry analyses. To test the potential ability of EVs to activate APCs, rat islet-EVs were incubated with DR4^{+/+} BMDCs. During 24 hours incubation, secretion of the pro-inflammatory molecules TNFα, IL6 and IL1β was significantly increased in the presence of islet-EVs compared to PBS (**Figure 3C**). Taken together, the results suggest that EVs from primary islets are efficiently taken up by APCs resulting in their stimulation.
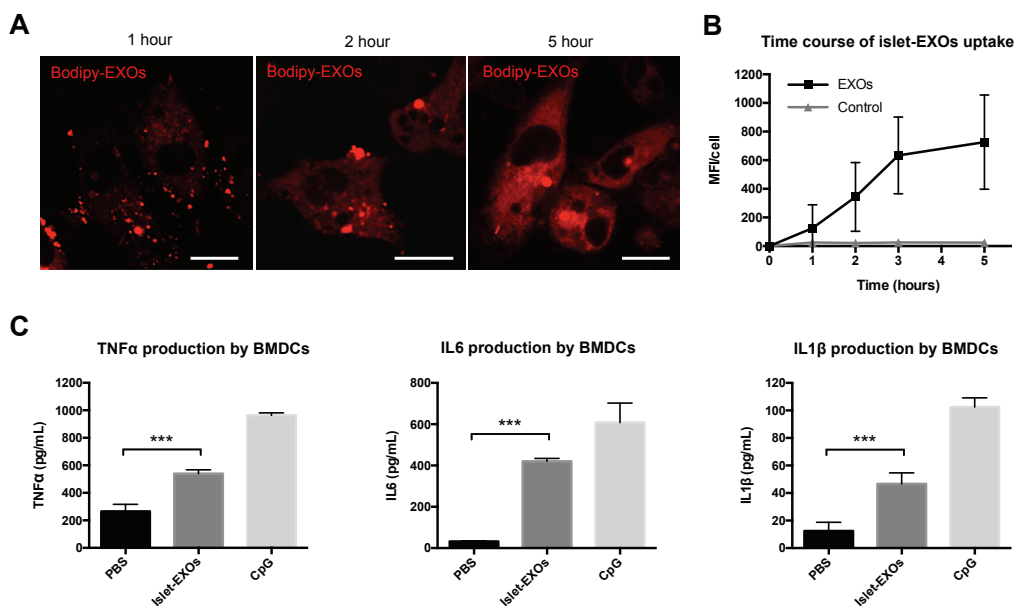


137

**Figure 3. Activation of BMDCs upon uptake of islet-exosomes.**
(**A**) Uptake of Bodipy-Ceramide labeled rat islet-exosomes by bone marrow-derived DR4$^{+/+}$ dendritic cells analyzed by confocal live cell image acquisitions. At one hour, Bodipy-exosomes were detected at the surface of cells. Exosome internalization was observed around two hours after incubation, while a more diffuse red staining was detected at five hours, indicating diffusion of the dye within the cells. Scale bars: 10 μm. (**B**) Uptake of Bodipy-exosomes by BMDCs. Free Bodipy dye processed the same way as the Bodipy-labeled islet-exosomes was used as a control. The results are shown as mean fluorescence intensity (MFI) ± SD for a total of 20 cells sampled from three different fields. (**C**) Secretion of the pro-inflammatory cytokines TNFα, IL6, and IL1β by DR4$^{+/+}$ BMDCs after stimulation by rat islet-exosomes or PBS and CpG as negative and positive controls respectively. Analyses were performed in technical triplicates. The results are reported as mean ± SD and are representative of two independent experiments. Statistical analyses were performed using a one-way ANOVA analysis (p***<0.001).

## 4.4.4 GAD65 exosome mimetics activate GAD65-specific T cells

In order to investigate the potential autoantigenicity of GAD65 in islet exosomes, we used the GAD65-specific T cell hybridoma, T33.1, which recognizes the GAD65$^{274-286}$ peptide in the context of HLA-DR4 (25,46). T33.1 cells require ~1-5 μg/ml GAD65 for stimulation as measured by IL-2 secretion. Since the quantity of EVs that can be isolated from primary islets is limited (~2-3 μg/day from 10,000 islets) and the concentration of GAD65 in islet-EVs is low (~0.05% of total exosomal protein), we sought to engineer an analog for antigen presentation of GAD65 that mimicked features of natural islet exosomes. Purified endotoxin free human recombinant GAD65 antigen was inserted in liposomes that approximated the size and membrane lipid composition of exosomes (10): unilamellar vesicles, 100 nm in diameter, containing cholesterol, sphingomyelin and ganglioside GM3 (**Figure 4A**).

Different concentrations of either free GAD65 antigen or GAD65 bound to liposomes were incubated for 24 hours with DR4$^{+/+}$ BMDCs as APCs, and then T33.1 hybridoma cells (GAD65-specific T cells) were added and incubated for 24 hours. This concentration range of GAD65 induces activation of T33.1 hybridoma cells and release of interleukin-2 (IL2) in a dose dependent manner (25,46). The GAD65$^{274-286}$ peptide was used as a positive control at a concentration that consistently induces

IL2 release at around 150-200 μg/ml from T33.1 cells. Analyses of the IL2 concentration in the supernatant revealed a 50-fold increase in T33.1 activation by GAD65-liposomes compared to the free autoantigen (**Figure 4B**), suggesting that presentation of GAD65 in the context of liposomes possessing lipids characteristic of exosomes significantly enhances T cell stimulation of the protein compared to free antigen. In a recent study (18), we have shown that compared to free GAD65, palmitoylated GAD65 more efficiently taken up by APCs and enhances stimulation of T cells consistent with the notion that in general, GAD65 inserted in a membrane is more immunogenic than free GAD65.
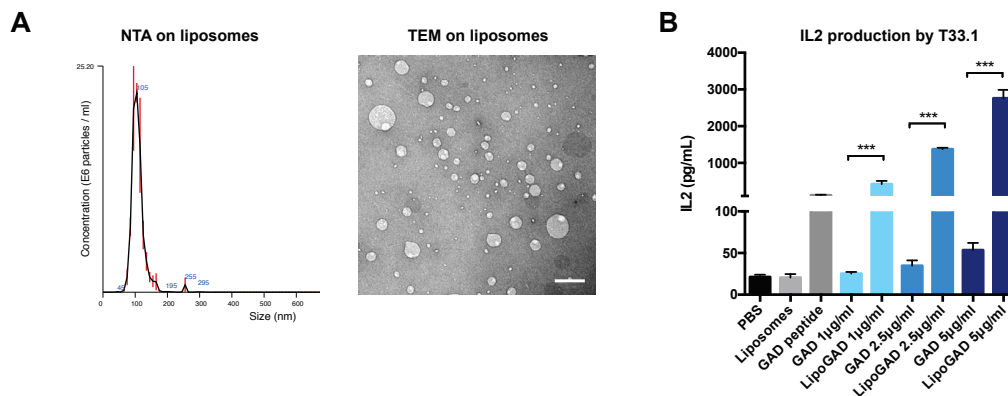


**Figure 4. GAD65-exosome mimetics induce strong GAD65-specific T cell activation.**
(**A**) Nanoparticle tracking analyses and transmission electron microscopy analyses of exosome-mimetic liposomes reveal an average size of ~100 nm. Scale bar: 200 nm. (**B**) Activation of GAD65-specific DR4-restricted T33.1 hybridoma cells by DR4$^{+/+}$ BMDCs that had been incubated with either free GAD65 protein or GAD65 anchored to liposomes and using PBS, empty liposomes, or GAD$_{274-286}$ peptide (0.5 μg/ml) as negative and positive controls. Analyses were performed in technical triplicates. Statistical analyses were performed using a one-way ANOVA (p***<0.001). The results are representative of two independent experiments.

## 4.4.5 Cytokine-induced ER stress increases EV release by pancreatic islets and induces the expression of immune stimulatory chaperones

ER stress and the resulting beta cell dysfunction are implicated in the pathogenesis of T1D (3,47). We addressed the question whether induction of ER stress in primary beta cells by Th1 cytokines affects the quantity and/or composition

of released EVs. Rat islets were incubated with or without low concentrations (10 U/ml) of IL1β and IFNγ. We confirmed induction of ER stress in cytokine-treated primary beta cells by detecting upregulation and nuclear translocation of the transcription factor CHOP (2) (**Figure 5A**).
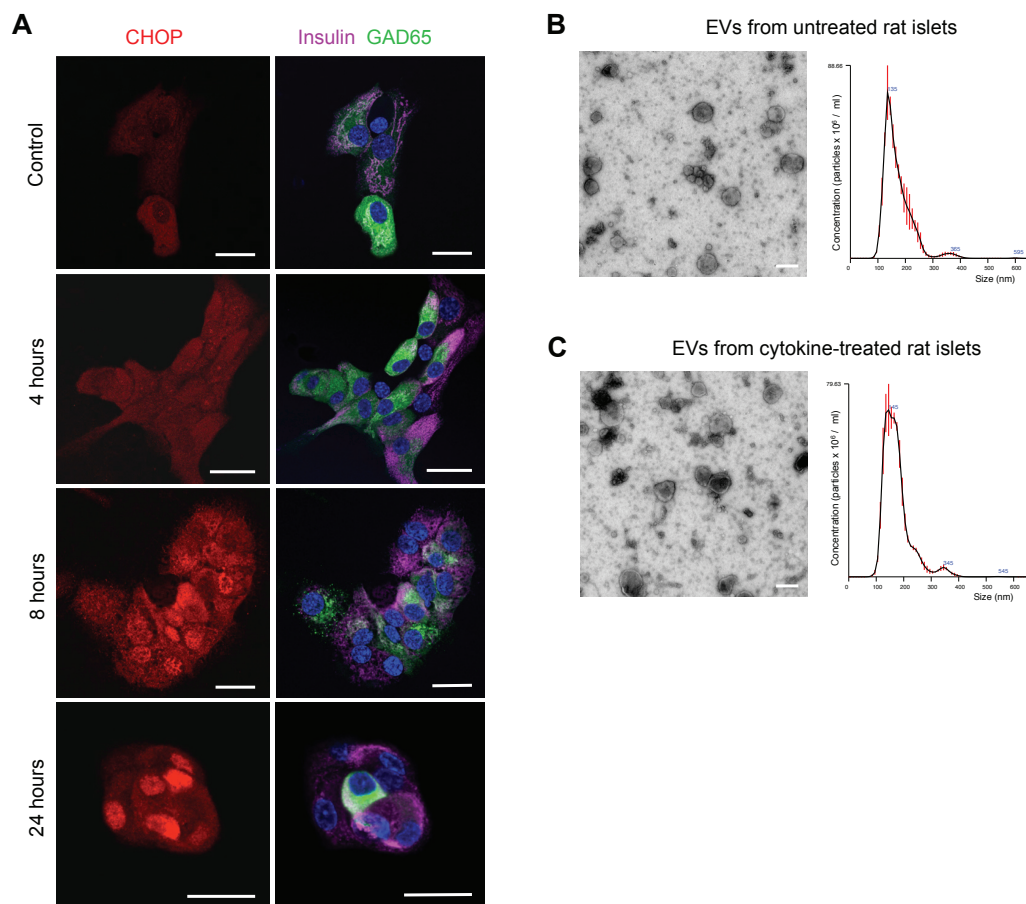


**Figure 5. Cytokine-induced ER stress does not affect the size and physical properties of exosomes released by rat pancreatic islets.**

(**A**) Primary pancreatic islet cells immunostained for the stress marker CHOP (left panels) and insulin and GAD65 (right panels), upon cytokine exposure for the indicated number of hours. Nuclei are stained in blue with DAPI. The progressive upregulation and nuclear translocation of the transcription factor CHOP indicates the induction of ER stress in treated cells. Scale bar: 30 μm. (**B-C**) Transmission electron microscopy and nanoparticle-tracking analyses on EVs isolated from untreated islets (**B**) and cytokine-treated islets (**C**). NTA indicates the presence of a uniform size distribution of EVs, with a similar major peak for untreated (141±4 nm) and cytokine-treated islets (144 ±10 nm). Scale bars: 200 nm.

No differences in the morphology and size of vesicles from cytokine-treated and untreated islets were observed by TEM or NTA (**Figure 5B and 5C**). However, analyses of total protein content measured by BCA and the total number of EVs measured by NTA revealed a 2-3-fold increase in EVs released from cytokine-treated islets vs non-treated islets (**Figure 6A and 6B)**.

LC-MS/MS analyses of the protein profile of EVs isolated from cytokine-treated islets revealed upregulation of immunomodulatory proteins involved in the ER stress response. These included the chaperones Gp96, calreticulin and the hypoxia-upregulated protein, ORP150, which were increased 2, 3 and 3.5-fold, respectively, in EVs from cytokine-treated compared to untreated islets (**Figure 6C**). These proteins have been shown to be highly immunogenic when they leave the ER and appear on the surface of cells or outside cells (48). In contrast, other proteins were found at similar concentrations in cytokine-treated vs. untreated preparations, including exosomal markers (CD9, CD81 and flotillin1), GAPDH, and proteins involved in the cytosolic stress response, such as Hsp90 (**Figure 6C**). WB analyses confirmed the induction of the ER-chaperones calreticulin and Gp96 in exosomes from cytokine-treated islets, while exosomes from untreated cells were negative. In contrast, the ER-chaperone protein disulfide isomerase (PDI), which can also be detected on the surface of cells and secreted from cells (49), was detected at similar levels in exosomes from treated and untreated islets, suggesting that induction of calreticulin, Gp96 and ORP150 in islet-exosomes by cytokines is a selective process. The concentrations of GAD65, IA-2, insulin and flotillin1, however, were similar in EVs from cytokine-treated and untreated islets although their total amount was increased commensurate with the increase in released EVs (**Figure 6D** and results not shown). The data presented here suggest that induction of ER stress in beta cells can result in targeting of selected immunostimulatory ER chaperones to exosomes. Furthermore, exosomes isolated from human islets treated with IL1β and IFNγ (20 U/ml and 10 U/ml respectively) induced a stronger activation of the DR4^{+/+} BMDCs

compared to those isolated from untreated islets, as shown by secretion of the immunostimulatory cytokines IL6 and TNFα (**Figure 6E-F**).
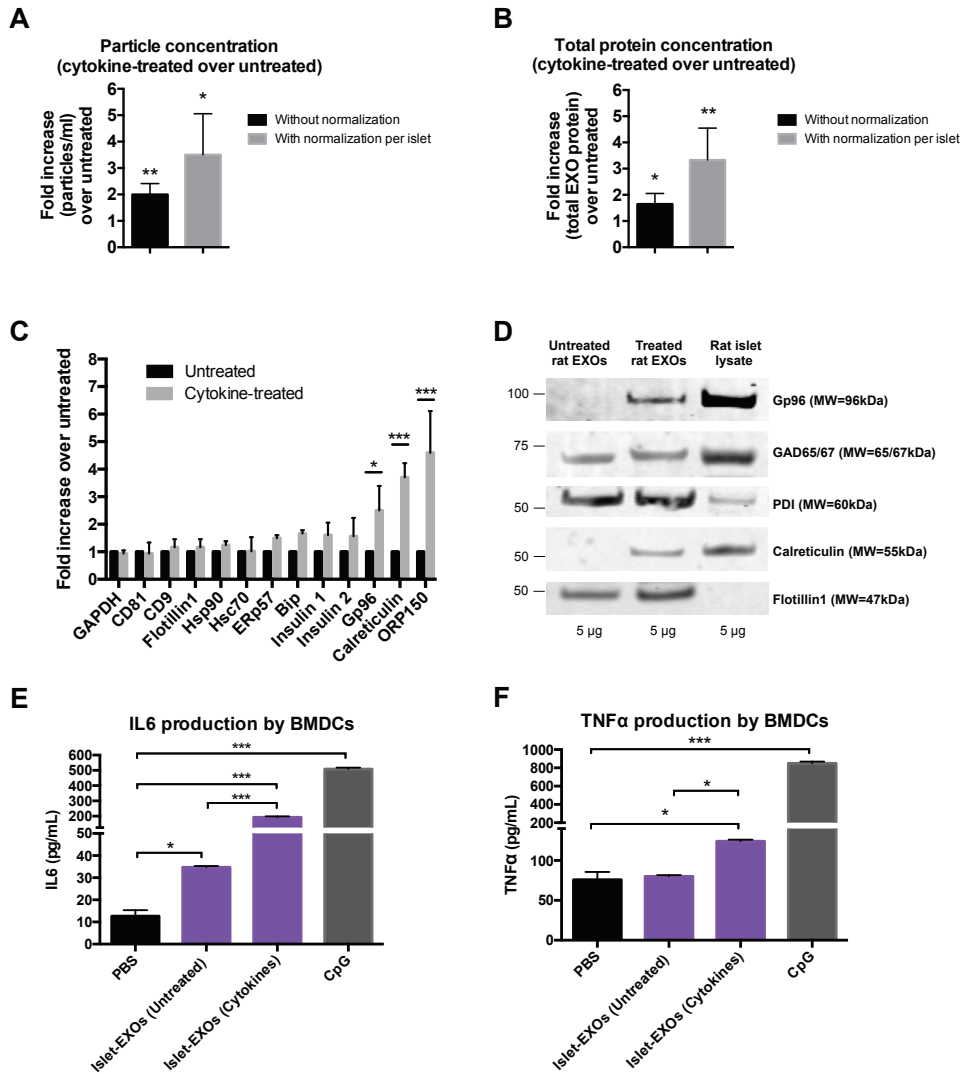


**Figure 6. Th1 cytokine treatment results in increased exosome release and co-release of immunogenic chaperones by islets cells.**

(**A-B**) Release, over a total period of 6 days, of exosomes from cytokine-treated (10 U/ml IFNγ and 10 U/ml IL1β) vs untreated rat islets shown as (**A**) particle concentration by nanoparticle tracking analyses and (**B**) total protein content by BCA. Bars represent quantitation of exosome secretion without (black bars) and with (grey bars) correction for the number of islets. Data are expressed as mean ± SD of 4 independent experiments. Statistical analyses were performed using a paired *t* test  (p*<0.05, p**<0.01). (**C**) Ratio of LC-MS/MS analyses of EV proteins from cytokine treated and untreated rat islet cells showing cytokine-induced upregulation of proteins involved in the ER stress response. Data are expressed as mean ± SD of 3 independent experiments. Statistical analyses were performed using a

one-way ANOVA (p*<0.05, p***<0.001). (**D**) Western blot analyses of EVs isolated from cytokine treated and untreated rat islet cells showing specific induction of the ER chaperones Gp96, Calreticulin and ORP150 by cytokine treatment. Data are representative of 3 independent experiments. (**E-F**) Exosomes isolated from untreated and cytokine-treated human islets were incubated (50 µg/ml) with DR4+/+ BMDCs for 24h. CpG (5 µg/ml) was used as positive control. Activation of the BMDCs was assessed by secretion of the pro-inflammatory cytokines IL6 (**E**) and TNFα (**F**). Data are expressed as mean ± SEM (n=3) and are representative of 2 independent experiments. Statistical analyses were performed using a one-way ANOVA (p*<0.05, p***<0.001).

## 4.5  DISCUSSION

It is not known why the GAD65, IA-2 and insulin/proinsulin autoantigens in human T1D are so susceptible to becoming targets of autoimmunity, nor is it known how they initially attract the attention of the immune system. Notably, GAD65 and IA-2 are scarce intracellular beta cell membrane proteins, which are processed in the ER and Golgi compartments before targeting to secretory pathways. IA-2 is a transmembrane proteins localized in the limiting membrane of large dense core insulin secretory vesicles, whereas GAD65 is a peripheral membrane protein found in the membrane of distinct smaller microvesicles (15). While mature insulin is present in sufficient amounts in the circulation to induce and maintain immunological tolerance, proinsulin is an intracellular beta cell protein targeted by autoimmunity in NOD mice and man (7,9). It has been proposed that the initiation of T1D autoimmunity follows a period of prolonged ER stress, induced by inflammatory cytokines, and resulting in apoptosis (47) and presentation of beta cell proteins to self-reactive T cells. The data presented here reveal that primary islets release immunogenic exosomes containing the beta cell intracellular autoantigens, GAD65 and IA-2, and proinsulin. Hybrid peptides between proinsulin and other secretory granule proteins are targets of CD4 T cells in T1D and are implicated in loss of self-tolerance to insulin in human T1D (8).

As shown previously for exosomes from insulinoma cell lines (9), EVs from primary islets are rapidly and efficiently taken up by APCs resulting in their activation.

The exosomal markers flotillin1, CD9 and CD81 were detected in islet-EVs. The biogenesis pathway for exosomes expressing those markers may originate in the TGN and involve Rab11-controlled transport through recycling endosomes (10). The data presented here suggest that trafficking of GAD65 from TGN to exosomes may follow this pathway.

Beta cells have an extensive and highly active ER, reflecting their role in synthesizing and secreting large amounts of insulin. The enormous protein synthesis capacity of beta cells, however, makes them markedly susceptible to ER stress. Th1 cytokines secreted by inflammatory cells induce ER stress in beta cells (47). Disturbances in the normal function of the ER to modify and fold newly synthesized proteins results in induction of the unfolded protein response, which is aimed at restoring cell ER homeostasis but can eventually trigger apoptosis if an imbalance in the folding capacity persists. In this study we show that induction of ER stress by pro-inflammatory cytokines results in a 2-3 fold increase in exosome secretion by islet cells and consequently the proteins in them. We have recently shown (18) that ER stress induced by three different regimens results in perturbation of the palmitoylation cycle controlling GAD65 endomembrane distribution and accumulation of an immunogenic palmitoylated form of the protein in TGN membranes. We propose that aberrant trafficking during ER stress diverts more GAD65 to the exosomal pathway to maintain a similar concentration of the protein in exosomes during increased secretion.

Different possibilities can be suggested to explain the increased release in EVs from beta cells in ER stress conditions. First, exosomes have been suggested to play a role in intercellular communication (10), and increased secretion may serve to signal ER stress conditions to neighboring cells. Second, exosomes may be a vehicle for disposing of cell material that is not needed or desirable for optimal responses to ER stress in a cell seeking to regain homeostasis.

Cytokine treatment also resulted in a change in the composition of EVs. Whereas the composition and relative quantity of autoantigens and exosome markers were similar with and without cytokine treatment, the latter resulted in a co-release of ER-chaperone proteins known to act as strong pro-inflammatory molecules (50,51). These proteins, calreticulin, Gp96 and ORP150, can be found outside the ER, on the cell surface and released extracellularly (48). They are known for their role in triggering immune responses by promoting phagocytosis and/or by directly exerting adjuvant capacity (48,51). Some of these ER proteins or antibodies to them have been implicated in autoimmunity (52). It is possible that islet-exosomes carrying a combination of autoantigens and pro-inflammatory signals may be particularly immunogenic.

We considered the possibility that the ER chaperones detected in exosome preparations from stressed beta cells originated from ER microsomes generated during cytokine-induced islet cell death that coincidentally co-purified with exosomes. While this possibility cannot be formally excluded, several factors argue against a significant contribution of ER-derived microsomes to our EV preparations. First, the relative amount of exosomal markers and autoantigens in EVs was similar with and without cytokine treatment. Thus a dilution effect of contaminating microsomes was not observed. Second, in contrast to the immunogenic ER chaperones mentioned above, the relative amount of PDI, an ER chaperone, which is not associated with induction of immunogenicity (53) (Schild and Rammensee personal communication), was not increased in EVs by cytokine treatment, suggesting that only specific ER proteins were enhanced. Third, the morphology and size of exosomes remained similar with cytokine treatment, consistent with a lack of the heterogeneity, which would be expected with addition of ER microsomes.

The pathway involved in transport of ER proteins into exosomes under stress conditions has not been elucidated. Islet-EVs were particularly enriched in Rab1, which is involved in vesicle transport from ER-to-Golgi membranes. During

145

immunogenic cell death, calreticulin undergoes an ER-to-Golgi anterograde transport (54). An ER-to-Golgi anterograde transport of the ER proteins in conditions of ER stress would be consistent with a Golgi origin of some islet-exosomes and a trafficking pathway where autoantigens, exosome markers and heat shock proteins assemble in exosomes. Alternatively, as several studies have identified contact sites and interaction between ER membranes and endosomal compartments (55) including MVBs (56), it is possible that the ER chaperones are transported directly from the ER to endosomal compartments. Cytokine treatment of mouse islets to induce ER stress has also been shown to result in a detection of another ER chaperone, glucose-regulated protein 78 (GRP78), in the plasma membrane of primary islet cells and GRP78 was detected in the medium of cytokine treated INS-1E cells. These findings support the notion that inflammatory conditions induced by IL1b and IFNg may results in aberrant surface location and secretion of some ER chaperones. Interestingly, cytokine treatment was also shown to result in citrullination of GRP78 and targeting of a citrullinated peptide by both B cells and T cells in NOD mice (57). Thus, additional studies are important for identification of potential post-translational modifications of ER chaperones and autoantigens associated with islet-exosomes in order to better understand their contribution to the induction of autoimmunity.

Islet derived EVs are rapidly and efficiently taken up by APCs expressing the T1D susceptibility haplotype DRB1*0401, resulting in their activation. To investigate the potential auto-antigenicity of islet-exosomes, we adopted an established GAD65-specific T cell assay using DR4$^{+/+}$APCs and a DR4-restricted GAD65 specific T cell hybridoma (25). The amount of GAD65 required for antigen specific stimulation of T33.1 cells could not be achieved from the limited amount of exosomes that can be obtained from primary islets. Instead, we developed a platform where purified GAD65 was bound to liposomes approximating the size and lipid composition of islet-exosomes. APCs loaded with GAD65 liposomes were 1-2 orders of magnitude more

efficient in inducing activation of autoreactive T cells compared to the free antigen. Furthermore, preliminary experiments revealed that compared to ovalbumin, calreticulin enhances the stimulatory effect of GAD65-liposomes on BMDCs and activation of GAD65 specific T33.1 cells (**Supporting Figure 4**).

The engineered platform based on exosome mimetics presents an initial attempt to assess the immunogenic potential of GAD65 in lipid membranes with some characteristics of exosomes and it is not perfect. For instance, the liposomes carry GAD65 on the surface rather than on the luminal face, which is more likely the position of GAD65 in exosomes. Furthermore, the immunogenicity of natural exosomes is likely the results of a particular compositions of proteins and lipids, some enhancing the uptake and presentation by APCs, others functioning as accessory molecules in the immune response. However, the reductionist approach of the liposomal platform can be explored to investigate the role of individual components in APC activation and antigen presentation. With further development, exosome-mimetics may become useful as therapeutic strategy to generate tolerance versus immunity to GAD65 and other autoantigens, when combined with molecules with known anti-inflammatory properties.

In conclusion, we propose (**Figure 7**) that the release of the autoantigens GAD65, IA-2 and insulin/proinsulin in exosomes from pancreatic beta cells may play a role in triggering autoimmunity, especially in pro-inflammatory conditions eliciting ER stress and dysfunction, with consequent co-release of immunostimulatory ER chaperones. With time it may become feasible to test the role of immunogenic chaperones using natural exosomes isolated from primary islets exposed to inflammatory stress. This approach may benefit from first testing the *in vitro* stimulatory effect on T cells specific for the more abundant exosomal autoantigens proinsulin and/or insulin and then taking advantage of the NOD mouse for *in vivo* studies targeting these proteins.
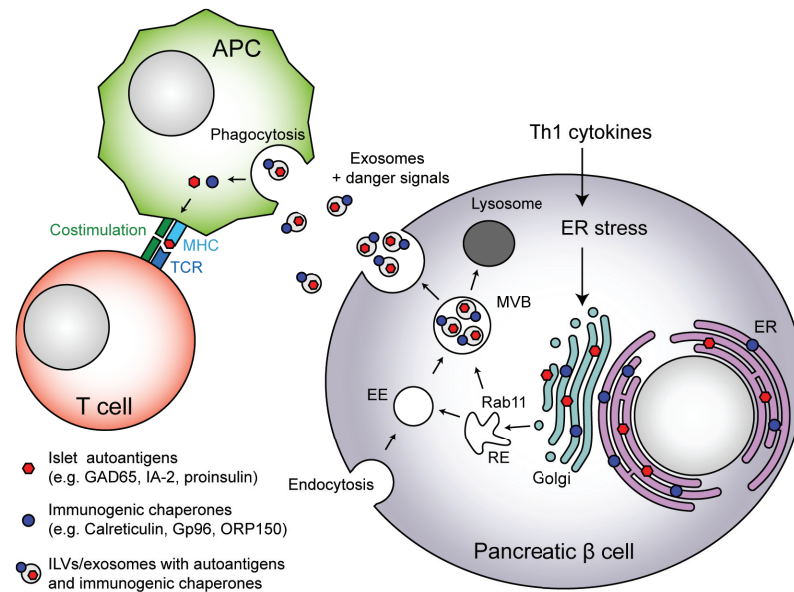
**Figure 7. Proposed schematic model of combined release of autoantigens and pro-inflammatory ER proteins in beta cell exosomes under cytokine-induced ER stress conditions.**

ER stress can be induced in pancreatic beta cells by Th1 cytokines and other inflammatory factors, leading to upregulation of ER proteins involved in the unfolded protein response, and possibly their translocation to the Golgi. Once in the Golgi, these ER proteins can be transferred, loaded into the ILVs of MVBs, and released in exosomes. A localization in common between the islet autoantigens during their biosynthesis pathway is the Golgi compartment, thus their loading into exosomes, together with ER proteins is a possibility. In addition, ER stress can induce an increase in the amount of exosomes released by pancreatic beta cells. ER proteins outside the cell may be recognized as danger signals by APC, leading to cell activation and phagocytosis of autoantigen-containing exosomes. This may result in autoantigens being processed and presented to self-reactive T cells, triggering autoimmunity against pancreatic beta cells. (ER, Endoplasmic Reticulum; EE, Early Endosome; RE, Recycling Endosome; MVB, Multivesicular Body; ILVs, Intraluminal Vesicles; APC, Antigen Presenting Cell; TCR, T Cell Receptor).

## 4.6  CONTRIBUTION OF THE DOCTORAL CANDIDATE

The doctoral candidate conceived the study. She designed the study together with E.A.P and S.B. She directly performed all the experiments reported in the manuscript, except the LC-MS/MS analyses that were performed by the Proteomics core facility of EPFL, and she analyzed the data together with S.B. She wrote the paper together with the corresponding author and thesis advisor S.B.

# 4.7 SUPPLEMENTARY INFORMATION

| Pathway | Protein | Uniprot Accession Number | Matched Unique Peptides | | Uniprot Accession Number | Matched Unique Peptides | Reference |
|---|---|---|---|---|---|---|---|
| | | | Rat islets | INS-1E | | Human islets | |
| *Cytoskeleton associated* | Beta tubulin | P69897 | 26 | 22 | P68371 | 20 | (1) |
| | Alpha Tubulin | Q6P9V9 | 27 | 16 | P68363 | 18 | (2) |
| | Actin | P63259 | 44 | 24 | P63261 | 30 | (3) |
| | Moesin | F1LP60 | 19 | 1 | P26038 | 17 | (3) |
| | Ezrin | P31977 | 3 | 0 | P15311 | 35 | (4) |
| | Profilin1 | P62963 | 5 | 3 | P07737 | 6 | (5) |
| | Cofilin1 | P45592 | 5 | 8 | P23528 | 9 | (1) |
| *Signaling* | 14-3-3 protein zeta/delta | P63102 | 26 | 12 | P63104 | 12 | (1) |
| | 14-3-3 protein epsilon | P62260 | 12 | 8 | P62258 | 8 | (3) |
| | Elongation factor 1-alpha 1 | P62630 | 16 | 14 | P68104 | 18 | (6) |
| *Membrane trafficking* | Annexin 2 | Q07936 | 11 | 0 | P07355 | 25 | (6) |
| | Annexin 6 | D4ABR6 | 15 | 0 | P08133 | 35 | (7) |
| | Rab1 | E9PU16 | 5 | 3 | P62820 | 3 | (8) |
| | Rab11a | P62494 | 10 | 2 | P62491 | 4 | (9) |
| | Rab27a | P23640 | 2 | 0 | H3BN55 | 3 | (10) |
| | Rab27b | Q99P74 | 5 | 0 | O00194 | 0 | (10) |
| | Rab35 | Q5U316 | 2 | 1 | F5H157 | 2 | (11) |
| | Flotillin1 | Q9Z1E1 | 2 | 0 | O75955 | 0 | (12) |
| | Clathrin heavy chain | F1M779 | 67 | 89 | Q00610 | 52 | (2) |
| *Tetraspanins* | CD9 | P40241 | 1 | 0 | A6NNI4 | 2 | (13) |
| | CD81 | Q6P9V1 | 3 | 5 | A6NMH8 | 3 | (6) |
| *Late endosome/ Lysosome* | LAMP1 | P14562 | 1 | 1 | P11279 | 4 | (13) |
| *Enzymes* | GAPDH | P04797 | 13 | 16 | P04406 | 22 | (2) |
| | Pyruvate kinase M2 isoform | P11980-2 | 18 | 17 | P14618 | 29 | (2) |
| *Heat shock response* | Hsc70 | P63018 | 24 | 37 | E9PKE3 | 19 | (1) |
| | Hsp70 | Q07439 | 12 | 2 | P08107 | 15 | (4) |
| | Hsp90alpha | P82995 | 3 | 4 | P07900 | 18 | (3) |
| | Hsp90beta | P63018 | 7 | 14 | P08238 | 13 | (3) |
| *Beta cell islet antigen* | Insulin1 | P01322 | 7 | 12 | P01308 | 20 | |
| | Insulin2 | P01323 | 4 | 11 | | | |

**Supplementary Table 1. Proteins identified by LC-MS/MS analysis in EV preparations from rat pancreatic islets, INS-1E cells and human pancreatic islets.**

The right column shows references for identification of each protein in exosomal preparations from other cell types.

**References listed in Supplementary Table 1**

1.  Théry C, Boussac M, Véron P, Ricciardi-Castagnoli P, Raposo G, Garin J, et al. Proteomic analysis of dendritic cell-derived exosomes: a secreted subcellular compartment distinct from apoptotic vesicles. J Immunol 2001;166(12):7309–18
2.  Wubbolts R, Leckie RS, Veenhuizen PTM, Schwarzmann G, Möbius W, Hoernschemeyer J, et al. Proteomic and biochemical analyses of human B cell-derived exosomes. Potential implications for their function and multivesicular body formation. J Biol Chem 2003;278(13):10963–72
3.  Carayon K, Chaoui K, Ronzier E, Lazar I, Bertrand-Michel J, Roques V, et al. Proteolipidic composition of exosomes changes during reticulocyte maturation. J Biol Chem 2011;286(39):34426–39
4.  Hegmans JPJJ, Bard MPL, Hemmes A, Luider TM, Kleijmeer MJ, Prins J-B, et al. Proteomic analysis of exosomes secreted by human mesothelioma cells. Am J Pathol 2004;164(5):1807–15
5.  Fevrier B, Vilette D, Archer F, Loew D, Faigle W, Vidal M, et al. Cells release prions in association with exosomes. Proc Natl Acad Sci U S A 2004;101(26):9683–8
6.  Conde-Vancells J, Rodriguez-Suarez E, Embade N, Gil D, Matthiesen R, Valle M, et al. Characterization and comprehensive proteome profiling of exosomes secreted by hepatocytes. J Proteome Res 2008;7(12):5157–66
7.  Pisitkun T, Shen R-F, Knepper MA. Identification and proteomic profiling of exosomes in human urine. Proc Natl Acad Sci U S A  2004;101(36):13368–73
8.  Hassani K, Olivier M. Immunomodulatory Impact of Leishmania-Induced Macrophage Exosomes: A Comparative Proteomic and Functional Analysis. Milon G, editor. PLoS Negl Trop Dis 2013;7(5):e2185
9.  Savina A, Vidal M, Colombo MI. The exosome pathway in K562 cells is regulated by Rab11. J Cell Sci 2002;115(Pt 12):2505–15
10. Ostrowski M, Carmo NB, Krumeich S, Fanget I, Raposo G, Savina A, et al. Rab27a and Rab27b control different steps of the exosome secretion pathway. Nat Cell Biol 2010;12(1):19–30; sup pp 1–13
11. Hsu C, Morohashi Y, Yoshimura S-I, Manrique-Hoyos N, Jung S, Lauterbach MA, et al. Regulation of exosome secretion by Rab35 and its GTPase-activating proteins TBC1D10A-C. J Cell Biol 2010;189(2):223–32
12. Strauss K, Goebel C, Runz H, Möbius W, Weiss S, Feussner I, et al. Exosome secretion ameliorates lysosomal storage of cholesterol in Niemann-Pick type C disease. J Biol Chem 2010;285(34):26279–88
13. Nazarenko I, Rana S, Baumann A, McAlear J, Hellwig A, Trendelenburg M, et al. Cell surface tetraspanin Tspan8 contributes to molecular pathways of exosome-induced endothelial cell activation. Cancer Res 2010;70(4):1668–78
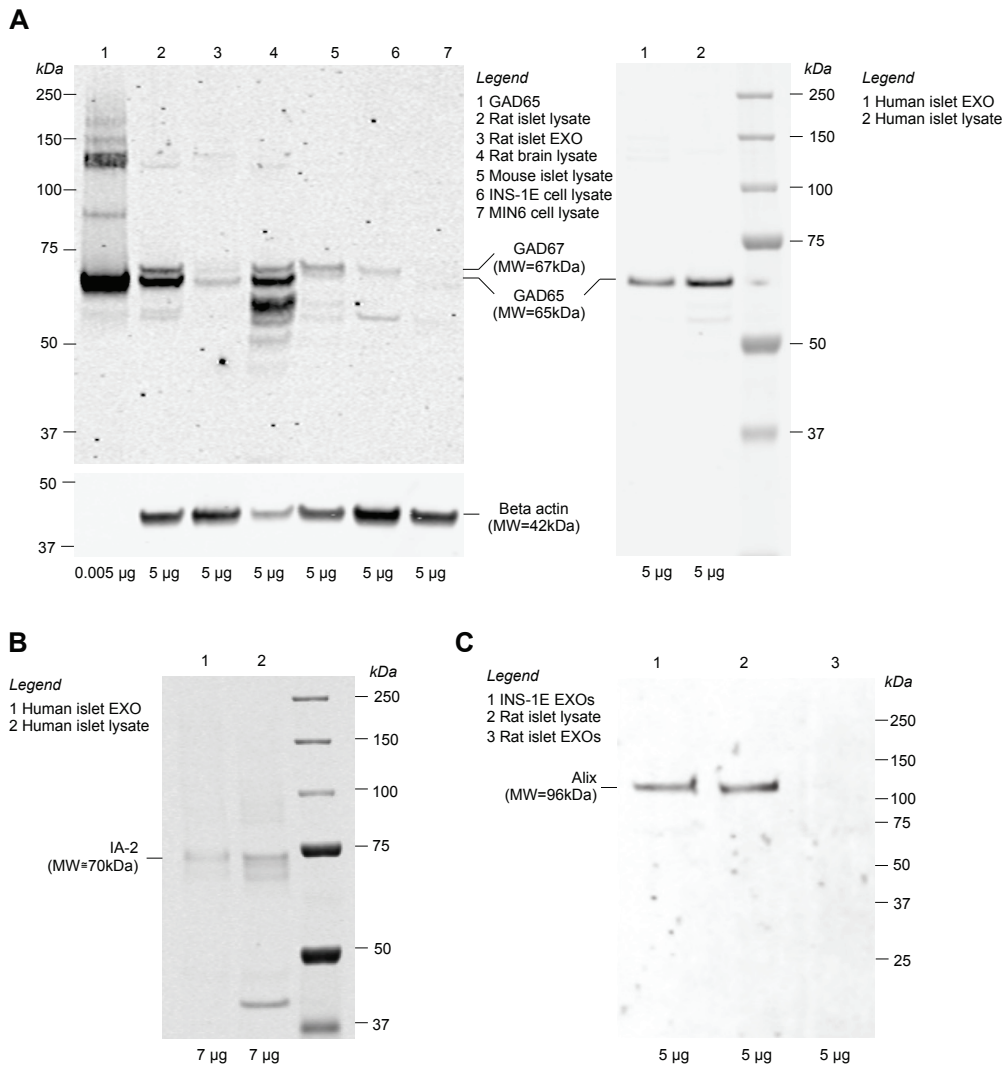
**Supplementary Figure 1. Analyses of protein expression in exosomes isolated from primary islets or insulinoma cells.**

(**A**) Uncropped scan related to the cropped scan of a Western blot showing GAD65/GAD67 in rat and human islets and exosomes in Figure 1. The uncropped Western blot shows rat, mouse and human islet proteins, rat and human exosome proteins and rat and mouse insulinoma protein immunostained using the GAD1701 antiserum that recognizes both GAD65 and GAD67. Rat islets express both GAD65 and the non-autoantigenic isoform GAD67 (left panel), while human islets only express the GAD65 isoform of GAD (right panel). Mouse islets and rat INS-1E cells only express GAD67, while mouse MIN6 cells express neither GAD isoform (left panel). Human recombinant GAD65, rat brain lysate and rat islet lysate were used as positive controls. (**B**) Uncropped scan related to the cropped scan of a Western blot showing human IA-2 in human islets and exosomes in Figure 1E. The Western blot of human islet and exosome proteins was immunostained with the 76F-B4 mouse monoclonal antibody to IA-2. (**C**) Western blot of rat islet exosome proteins, rat islet proteins, and rat insulinoma cell line INS-1E exosome proteins immunostained with a monoclonal antibody to the exosomal marker Alix. (**A-C**) Data are representative of 2-5 independent experiments.

152
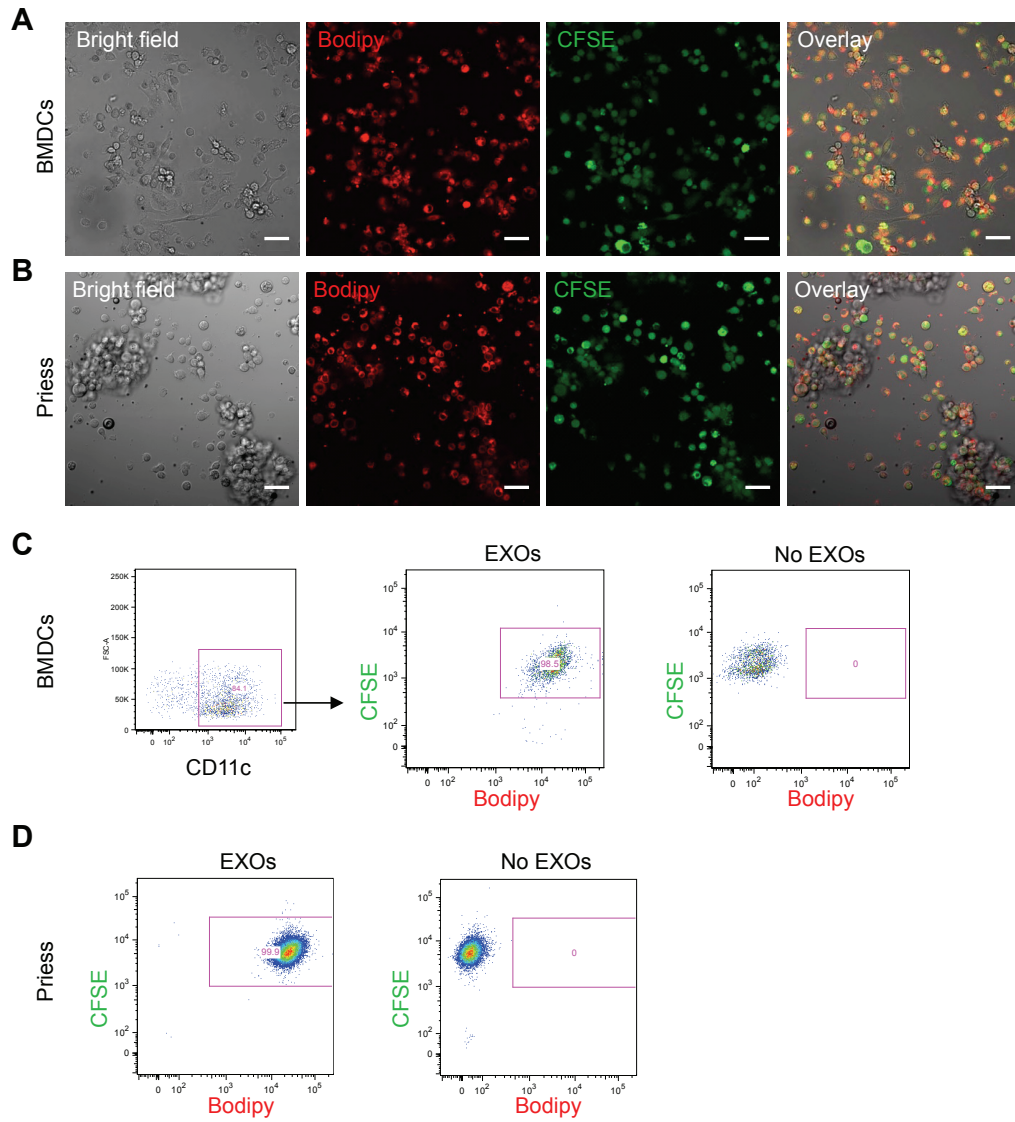
**Supplementary Figure 2. Uptake of islet exosomes by BMDCs and Priess B cells.**

Pancreatic islet derived-EVs were labeled with Bodipy-Ceramide and added at the concentration of 25 µg/ml to 100,000 CFSE-labeled DR4$^{+/+}$ BMDCs (**A, C**) or DR4$^{+/+}$ human Priess B cells (**B**, **D**). After five hours of incubation, cells were analyzed by live cell imaging (**A, B**) and flow cytometry (**C, D**). Confocal acquisitions of CFSE (green), Bodipy-Ceramide (red) and bright field channels show that both DCs (**A**) and B cells (**B**) are positive for Bodipy-Ceramide. In addition, a very high percentage (around 99%) of BMDCs cells (**C**) and B cells (**D**) are Bodipy-Ceramide-positive by flow cytometry. Analyses of BMDCs were performed on the cell population positive for the CD11c antigen expressed by mature dendritic cells. Scale bars: 30 µm.

## 4.8  SUPPORTING INFORMATION

**A**

**Cell viability of rat islets during supernatant collection for exosome isolation**

Method: Trypan Blue counting



**B**

**Cell viability of rat islet single cells**

Method: Annexin V Apoptosis detection kit
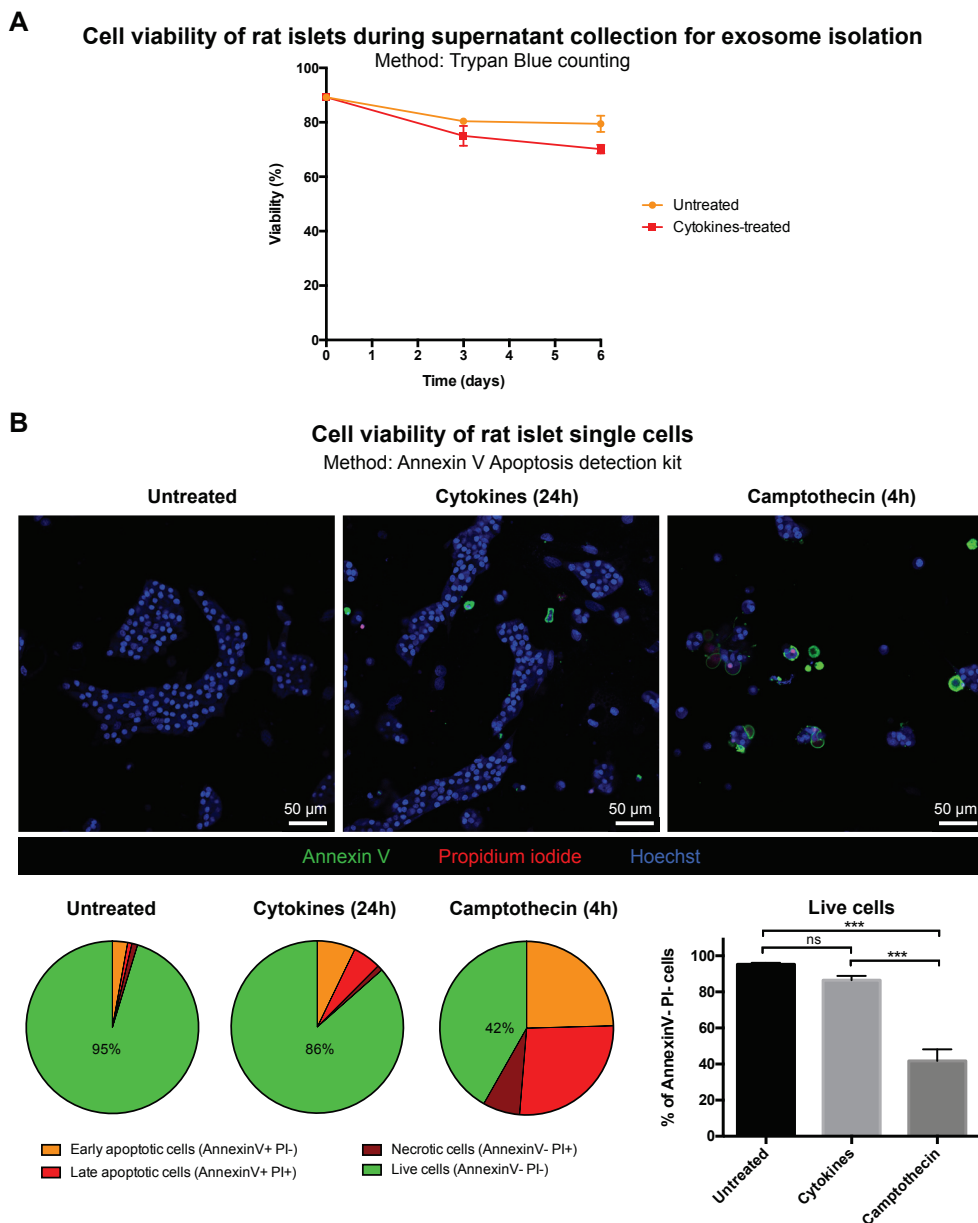


**Supporting Figure 1. Cell viability of untreated and cytokine-treated rat islets.**

(**A**) Rat islets were seeded in 10 cm Petri dishes (~500 islets/plate) and half of them were treated with 10 U/ml of rIL1β and 10 U/ml of rIFNγ for a total of 6 days. Supernatants were collected every two days for exosome isolation. Cell viability was assessed every 3 days by collecting a sample of islets from each dish. A pool of ~30 islets was dissociated with Trypsin/EDTA followed by a dilution in fresh medium containing serum.  Cells were then stained immediately by Trypan Blue and live vs dead cells counted in a counting chamber. Results are reported as mean ± SD (n=5 different cell countings per group). (**B**) Rat islet single cells prepared as described above were treated or not with either 10 U/ml of rIL1β and 10 U/ml of rIFNγ for 24h or 100 µM of the apoptosis inducing compound camptothecin for 4h. Cell viability was assessed by confocal microscope analyses using the Annexin V Apoptosis detection

kit (Invitrogen). Results are reported as mean ± SD (n=6 different fields per group). Statistical analyses were performed using a one-way ANOVA analysis (p***<0.001).

**A**

**Cell viability of human islets during supernatant collection for exosome isolation**

Method: Trypan Blue counting



**B**

**Cell viability of human islet single cells**

Method: Annexin V Apoptosis detection kit
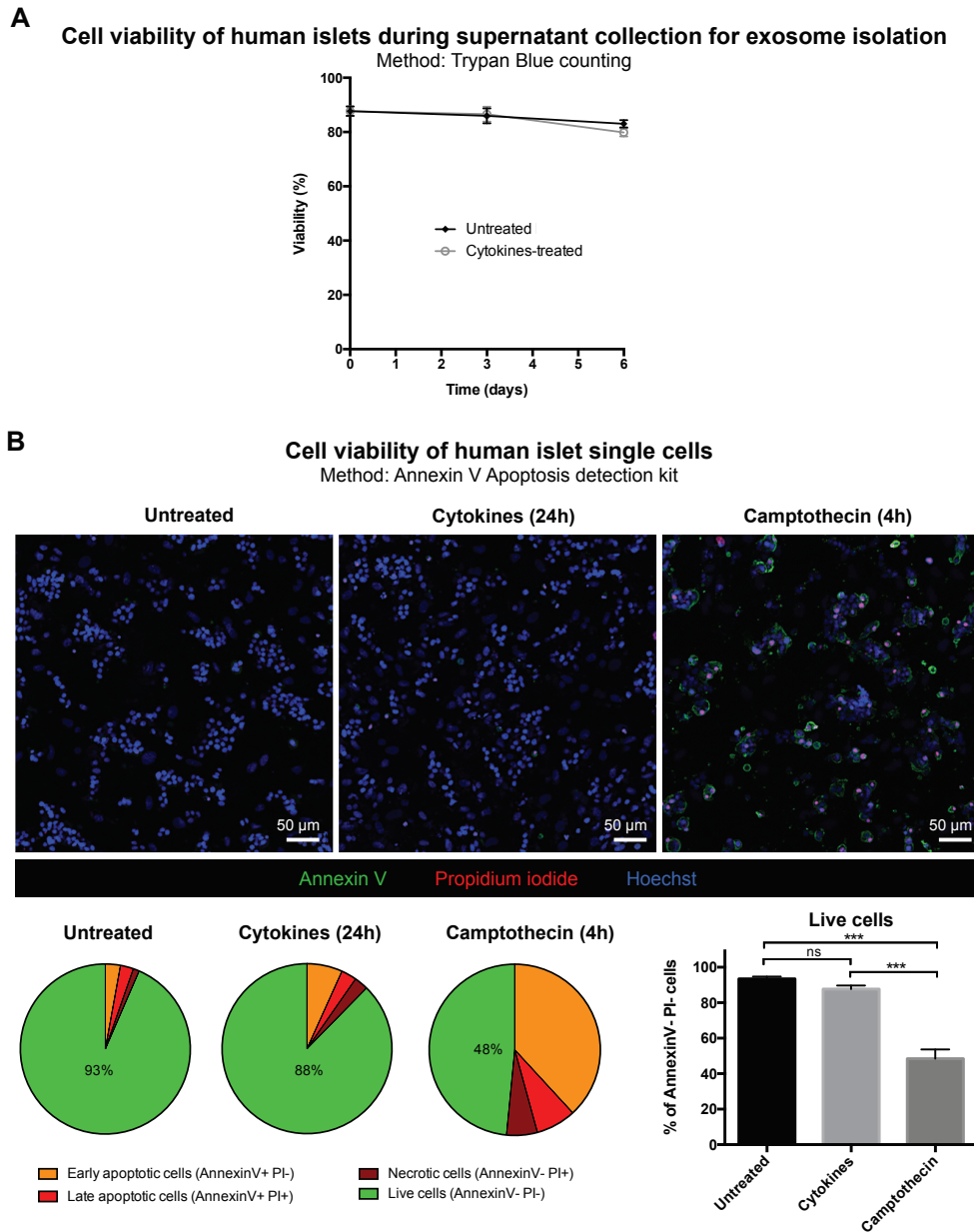


**Supporting Figure 2. Cell viability of untreated and cytokine-treated human islets.**

(**A**) Human islets were seeded in Petri dishes (~500 islets/plate) and half of them was treated with 20 U/ml of hIL1β and 10 U/ml of hIFNγ for a total of 6 days. Supernatants were collected every two days for exosome isolation. Cell viability was assessed every 3 days by collecting a sample of islets from each dish. A pool of ~30 islets was dissociated with Trypsin/EDTA followed by dilution in fresh medium containing serum. Cells were stained immediately by Trypan Blue and live vs dead cells counted using a counting chamber. Results are reported as mean ± SD (n=5 different cell countings per group). (**B**) Human islet single cells, prepared as described above, were treated or not with 20 U/ml of hIL1β and 10 U/ml of hIFNγ for 24h or 100 μM of the apoptosis inducing compound camptothecin for 4h. Cell viability was assessed by confocal microscope analyses using the Annexin V Apoptosis detection kit
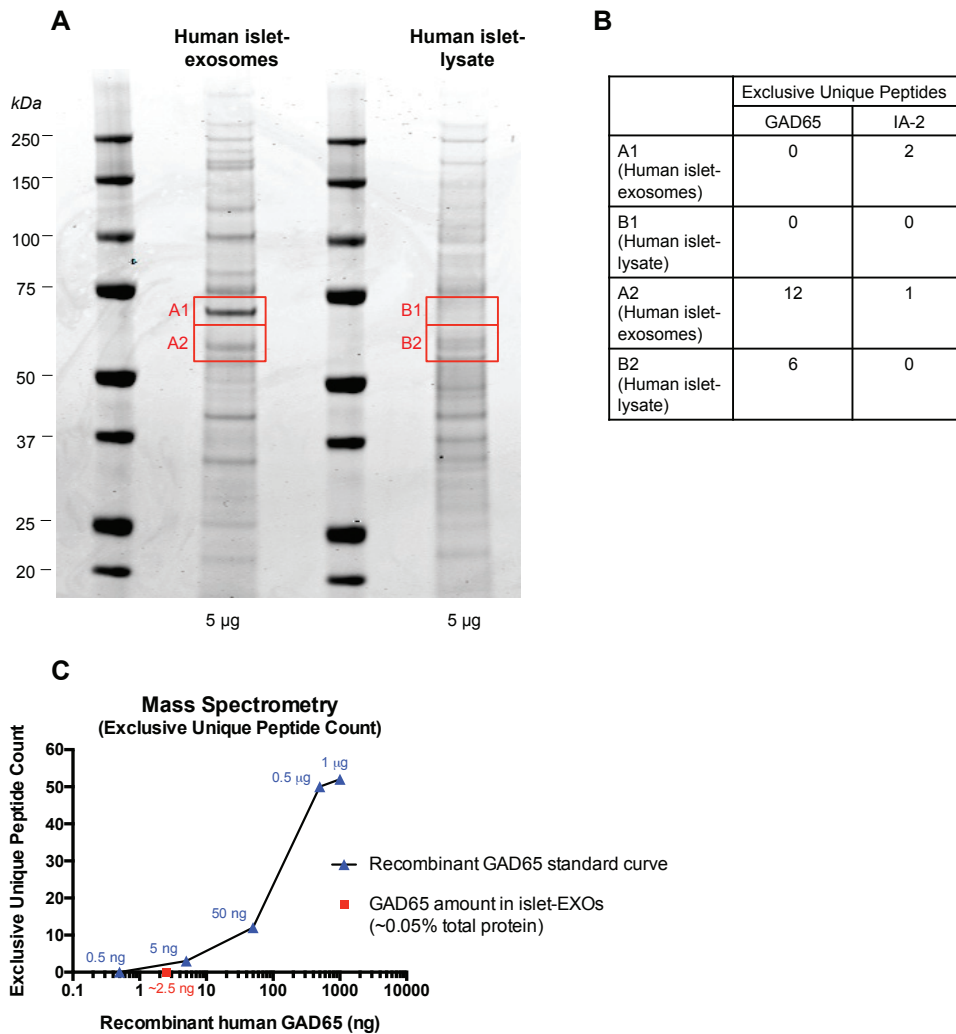
(Invitrogen). Results are reported as mean ± SD (n=6 different fields per group). Statistical analyses were performed using a one-way ANOVA analysis (p***<0.001).



**A**

Human islet-exosomes | Human islet-lysate

| | Exclusive Unique Peptides | |
|---|---|---|
| | GAD65 | IA-2 |
| A1 (Human islet-exosomes) | 0 | 2 |
| B1 (Human islet-lysate) | 0 | 0 |
| A2 (Human islet-exosomes) | 12 | 1 |
| B2 (Human islet-lysate) | 6 | 0 |

**Supporting Figure 3. Detection of GAD65 and IA-2 in human islet-exosomes by LC-MS/MS.**

Five µg of human islet-exosomes or human islet-lysate were separated on a denaturing 4-12% polyacrylamide gradient gel. (**A**) Gel slices were excised in the indicated areas and proteins were eluted and analyzed by LC-MS/MS. (**B**) Number of exclusive unique peptides identified for GAD65 and IA-2, showing the presence of both proteins in human islet-exosomes. (**C**) In order to define the threshold of detection of GAD65 by mass spectrometry, increasing amounts of recombinant human GAD65 (0.5 ng-1 µg) were analyzed in solution by LC-MS/MS. The amount of GAD65 in islet-exosomes was estimated by quantitative Western Blotting using serial dilutions of recombinant hGAD65 as a positive standard. Data show the limitations in detecting GAD65 by MS, which is likely due to its hydrophobicity and poor peptide ionization. While protein amounts of ≥5 ng are clearly identifiable by LC-MS/MS, the amount of GAD65 in 5 µg of islet-exosomes (2.5 ng) is close to the boundary of detection. The pre-purification step of exosome lysate by SDS-PAGE, however, improves the detection of GAD65 and also enables the detection of IA-2.
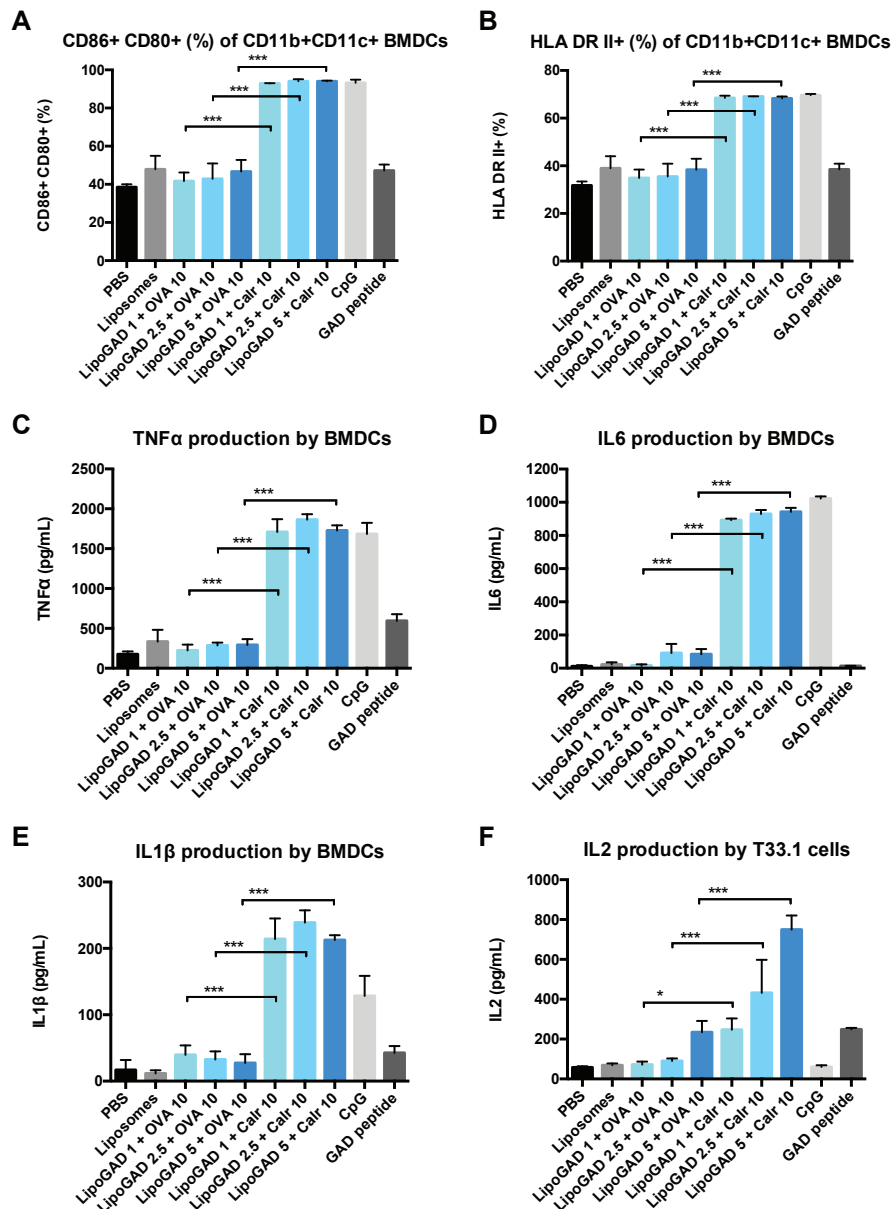
**Supporting Figure 4. Enhanced immunogenicity of GAD65-exosome mimetics in presence of the ER chaperone Calreticulin.**

Activation of BMDCs (**A**-**E**) and GAD65 specific T33.1 T cells (**F**) by 1, 2.5 and 5 µg/ml of liposome bound GAD65 combined with 10 µg/ml purified endotoxin-free recombinant calreticulin or ovalbumin (OVA). PBS, empty liposomes, CpG (5 µg/ml) and the GAD$_{274-286}$ peptide (0.5 µg/ml) were used as negative and positive controls respectively. (**A**-**B**) Flow cytometry analyses of BMDC expression of the costimulatory molecules CD80 and CD86 (**A**) and HLA-class II DR antigen expression (**B**). (**C**-**E**) ELISA analysis of TNFα (**C**), IL6 (**D**) and IL1β (**E**) secretion by BMDCs. (**A**-**E**) Data show the BMDC stimulation by calreticulin compared to the negative control protein OVA. The stimulation of BMDCs is not antigen dependent. (**F**) ELISA analysis of IL2 secretion by T33.1 T cells, showing significantly increased activation by liposomal GAD65 in combination with calreticulin versus OVA. Analyses were performed in technical triplicates. A one-way ANOVA was used for statistical analyses ($p* < 0.05$; $p*** < 0.001$). Immunogenic properties of calreticulin were observed in four different independent experiments.

## 4.9 REFERENCES

1. Lehuen A, Diana J, Zaccone P, Cooke A. Immune cell crosstalk in type 1 diabetes. Nat Rev Immunol 2010;10(7):501–13
2. Tersey SA, Nishiki Y, Templin AT, Cabrera SM, Stull ND, Colvin SC, et al. Islet β-cell endoplasmic reticulum stress precedes the onset of type 1 diabetes in the nonobese diabetic mouse model. Diabetes 2012;61(4):818–27
3. Engin F, Yermalovich A, Nguyen T, Ngyuen T, Hummasti S, Fu W, et al. Restoration of the unfolded protein response in pancreatic β cells protects mice against type 1 diabetes. Sci Transl Med 2013;5(211):211ra156
4. Baekkeskov S, Aanstoot HJ, Christgau S, Reetz A, Solimena M, Cascalho M, et al. Identification of the 64K autoantigen in insulin-dependent diabetes as the GABA-synthesizing enzyme glutamic acid decarboxylase. Nature 1990;347(6289):151–6
5. Payton MA, Hawkes CJ, Christie MR. Relationship of the 37,000- and 40,000-M(r) tryptic fragments of islet antigens in insulin-dependent diabetes to the protein tyrosine phosphatase-like molecule IA-2 (ICA512). J Clin Invest 1995;96(3):1506–11
6. Bonifacio E. Predicting type 1 diabetes using biomarkers. Diabetes Care 2015;38(6):989–96
7. Arvan P, Pietropaolo M, Ostrov D, Rhodes CJ. Islet autoantigens: structure, function, localization, and regulation. Cold Spring Harb Perspect Med 2012;2(8):a007658
8. Delong T, Wiles TA, Baker RL, Bradley B, Barbour G, Reisdorph R, et al. Pathogenic CD4 T cells in type 1 diabetes recognize epitopes formed by peptide fusion. Science 2016;351(6274):711–4
9. Sheng H, Hassanali S, Nugent C, Wen L, Hamilton-Williams E, Dias P, et al. Insulinoma-released exosomes or microparticles are immunostimulatory and can activate autoreactive T cells spontaneously developed in nonobese diabetic mice. J Immunol. 2011;187(4):1591–600
10. Colombo M, Raposo G, Théry C. Biogenesis, Secretion, and Intercellular Interactions of Exosomes and Other Extracellular Vesicles. Annu Rev Cell Dev Biol 2014;30(1):255–89
11. Robbins PD, Morelli AE. Regulation of immune responses by extracellular vesicles. Nat Rev Immunol 2014;14(3):195–208
12. Bashratyan R, Sheng H, Regn D, Rahman MJ, Dai YD. Insulinoma-released exosomes activate autoreactive marginal zone-like B cells that expand endogenously in prediabetic NOD mice. Eur J Immunol 2013;43(10):2588–97
13. Rahman MJ, Regn D, Bashratyan R, Dai YD. Exosomes released by islet-derived mesenchymal stem cells trigger autoimmune responses in NOD mice. Diabetes 2014;63(3):1008–20
14. Kim J, Richter W, Aanstoot HJ, Shi Y, Fu Q, Rajotte R, et al. Differential expression of GAD65 and GAD67 in human, rat, and mouse pancreatic islets. Diabetes 1993;42(12):1799–808
15. Kanaani J, Cianciaruso C, Phelps E a., Pasquier M, Brioudes E, Billestrup N, et al. Compartmentalization of GABA synthesis by GAD67 differs between pancreatic beta cells and neurons. PLoS One 2015;10(2):e0117130
16. Kash SF, Condie BG, Baekkeskov S. Glutamate decarboxylase and GABA in pancreatic islets: lessons from knock-out mice. Horm Metab Res 1999;31(5):340–4
17. Kubosaki A, Gross S, Miura J, Saeki K, Zhu M, Nakamura S, et al. Targeted disruption of the IA-2beta gene causes glucose intolerance and impairs insulin secretion but does not prevent the development of diabetes in NOD mice. Diabetes 2004;53(7):1684–91
18. Phelps EA, Cianciaruso C, Michael IP, Pasquier M, Kanaani J, Nano R, et al.

Aberrant Accumulation of the Diabetes Autoantigen GAD65 in Golgi Membranes in Conditions of ER Stress and Autoimmunity. Diabetes 2016;65(9):2686–99

19. Zmuda EJ, Powell CA, Hai T. A Method for Murine Islet Isolation and Subcapsular Kidney Transplantation. J Vis Exp 2011;(50):e2096

20. Congia M, Patel S, Cope AP, De Virgiliis S, Sønderstrup G. T cell epitopes of insulin defined in HLA-DR4 transgenic mice are derived from preproinsulin and proinsulin. Proc Natl Acad Sci U S A. 1998;95:3833–8

21. Rutti S, Sauter NS, Bouzakri K, Prazak R, Halban PA, Donath MY. In vitro proliferation of adult human beta-cells. Maedler K, editor. PLoS One 2012;7(4):e35801

22. Lutz MB, Kukutsch N, Ogilvie AL, Rössner S, Koch F, Romani N, et al. An advanced culture method for generating large quantities of highly pure dendritic cells from mouse bone marrow. J Immunol Methods 1999;223(1):77–92

23. Merglen A, Theander S, Rubi B, Chaffard G, Wollheim CB, Maechler P. Glucose Sensitivity and Metabolism-Secretion Coupling Studied during Two-Year Continuous Culture in INS-1E Insulinoma Cells. Endocrinology 2004;145(2):667–78

24. Minami K, Yano H, Miki T, Nagashima K, Wang CZ, Tanaka H, et al. Insulin secretion and differential gene expression in glucose-responsive and -unresponsive MIN6 sublines. Am J Physiol Endocrinol Metab 2000;279(4):E773–81

25. Houlihan JL, Metzler JJ, Blum JS. HSP90alpha and HSP90beta isoforms selectively modulate MHC class II antigen presentation in B cells. J Immunol 2009;182(12):7451–8

26. Théry C, Amigorena S, Raposo G, Clayton A. Isolation and characterization of exosomes from cell culture supernatants and biological fluids. Curr Protoc Cell Biol 2006;Chapter 3:Unit 3.22

27. Chopra T, Hamelin R, Armand F, Chiappe D, Moniatte M, McKinney JD. Quantitative Mass Spectrometry Reveals Plasticity of Metabolic Networks in Mycobacterium smegmatis. Mol Cell Proteomics 2014;13(11):3014–28

28. Piquer S, Valera L, Lampasona V, Jardin-Watelet B, Roche S, Granier C, et al. Monoclonal antibody 76F distinguishes IA-2 from IA-2β and overlaps an autoantibody epitope. J Autoimmun. 2006;26(3):215–22.

29. Warren G. Transport through the Golgi in Trypanosoma brucei. Vol. 140, Histochemistry and Cell Biology. 2013. p. 235–8

30. Lock JG, Stow JL. Rab11 in recycling endosomes regulates the sorting and basolateral transport of E-cadherin. Mol Biol Cell. 2005;16(4):1744–55.

31. Laulagnier K, Vincent-Schneider H, Hamdi S, Subra C, Lankar D, Record M. Characterization of exosome subpopulations from RBL-2H3 cells using fluorescent lipids. Blood Cells, Mol Dis. 2005;35:116–21

32. Masserini M, Palestini P, Pitto M, Chigorno V, Sonnino S. Preparation and Use of Liposomes for the Study of Sphingolipid Segregation in Membrane Model Systems. In: Liposome Methods and Protocols New Jersey: Humana Press; 2002. p. 17–28

33. Baekkeskov S, Kanaani J. Palmitoylation cycles and regulation of protein function (Review). Mol Membr Biol 2009;26(1–2):42–54

34. Cossetti C, Iraci N, Mercer TR, Leonardi T, Alpi E, Drago D, et al. Extracellular vesicles from neural stem cells transfer IFN-γ via Ifngr1 to activate Stat1 signaling in target cells. Mol Cell 2014;56(2):193–204

35. Meister M, Tikkanen R. Endocytic trafficking of membrane-bound cargo: A flotillin point of view. Vol. 4, Membranes. 2014. p. 356–71

36. Andreu Z, Yáñez-Mó M. Tetraspanins in extracellular vesicle formation and function. Front Immunol 2014;5:442

37. Perez-Hernandez D, Gutiérrez-Vázquez C, Jorge I, López-Martín S, Ursa A, Sánchez-Madrid F, et al. The intracellular interactome of tetraspanin-enriched

microdomains reveals their function as sorting machineries toward exosomes. J Biol Chem 2013;288(17):11649–61

38. Savina A, Vidal M, Colombo MI. The exosome pathway in K562 cells is regulated by Rab11. J Cell Sci 2002;115(Pt 12):2505–15

39. Hsu C, Morohashi Y, Yoshimura S-I, Manrique-Hoyos N, Jung S, Lauterbach MA, et al. Regulation of exosome secretion by Rab35 and its GTPase-activating proteins TBC1D10A-C. J Cell Biol 2010;189(2):223–32

40. Plutner H, Cox AD, Pind S, Khosravi-Far R, Bourne JR, Schwaninger R, et al. Rab1b regulates vesicular transport between the endoplasmic reticulum and successive Golgi compartments. J Cell Biol 1991;115:31–43

41. Christgau S, Schierbeck H, Aanstoot HJ, Aagaard L, Begley K, Kofod H, et al. Pancreatic beta cells express two autoantigenic forms of glutamic acid decarboxylase, a 65-kDa hydrophilic form and a 64-kDa amphiphilic form which can be both membrane-bound and soluble. J Biol Chem 1991;266(31):21257–64

42. Roucourt B, Meeussen S, Bao J, Zimmermann P, David G. Heparanase activates the syndecan-syntenin-ALIX exosome pathway. Cell Res 2015;25(4):412–28

43. Kanaani J, Patterson G, Schaufele F, Lippincott-Schwartz J, Baekkeskov S. A palmitoylation cycle dynamically regulates partitioning of the GABA-synthesizing enzyme GAD65 between ER-Golgi and post-Golgi membranes. J Cell Sci 2008;121(Pt 4):437–49

44. Kelly EE, Horgan CP, McCaffrey MW. Rab11 proteins in health and disease. Biochem Soc Trans 2012;40(6):1360–7

45. Savina A, Fader CM, Damiani MT, Colombo MI. Rab11 promotes docking and fusion of multivesicular bodies in a calcium-dependent manner. Traffic. 2005;6(2):131–43

46. Wicker LS, Chen SL, Nepom GT, Elliott JF, Freed DC, Bansal A, et al. Naturally processed T cell epitopes from human glutamic acid decarboxylase identified using mice transgenic for the type 1 diabetes-associated human MHC class II allele, DRB1*0401. J Clin Invest 1996;98(11):2597–603

47. Eizirik DL, Cardozo AK, Cnop M. The Role for Endoplasmic Reticulum Stress in Diabetes Mellitus. Endocr Rev 2008;29(1):42–61

48. Graner MW, Lillehei KO, Katsanis E. Endoplasmic Reticulum Chaperones and Their Roles in the Immunogenicity of Cancer Vaccines. Front Oncol 2015;4:379

49. Turano C, Coppari S, Altieri F, Ferraro A. Proteins of the PDI family: Unpredicted non-ER locations and functions. J Cell Physiol. 2002;193(2):154–63

50. Obeid M, Tesniere A, Ghiringhelli F, Fimia GM, Apetoh L, Perfettini J-L, et al. Calreticulin exposure dictates the immunogenicity of cancer cell death. Nat Med 2007;13(1):54–61

51. Yang Y, Liu B, Dai J, Srivastava PK, Zammit DJ, Lefrançois L, et al. Heat shock protein gp96 is a master chaperone for toll-like receptors and is important in the innate function of macrophages. Immunity 2007;26(2):215–26

52. Morito D, Nagata K. ER Stress Proteins in Autoimmune and Inflammatory Diseases. Front Immunol 2012;3:48

53. Schild H, Rammensee H. gp96 — The immune system's Swiss army knife. Nat Immunol 2000;1(2):1–2

54. Galluzzi L, Kepp O, Kroemer G. Enlightening the impact of immunogenic cell death in photodynamic cancer therapy. EMBO J 2012;31(5):1055–7

55. Rowland AA, Chitwood PJ, Phillips MJ, Voeltz GK. ER contact sites define the position and timing of endosome fission. Cell 2014;159(5):1027–41

56. Eden ER, White IJ, Tsapara A, Futter CE. Membrane contacts between endosomes and ER provide sites for PTP1B-epidermal growth factor receptor interaction. Nat Cell Biol. 2010;12(3):267–72

57. Rondas D, Crèvecoeur I, D'Hertog W, Ferreira GB, Staes A, Garg AD, et al. Citrullinated glucose-regulated protein 78 is an autoantigen in type 1 diabetes. Diabetes 2015;64(2):573–86

# CHAPTER 5

# Conclusion

## 5.1  SUMMARY AND DISCUSSION

T1D is an autoimmune disease characterized by T cell infiltration in the islets of Langerhans and destruction of insulin-producing beta cells. The multifactorial aspect of the disease makes the research on the biological mechanisms implicated in the development of autoimmunity highly complex and challenging. Although much progress has been achieved and several biological predictive biomarkers of the disease are now known, a comprehensive and complete view including all the causes involved in the onset of the disease is not available yet.

In addition to identified anomalies in the immune system of T1D patients (1), a recent and recognized key factor in the initiation of autoimmunity directly involves the tissue that is target of the disease, particularly the pancreatic beta cells (2-4). The enormous protein synthesis capacities of these cells makes them highly susceptible to stress, leading to the initiation of self-defense processes that can either restore the normal cell function and homeostasis or lead to a cell "suicide", which could attract the attention of the immune system.

The purpose of my thesis was to give a close look at beta cells in order to find out which potential intracellular abnormalities and pathways might be responsible for making beta cell antigens so vulnerable for the attack of the immune system.

Thus, having the opportunity of looking inside a beta cell, with such a level of resolution that permits to visualize trafficking of autoantigens, is of high importance for investigating the pathogenesis of T1D. In the first manuscript (Chapter 2) we described a method that allows for the successful culture of monolayers of pancreatic islet cells. Although culturing techniques in 2D systems have been extensively reported for many different cell types, several difficulties have been encountered with

primary pancreatic islets. These mini-organs are indeed constituted by cells that work in close operation to maintain their homeostasis, and they usually loose their properties or do not survive when they are dissociated and separated from each other. We identified key factors (such as medium constituents and specific ECM molecules) that allow beta cells to survive after their dissociation, maintain their phenotype, adhere and spread well on surfaces. This allows the visualization of subcellular phenomena and details that could have not been observed in conditions where instead the cells look rounded and unhealthy. Also, this method represents the first successful attempt in culturing pancreatic islet cells not only on plastic coverslips, but also on glass surfaces, condition that is required for the application of super resolution imaging techniques such as STED.

Therefore, the protocol for culturing monolayer of pancreatic islet cells described here might represent a breakthrough in the field of beta cell biology. This method could be useful not only for all the scientists studying T1D, but also for those focused on Type 2 Diabetes (T2D), another worldwide multifactorial disease affecting pancreatic beta cells and characterized by insulin resistance (5).

Moreover, this method allowed us to identify a cilia-centric mechanism of beta cell proliferation. We discovered that culture conditions capable of boosting beta cell spreading, such as switching from low to high glucose concentration combined with serum starvation and its reintroduction, are capable of inducing reabsorption of primary cilia in beta cells, which are then stimulated to proliferate. Similarly to the protocol for monolayer islet cell culture, the method of cilia disassembly proposed in Chapter 2 might be of inspiration for many people working on T1D and T2D. Restoring beta cell mass and function through induction of beta cell proliferation is currently one of most investigated alternatives to overcome the issue of insulin deficiency that affects both types of Diabetes (6).

Our method for culturing islet monolayer also allowed us to perform high-resolution microscopy studies on beta cells and obtain most of the results reported in

the other two manuscripts (Chapters 3 and 4), which illustrate two interconnected mechanisms that could be responsible for the initiation of autoimmunity in T1D.

The first one (Chapter 3) shows how ER stress induced by pro-inflammatory factors or a saturated fatty acid can block the palmitoylation cycle of the antigen GAD65, leading to an accumulation of the palmitoylated form of the protein in the Golgi compartment. Furthermore, we show that the palmitoylated form of GAD65 is more immunogenic and can stimulate a stronger activation of GAD65-specific T cells compared to the form not carrying this post-translation modification. Since palmitoylation facilitates the interaction of proteins with cell membranes, the increased immunogenicity of the palmitoylated form of GAD65 is probably due to the fact that, once released in the extracellular space, the antigen has a stronger affinity for the plasma membrane of APCs and is taken up by more efficiently.

In addition, aberrant trafficking of GAD65 seems to be an active phenomenon during development of autoimmunity in T1D: immunostaining on human pancreatic sections from pre-diabetic GAD65-autoantibody positive individuals and patients with ongoing T cell infiltration in the islets reveals a significantly higher accumulation of GAD65 in the Golgi compartment compared to healthy controls.

Accumulation of GAD65 in trans-Golgi membranes might also be involved in another biological mechanism implicated in the initiation of autoimmunity, which is illustrated in the third and last manuscript (Chapter 4). Specifically beta cells seem to secrete autoantigens in a subtype of exosomes involving a biogenesis pathway originating in the trans-Golgi network and intersecting with recycling endosomes and Rab11.

Our work represents the first extensive characterization of exosomes and their protein content isolated from primary human and rat pancreatic islet cells. Given the limited availability of primary islets of Langerhans in general and human islets in particular, this study is probably unique at this time. We show that both human and rat islet-exosomes contain major autoantigens in T1D, insulin, proinsulin, GAD65 and

IA-2. Some of these autoantigens are intracellular proteins normally not visible by the immune system; therefore, their release into the extracellular space in exosomes may represent a route of exposure to the immune system and a possible mechanism underlying the initiation of autoimmunity in T1D.

Interestingly, the release of exosomes, and consequently the amount of autoantigens contained in them, is enhanced when primary pancreatic islets are exposed to pro-inflammatory cytokines. Since a strong connection between Th1 cytokines and induction of ER stress in beta cells has been observed by our group and others (7,8), it is likely that ER stress by itself may be responsible for the increased exosome release, but this aspect was not directly investigated in our work. In addition, pro-inflammatory cytokines strongly induce or upregulate the presence in exosomes of chaperones resident in the ER and involved in ER stress response, such as calreticulin, gp96 and ORP150. In addition to their role in restoring the correct protein folding and homeostasis in cell stress conditions, these chaperones, once released in the extracellular space, can act as "danger signals" and initiate inflammatory immune responses (9,10).

We also show that islet-exosomes can be efficiently taken up by APCs, such as BMDCs and B lymphocytes. Furthermore, activation of dendritic cells is enhanced when these APCs are incubated with exosomes from cytokine-treated islets compared to those isolated from untreated islets, suggesting that the presence of pro-inflammatory ER chaperones may be responsible for the increased exosome immunogenicity.

In addition to an effect of exosomes on the innate branch of the immune system, the presence of autoantigens in islet-exosomes may also enhance activation of an adaptive immune response. To test this hypothesis, we took advantage of an established in vitro assay constituted by GAD65-specific T cells and BMDCs carrying the HLA class II DR4. While this system works very well when the antigen is administered in a pure context (see for instance Chapter 3.3.4), two major issues do

not make this assay ideal for investigating more complex biological scenarios and conditions (including islet-lysates and islet-exosomes): first, the limited sensitivity due to which relatively high protein concentrations are required to induce a T cell response, and second, the presence of other proteins and possibly other beta cell antigens that might compete for uptake and presentation.

Thus, in order to analyze the immunogenicity of the autoantigen GAD65 associated to biological EVs, we engineered a liposome-based system mimicking the features of the natural exosomes, and to which we anchored the GAD65 recombinant protein. We used this system to test the T cell activation induced by GAD65-exosome mimetics compared to a scenario in which the protein is present as free antigen. In order to make a direct and reliable comparison between these two conditions, we administered the same exact concentrations of protein (both unbound and liposome-bound). In this manner, we were able to show that the T cell activation is about 50 times more efficient when GAD65 is bound to the exosome-mimetics compared to when is present as free protein. This system also allowed us to investigate the contribution of the ER chaperone calreticulin in increasing the immunogenicity of the GAD65-exosome mimetics. In this way, we observed that adding calreticulin (but not a control protein like OVA) to the GAD65-liposomes not only boosts the activation of the BMDCs used as APCs but also of the GAD65 autoreactive T cells.

## 5.2  FUTURE DIRECTIONS

The engineered platform based on exosome mimetics constitutes an initial attempt to assess the immunogenic potential of autoantigens associated to lipid membranes with some features of exosomes and has its limitations. For instance, the liposomes carry GAD65 on the surface rather than on the luminal face, which is more likely the position of GAD65 in exosomes. Furthermore, the immunogenicity of exosomes is likely the results of a particular compositions of proteins and lipids, some enhancing the uptake and presentation by APCs, others functioning as "danger signal" molecules in the immune response. However, the reductionist approach of the liposomal platform represents a reproducible and useful tool to explore the role of individual components in APC activation and antigen presentation. When combined with molecules with known anti-inflammatory properties, exosome-mimetics may become useful as therapeutic strategy to generate tolerance versus immunity to GAD65 and other autoantigens.

Finally, the discovery that pro-inflammatory ER chaperones can be released in association to exosomes, especially under cytokine-induced stress conditions, opens the possibility for investigating novel pharmaceutical approaches to prevent or cure T1D. For instance, administration of antibodies or blocking peptides against CD91, a known receptor for calreticulin and gp96 (11) that is highly expressed on macrophages (12) and a subtype of dendritic cells (13,14), could be exploited as a therapeutic strategy to prevent the uptake and activation of APCs by islet-exosomes.

## 5.3 REFERENCES

1. Roep BO, Tree TIM. Immune modulation in humans: implications for type 1 diabetes mellitus. Nat Rev Endocrinol 2014;10(4):229–42
2. Mathis D, Vence L, Benoist C. beta-Cell death during progression to diabetes. Nature 2001;414(6865):792–8
3. Eizirik DL, Miani M, Cardozo AK. Signalling danger: endoplasmic reticulum stress and the unfolded protein response in pancreatic islet inflammation. Diabetologia 2013;56(2):234–41
4. Todd DJ, Lee A-H, Glimcher LH. The endoplasmic reticulum stress response in immunity and autoimmunity. Nat Rev Immunol 2008;8(9):663–74
5. Kahn SE, Cooper ME, Del Prato S. Pathophysiology and treatment of type 2 diabetes: perspectives on the past, present, and future. Lancet (London, England) 2014;383(9922):1068–83
6. Wang P, Fiaschi-Taesch NM, Vasavada RC, Scott DK, García-Ocaña A, Stewart AF. Diabetes mellitus-advances and challenges in human β-cell proliferation. Nat Rev Endocrinol 2015;11(4):201–12
7. Brozzi F, Nardelli TR, Lopes M, Millard I, Barthson J, Igoillo-Esteve M, et al. Cytokines induce endoplasmic reticulum stress in human, rat and mouse beta cells via different mechanisms. Diabetologia 2015;58(10):2307–16
8. Eizirik DL, Colli ML, Ortis F. The role of inflammation in insulitis and beta-cell loss in type 1 diabetes. Nat Rev Endocrinol 2009;5(4):219–26
9. Morito D, Nagata K. ER Stress Proteins in Autoimmune and Inflammatory Diseases. Front Immunol 2012;3:48
10. Graner MW, Lillehei KO, Katsanis E. Endoplasmic Reticulum Chaperones and Their Roles in the Immunogenicity of Cancer Vaccines. Front Oncol 2015;4:379
11. Basu S, Binder RJ, Ramalingam T, Srivastava PK. CD91 is a common receptor for heat shock proteins gp96, hsp90, hsp70, and calreticulin. Immunity. 2001;14(3):303–13
12. Pawaria S, Binder RJ. CD91-dependent programming of T-helper cell responses following heat shock protein immunization. Nat Commun 2011;2:521
13. Hart JP, Gunn MD, Pizzo S V. A CD91-positive subset of CD11c+ blood dendritic cells: characterization of the APC that functions to enhance adaptive immune responses against CD91-targeted antigens. J Immunol. 2004;172(1):70–8
14. Cappelletti M, Presicce P, Calcaterra F, Mavilio D, Della Bella S. Bright expression of CD91 identifies highly activated human dendritic cells that can be expanded by defensins. Immunology 2015;144(4):661–7

# Curriculum vitae

## Chiara Cianciaruso

*Gender* Female | *Date of birth* 25/05/1988 | *Nationality* Italian
*Address* Avenue de Sévelin 13e, Lausanne, Switzerland, 1004
*Phone*: (+41) 789765486 | *Email*: c.chiara88@gmail.com

## WORK EXPERIENCE

*2013 – 2016*

### PhD student in Bioengineering and Biotechnology at EPFL (Lausanne)

**Laboratory of Immunopathology and Cell Biology of Autoantigens**
Prof. Baekkeskov's research group (http://baekkeskov-group.epfl.ch)
**École Polytechnique Fédérale de Lausanne**
Route Cantonale, 1015 Lausanne, Switzerland

Principal subject/s covered
- *Investigate the mechanisms leading to autoimmunity against the autoantigens GAD65 in Type 1 Diabetes*
  Responsibilities
- *Primary cell isolation (rat pancreatic islets, hippocampal neurons and dendritic cells), cell culture (human pancreatic islets, insulinoma cell lines, B cell line, GAD65-specific T cell hybridomas) and co-culture of human/rat pancreatic islet cells with neurons*
- *In vitro immunogenicity assays (FACS, ELISA, ELISPOT, T cell assays)*
- *In vivo vaccination studies (intra-footpad injections of adjuvant and antigens, blood and organ harvesting)*
- *Isolation and characterization of extracellular vesicles from cell culture supernatant and sera (electron microscopy, western blot and nanoparticle tracking analyses)*
- *Liposome preparation and protein conjugation*

Teaching assistant in the following classes:
- *Scientific literature analyses in Bioengineering*
- *Neuroscience*
- *Physiology lab (Topics: active sodium transport | ECG, electrocardiogram)*

*2012 – 2013*

### Research fellow in the Experimental Imaging Center at San Raffaele Institute (Milan)

**Laboratory activity in Neuroradiology Research Unit**
**Scientific Institute San Raffaele Hospital**
Via Olgettina, 58, 20132 Milano, Italy

Principal subject/s covered
- *Magnetic Resonance Imaging (MRI) and cell labeling with MRI contrast agents (SPIOs)*

Responsibilities
- *Isolation of hippocampal neurons and cell culture (embryonic stem cells, neural stem cells, cell lines)*
- *Cloning, lentiviral vector production, genomic DNA extraction, RT-PCR*
- *Stereotaxic brain injections of SPIO-labeled cells in mice, in vitro and in vivo bioluminescence*
- *Use of vibratome and cryostat, Prussian Blue staining, immunofluorescence, confocal microscopy*

## EDUCATION

*2013 – 2016*

**PhD student in Bioengineering and Biotechnology (EDBB doctoral program)**

**École Polytechnique Fédérale de Lausanne**
Route Cantonale, 1015 Lausanne, Switzerland
Thesis title: "Investigating the Biological Mechanisms underlying the Initiation of Autoimmunity against Beta Cell Antigens in Type 1 Diabetes".

*2010 – 2012*

**Master Degree in Medical, Cellular and Molecular Biotechnology**

**"Vita-Salute" San Raffaele University**
Via Olgettina, 58, 20132 Milan, Italy
Thesis title: "Cellular MR Imaging with Iron Oxide Nanoparticles: the Issue of Specificity".
Final score of 110/110 cum laude.

Principal subjects covered and acquired skills
▪ *Knowledge of cellular and molecular biology, gene expression, proteomics, genetics, microbiology, diagnostics, pathology, immunology, pharmacology and physiology*
▪ *Laboratory experience in protein expression and purification, cell culture, genetic engineering and bioimaging*

*2007 – 2010*

**First Level Degree in Pharmaceutical and Medical Biotechnology**

**"Vita-Salute" San Raffaele University**
Via Olgettina, 58, 20132 Milan, Italy
Thesis title: "Studies on Breast Cancer Genetic Susceptibility and Potential Diagnostic Applications".
Final score of 109/110.

*2002 – 2007*

**High School Scientific Lyceum Diploma**
"Galileo Galilei" Institute, Erba (CO), Italy
Final score of 98/100.

## PERSONAL SKILLS

*Languages*

Italian (native) | English (fluent) | French (basic)

*Computer skills*

European Computer Driving License (ECDL) | Microsoft Office™ tools | Scientific software (Flow Jo, Vector NTI, Prism, ImageJ) | Adobe Illustrator

*Driving licence*

For car (category B)

## PUBLICATIONS

**Cellular magnetic resonance with iron oxide nanoparticles: long-term persistence of SPIO signal in the CNS after transplanted cell death**
Chiara Cianciaruso, Antonella Pagani, Cristina Martelli, Marco Bacigaluppi, Mario L. Squadrito, Alessia Lo Dico, Michele De Palma, Roberto Furlan, Giovanni Lucignani, Andrea Falini, Alessandra Biffi, Luisa Ottobrini, Letterio S. Politi
*Nanomedicine (Lond) 2014; 9(10):1457-74*

**Compartmentalization of GABA synthesis by GAD67 differs between pancreatic beta cells and neurons**
Jamil Kanaani, Chiara Cianciaruso, Edward A. Phelps, Miriella Pasquier, Estelle Brioudes, Nills Billestrup, Steinunn Baekkeskov
*PLoS One 2015; 10(2):e0117130*

**Aberrant accumulation of the diabetes autoantigen GAD65 in Golgi membranes in conditions of ER stress and autoimmunity**
Edward A. Phelps, Chiara Cianciaruso, Iacovos P. Michael, Miriella Pasquier,
Jamil Kanaani, Rita Nano, Vanessa Lavallard, Nils Billestrup, Jeffrey A. Hubbell,
Steinunn Baekkeskov
*Diabetes 2016; 65(9):2686-99*

**Primary human and rat beta cells release the intracellular autoantigens GAD65, IA-2 and proinsulin in exosomes together with cytokine-induced enhancers of immunity**
Chiara Cianciaruso, Edward A. Phelps, Miriella Pasquier, Romain Hamelin, Davide Demurtas, Mohamed Alibashe Ahmed, Lorenzo Piemonti, Sachiko Hirosue, Melody Swartz, Michele De Palma, Jeffrey A. Hubbell, Steinunn Baekkeskov
*Diabetes 2016; db160671*

**Advances in pancreatic islet monolayer culture permit super-resolution microscopy and reveal a cilia-centric mechanism of beta cell proliferation**
Edward A. Phelps*, Chiara Cianciaruso*, Jaime Santo-Domingo, Miriella Pasquier, Gabriele Galliverti, Lorenzo Piemonti, Ekaterine Berishvili, Andreas Wiederkehr, Jeffrey A. Hubbell, Steinunn Baekkeskov
*Authors contributed equally
*In revision*

## CONFERENCES AND SEMINARS

Emerging Concepts and Targets in Islet Biology, Keystone 2014
Poster presentation: "Expression of Autoantigens and Interaction of Neurons and Pancreatic Islet Cells in a Co-culture System"

Bioengineering day, EPFL 2015
Poster presentation: "Pancreatic beta cells release the autoantigens GAD65 and IA-2 in exosomes together with cytokine induced enhancers of immunity"

IBI-EDBB Graduate Student Mini-Symposium, EPFL 2016
Oral presentation: "Extracellular Vesicles in the Immunopathogenesis of Type 1 Diabetes"